Hydrogeological Characterisation of the Impact of Climate Change and Anthropogenic Factors on Groundwater Resource in Klein Letaba River Catchment, Mopani District of Limpopo Province

by

Masilo Gladness Mohale

Thesis Submitted in fulfilments of the Requirements for the Degree of

Master of Science

in

Geology

in the

Faculty of Science and Agriculture
School of Physical and Mineral Sciences
(Department of Geology and Mining)

in the

University of Limpopo

Supervisor: Prof AZ Tessema

Co-supervisor: Prof KK Ayisi

March 2025

DECLARATION

I, Masilo Gladness Mohale, hereby declare that the work contained in this thesis submitted to the Department of Geology and Mining in the University of Limpopo, for an MSc Degree in Geology, is my original work and has not been previously submitted in this University or any other institution of higher learning and all reference materials contained therein have been fully and accordingly acknowledged.

Date: 16 March 2025

Acknowledgments

Financial support by the National Research Foundation (NRF) and Centre for Global Change at the Univerity of Limpopo. My sincere gratitude to Prof. Abera Tessema for the unwavering support, patience, guidance, and knowledge that he gave throughout the research study. To Manare Marweshi, you are a GOD sent and your kindness and steady support are highly appreciated. For the duration of this research study, I have received enormous support and would like to thank the following individuals and institutions:

- Mr. Mike Buttler from the iThemba Labs, Gauteng for the isotope analyses;
- Mr. Lucky Dlamini from the South African Weather Services (SAWS) and Mrs. Irene Joubert from the Agricultural Research Council Institute of Soil, Climate, and Water (ISCW) for providing climatic data for the project;
- Mr. Elias Nhlapo and Mr. Shonisani Mutheiwana from the Department of Water and Sanitation for providing monitoring data;
- Gidela Secondary School, Rotterdam Bricks and Clinic for allowing me to collect water samples at their facilities;
- Mr Robert Whitehead and Patric Mudau for their assistance during sampling.
- Patric Mudau for helping with borehole sampling;
- Most importantly, I would like to thank my husband and mentor Moropa Madisha, your support has been the ultimate source of my strength.
- To my children (Koketso, Olebogeng, Omphile, Molopolli and Khutso), Mom and Dad, your love, support and prayers helped me to overcome all the difficult times.
- To cousins, friends, and colleagues, your generosity has inspired me.
- Above all, I thank God for His Grace and mercy towards me and everyone during this research study.

Abstract

Groundwater is the primary source of water supply for domestic use, agricultural and mining sectors in the Klein Letaba River catchment, which is located in the central-eastern part of the Limpopo Province. As a result of the arid-to-semi-arid nature of the climate, there is limited surface water in this catchment, which partly contributed to groundwater as the only dependable source of water supply for various uses. Periodic measurements of water level in several boreholes in this catchment indicated that there is a continuous drop in piezometric surface from time to time. This persistent problem necessitated a detailed hydrogeological characterisation of the Klein Letaba River catchment to understand the extent of the impacts of climate change and anthropogenic factors on groundwater resource.

The main aim of the present study was to simulate groundwater flow, and evaluate the fluctuation of borehole water level in response to climate change and anthropogenic activities, thereby understand the extent of vulnerability of groundwater in the area. To achieve the aim, hydrogeological, geological, borehole logs, climate, soil, and digital elevation data, among many other spatial datasets were processed to determine aquifer parameters, MODFLOW layer groups, and develop boundary conditions. In addition, hydrochemical and environmental isotopes were used to trace the groundwater flow path, and to ascertain the inflows and outflow boundaries of the conceptual model of groundwater flow. The results show that groundwater recharge area occurs in the highly elevated south western sector, and it flows towards the low elevated north eastern part of the model boundary area. In addition, the tritium radiogenic isotope was employed to determine the mean residence time (MRT) of groundwater using the methods that were outlined in the previous studies. The results suggest that low tritium concentrations ranging from 0.2 to 1.9 TU correspond to the presence of old groundwater that resided in the aquifer for a prolonged period of time, probably prior to 1952 (<0.8 TU), while tritium values > 0.8 TU suggest the presence of a mixture of old and recently recharged water.

MODFLOW NWT, along with its upstream weighted flow package (UPW), was used to carry out three-dimensional steady state modelling of groundwater flow, and assess the response of the groundwater level due to the impacts of climate change and anthropogenic factors.

The results of the steady-state groundwater flow simulation indicated that recharge from the rainfall and river leakages are the most important components of the inflows that contribute to the availability of groundwater, accounting for 44% and 40%, respectively of the total inflows. The major outflow components include river leakage and evapotranspiration, which contribute 62% and 25%, respectively to the total discharge from the aquifer. These results show that groundwater and surface water interactions play an important role in the determination of the hydrological water balance. In that, the depletion of groundwater determines the fate of surface water and vice versa.

The results of the zone budgets suggest that the weathered aquifer acts as a medium through which the fractured aquifer and the rivers are being replenished. The weathered aquifer supplies approximately 36% and 23% of the total outflow volume from its zone to the fractured aquifer and rivers, respectively. At the same time, the dam gains a minor fraction of water from the weathered aquifer owing to an insignificant fluctuation of the hydraulic head and the conductivity of the bottom of the dam. Recharge from the rain largely replenishes the fractured aquifer via the weathered aquifer, while the internal boundaries such as rivers and dam gain water from the two aquifers and surface runoff. The zone budget further indicates that both aquifers are hydraulically connected and water availability in both permeable layers depends on the amount of rainfall recharge, evapotranspiration, and groundwater abstraction. Thus, climate change and anthropogenic activities play a significant role in determining the availability of sustainable water supply in the area. Furthermore, the results signify the importance of the underlying fractured aquifer as the main source of water owing to its good hydraulic conductivity compared to the weathered aquifer. In summary, climate change and anthropogenic activities are the main drivers of the scarcity of water resource in the area.

CONTENTS

List of Figures

List of Tables

CHAPTER 1 : INTRODUCTION

1.1 Background

Water resource is under threat due to population expansion, economic developments, land use and urbanization, environmental degradation, and other factors (Sophocleous, 2004). This has prompted the world to re-examine the relationship between water, climate and the environment to try and come up with management plans. South Africa is a semi-arid region in which both groundwater and surface water resources remain under threat as a result of the impacts of climate change and anthropogenic factors.

Dennis and Dennis (2011) noted that South Africa is currently facing a high level of water stress due to increasing problems related to water scarcity and water quality. The ever-increasing water demand and water scarcity have initiated water experts to shift their focus of research interest from surface water to groundwater as the primary source of water supply. Climate change is a topic of enormous scientific interest in various fields of studies and to the public in general due to its long-term direct impacts on natural resources and human livelihood (Nistor *et al.,* 2016).

This research project focuses on assessing the extent of groundwater resource vulnerability due to climate change and anthropogenic factors. The area of focus is mainly the Klein Letaba River catchment, which is situated in the north-eastern part of the Limpopo Province, in South Africa. In the Limpopo Province, the availability and quality of water have been affected by many factors, among which climate is one of the most important factors (Moseki, 2017). The impact is severe in some parts of the province where water scarcity has been observed due to the complex characteristics of the fractured crystalline basement rocks, limited rainfall and high evapotranspiration rates.

Groundwater Resource Information Project (GRIP) database of the Department of Water and Sanitation (DWS) indicates that groundwater is the main source of water supply for many communities in the Limpopo Province. In this province, groundwater plays a significant role for domestic water use, municipal bulk supplies, and agricultural purposes.

As a result, dependence on groundwater has increased significantly over the past few decades. However, the long-term high rate of abstraction put groundwater under threat, as it is the only sustainable source of water for various uses. In the study area (Klein Letaba River catchment), groundwater occurs in weathered and fractured rocks, and recharge mainly takes place through rainfall. In addition, recharge takes place through interaction between surface water bodies such as dams, rivers, lakes, and wetlands. As a result of this process, the direct influence of climate change on rainfall and surface water eventually affects the groundwater. Thus, understanding the impacts of climate change and anthropogenic variables is critical in determining a management plan that enables groundwater protection and long-term use (Ahzegbobor *et al.,* 2017).

Groundwater modelling has over the years become an indispensable tool in understanding aquifer dynamics, flow patterns, and management of the aquifers. It is one of the most important approaches that are used to understand the response of groundwater to stress such as rainfall, evapotranspiration, and abstractions. Also, modelling of groundwater flow can be used as a predictive tool, i.e., to forecast future scenarios based on analysis of the past and present hydrogeological observations. In this study, steady state three-dimensional numerical modelling of groundwater flow is implemented to understand the aquifer's response to changes in climate and human interactions.

1.2 Problem Statement

The Klein Letaba River catchment is characterised by prolonged periods of drought, low rainfall, high temperature, and evaporation which impact negatively on the quality and availability of water. Due to the limited availability of surface water, the principal source of water for domestic and agricultural usage is groundwater. Groundwater in this area occurs in crystalline rock aquifers which are characterised by a low intrinsic primary permeability and porosity (Holland, 2011). According to climate change estimates, the Mopani District will see rising temperatures and decreased rainfall patterns (Brodrick *et al.,* 2014). Climate change will have a consequential impact on the water resources and food security in the Mopani District (Turpie and Visser, 2012).

With continued unfavourable climate conditions and increasing use of groundwater, the vulnerability will likely increase. Urbanisation, deforestation, population increase, and industrialisation, as well as increasing demands from the domestic and agricultural sectors, all of which are exacerbated by climate change, are manmade causes that pose a threat to groundwater (Taylor, 2014; Van der Gun, 2012 and Mato, 2002;).

The dynamics and flow patterns in the research area can be better understood using a groundwater flow model and this can further assist in groundwater risk assessment which might emanate from the stress associated with the changes in climate and human interactions with the water resource. Moreover, the results of modelling enable the determination of measures to remedy potential risks.

1.3 Rational

The impacts of climate change and anthropogenic factors on groundwater resources can no longer be hidden. Recently, there has been an increase in the involvement for sustainable development and management of groundwater resources. This research study is important as the information gathered will help improve the understanding of the hydrogeological properties and groundwater flow dynamics in crystalline basement aquifers. The information generated here is crucial for water resource planning and management. In addition, the results of this work will be published in peer-reviewed journals, conference proceedings and used as a source for literature review for other studies in the future.

1.4 Hypothesis

The following are the hypotheses under consideration:

- Perennial rivers are the main source of groundwater,
- The Middle Letaba dam loses water to the aquifer via interaction between the bottom of the dam and the fluctuation of water level in the aquifer,
- Naturally, groundwater flows from recharge to discharge zones.

1.5 Research question and thesis statement

(ii) To what extent surface water fluctuations impacts on dynamics of groundwater level?

(ii) Is there an interaction between the Middle Letaba Dam and the groundwater aquifer?

(iii) What are the parameters that determine groundwater flow in the area?

The current study raises these questions to provide an understanding of the possible influence of geological structures, climate change, and anthropogenic factors on groundwater resources.

1.6 Aims and Objectives

This study aims to simulate groundwater flow and assess the extent of vulnerability of the groundwater resource due to the impacts of climate change and anthropogenic factors. The objectives are to evaluate and characterize the hydrogeology of the study area. The following activities were carried out to achieve the objectives:

i. compile relevant data that include hydrogeological and geological data obtained from various sources and fieldwork,

ii. collect additional field data (to fill in the gaps) such as water samples and carry out hydro-census, etc,

iii. process the spatial data that are relevant for defining hydraulic conductivity zones,

iv. compile relevant data that are required for the determination of groundwater recharge,

v. compile spatial data that are required for the construction of MODFLOW boundary conditions and layer group,

vi. Quantify the impacts of climate change (i.e., rainfall recharge and evapotranspiration) by investigating the interaction between various components of surface and groundwater, and

vii. Quantify the impacts of anthropogenic water abstraction from the aquifers and the effects it will have on the groundwater hydraulic gradient.

CHAPTER 2 : DESCRIPTION OF THE STUDY AREA

2.1 Location of the study area

There are three District Municipalities in the Klein Letaba River catchment, namely Mopani, Vhembe, and Capricorn. The area is located in the central-eastern sector of the Limpopo Province, and it covers approximately 5,455 sq. km, with an east-west length of ~150 km, and a width of ~40 km in the north-south direction (Figure 2-1).

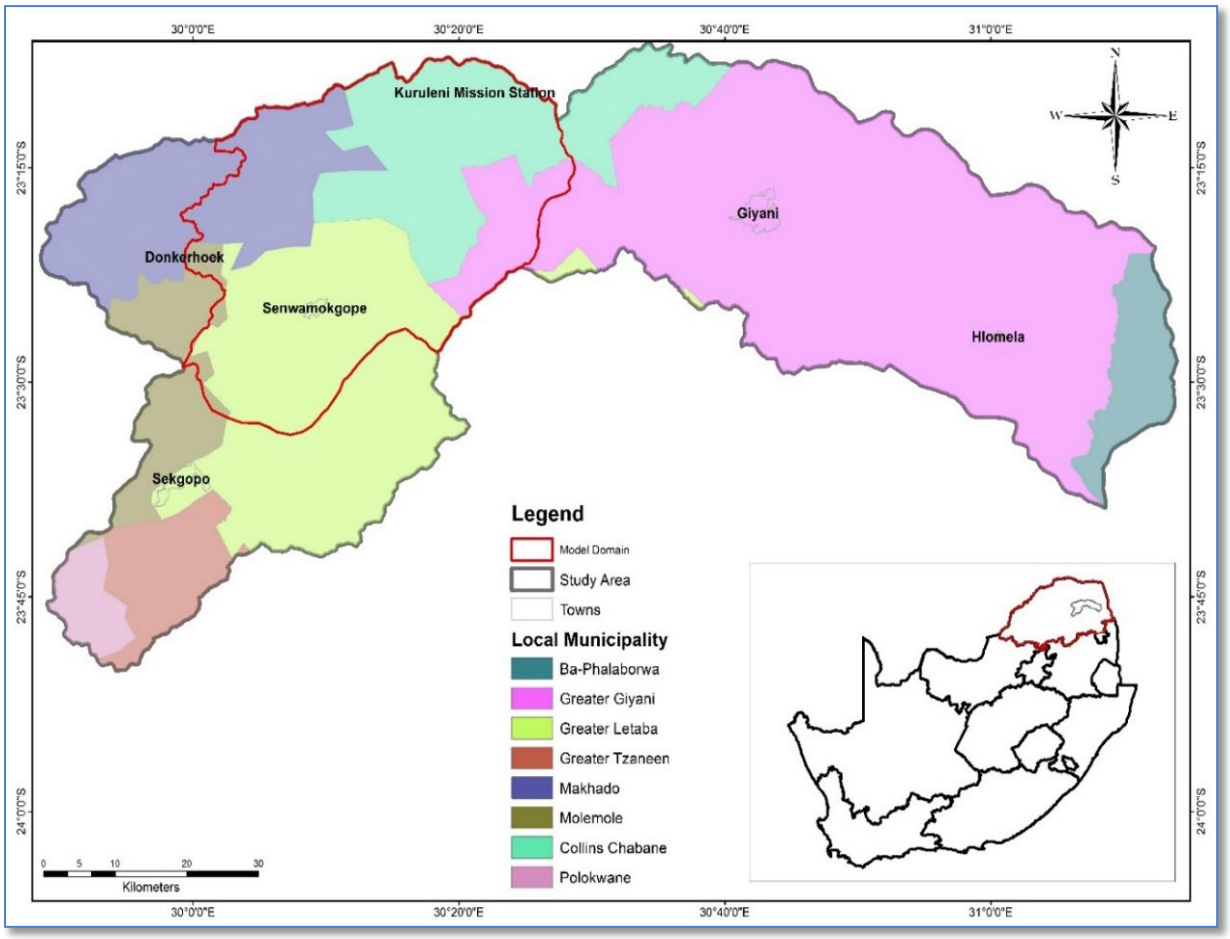

Figure 2-1: Location map of the study area showing local municipalities, towns and the outline of the model domain. The inset map shows the boundary of the study area and the Limpopo Province in South Africa.

2.2 Demography and Socio-Economics

According to Turpie and Visser (2012), Greater Letaba and Greater Giyani are said to be among the 20 local municipalities in South Africa that are at risk due to climate change relative to elsewhere in South Africa. Agriculture (livestock, fruits, and vegetables) is the main economic sector in the study area. At a district level, the mining sector also contributes about 30% to the Gross Domestic Product (GDP).

As a result of the limited water resources in the study area, groundwater plays a significant role in providing water to many households (±17%) and augmenting municipal bulk supply to >60 % of the population (Stats, 2011). Other sources of water (i.e., rain harvesting, dams, rivers, streams, and water tankers) account for more than 20% of the water supply in the study area.

2.3 Climate, Topography and Drainage

The climate in the study area is topographically controlled and it varies from the highveld in the western part to the lowveld in the eastern part of the study area. Moon and Heritage (2001), classified the area as a semi-arid to arid climate. Based on the soil terrain (SOTER) model classification (European Commission, 1995), the study area is classified as flat and undulating with isolated mountains surrounded by steep slope areas (Table 2-1). Elevation in the study area ranges between a minimum of 300 to a maximum of 1893 meters above mean sea level (m.a.m.s.l) with a general slopping(e) to the east (Figure 2-2).

The Klein Letaba River catchment consists of 8 Quaternary catchments, which form part of the Klein Letaba River Catchment of the Levuvhu and Letaba Water Management Area. The Middle and Klein Letaba Rivers are the main tributaries of the Klein Letaba River Catchment, which together with their tributaries form the watershed in the study area. There are three dams in the catchment, namely, the Lornadawn Dam in the southwest, the Middle Letaba and Nsami Dams in the central and eastern parts, respectively. The Middle Letaba Dam is supplied by Middle Letaba, Koedoes and Brandboontjies rivers as well as minor streams. Nsami Dam is dominantly supplied by Nsami River and additional water is transferred through a 70 km concrete-lined canal from Middle Letaba Dam.

Table 2-1: Slope classification based on soil terrain (SOTER) model, European Commission (1995).

Slope (%)	Classification
0-2	Flat
2-8	Undulating
8-15	Rolling
15-30	Moderately Steep
30-60	Steep

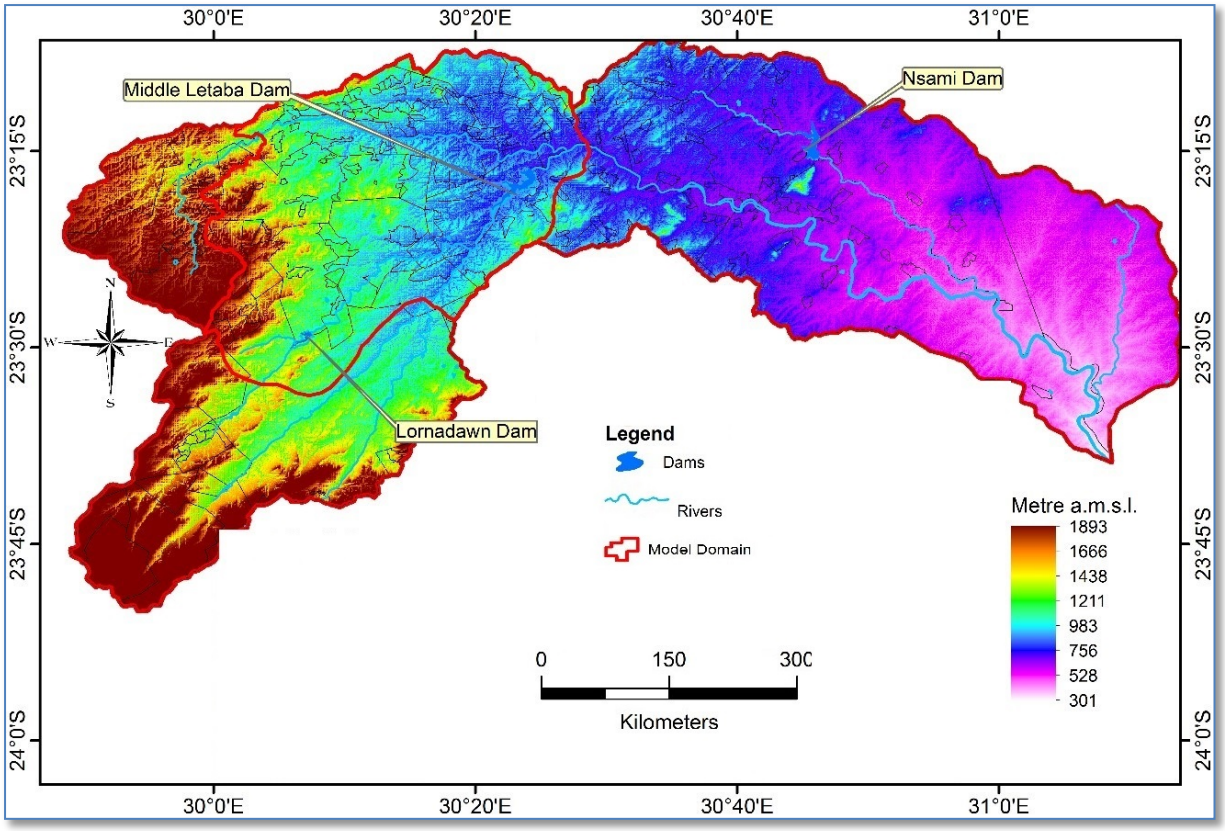

Figure 2-2: Surface drainage and topography of the Klein Letaba River catchment.

The source of the Middle Letaba River is the high tropical mountains of Magoebaskloof near Tzaneen, where rainfall is abundant during the Summer season. The inflow into the study area occurs at the topographically high recharge areas of the Soutpansberg and Magoebaskloof mountain ranges towards the west and south-western part of the study area, respectively. Discharge (outflow) occurs at the topographically low area towards the north-eastern side of the study area.

2.3.1 Climate Stations

Six climate stations were used based on the availability of the relevant data. All the stations used are in close proximity to the Klein Letaba River catchment. Table 2-2 and Figure 2-3 show a summary of the basic information and locations of the climate stations, respectively. For this research work, only stations with data covering 10 years and above were considered.

Table 2-2: Basic information of the Meteorological stations.

Station Number	Station Name	Latitude	Longitude	Information Available	Information Source
30760	Madombidza	-23.31134	30.69214	Rainfall, Temperature and Evapotranspiration	Agricultural Research Council
0679194 5	Tzaneen	-23.73670	30.11270	Rainfall and Temperature	South African Weather Services
0723020 0	Kleinfontein	-23.3240	30.0300	Rainfall	Department of Water and Sanitation
0723113 7	Voorspoed	-23.3730	30.0800	Rainfall	
B8E008	Nsami Dam	-23.26344	30.76552	Rainfall and Evapotranspiration	
B8R007	Middle Letaba	-23.27354	30.40348	Rainfall and Evapotranspiration	

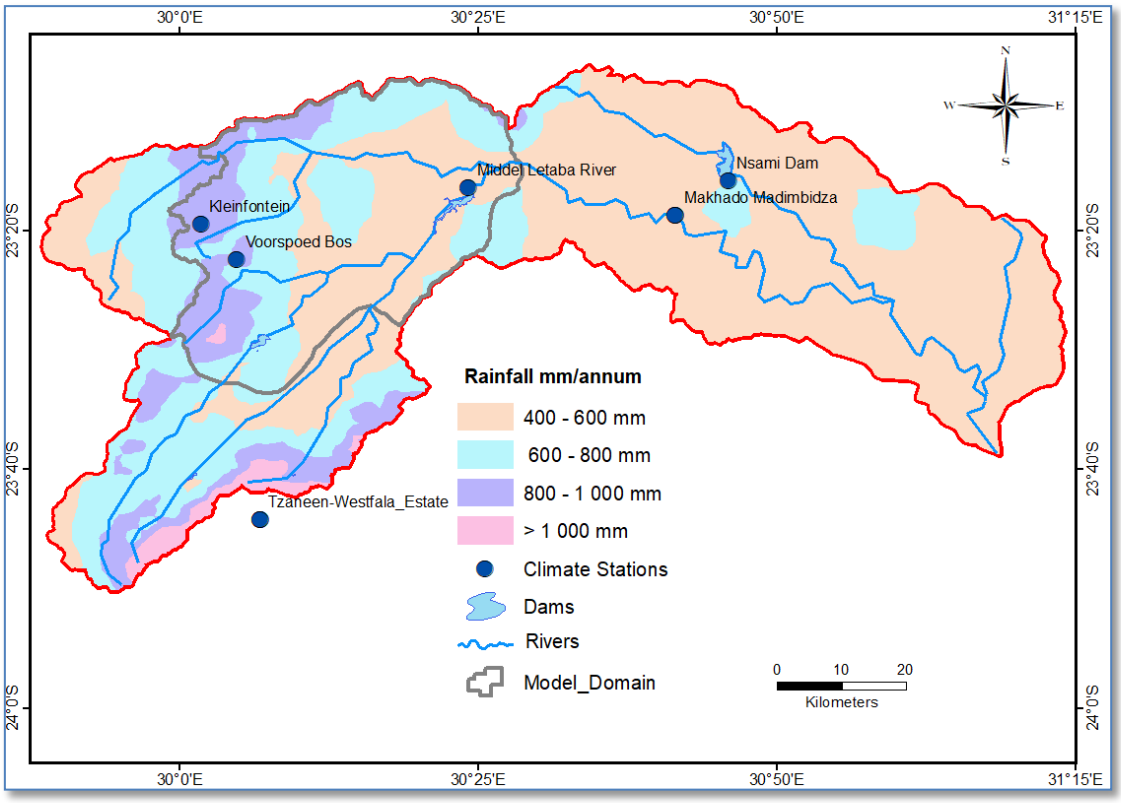

Figure 2-3: Location map of the meteorological stations where the mean annual rainfall was recorded.

2.3.2 Rainfall

Rainfall is the key driving force in most hydrogeological processes (Schulze, 1995), as well as the primary source of groundwater recharge and surface water bodies. Without rainfall, there can be no infiltration, evapotranspiration, surface runoff, baseflow or any other hydrologic process. The Lowveld region covers the largest portion of the study area, with average rainfall ranging between 400 and 600 mm per annum (Figure 2-3). The average monthly rainfall varies across different seasons (Table 2:3 and Figure 2-4) starting from Spring (October to November) with more rainfall occurring during Summer (December to February) and decreasing in Autumn (March and April). Less rainfall is received during the Winter (May, June, July, and August). The mean annual rainfall in the area climbed in November and December, with January being the wettest month of the year, with many stations receiving more than 100 mm per month. The rainfall then declines through March, April, and May. The months of June, July and August generally have low rainfall.

Table 2-3: Mean monthly rainfall.

	Highveld			Lowveld			
Months	**Tzaneen**	**Voorspoed**	**Kleinfontein**	**Middle Letaba**	**Nsami Dam**	**Madombidzha**	**MMR**
Oct	56	54	42	26	20	38	37
Nov	146	106	115	79	68	80	97
Dec	166	127	106	115	117	94	118
Jan	216	204	166	138	101	136	159
Feb	102	92	92	38	55	56	81
Mar	87	74	94	67	83	50	74
Apr	94	60	47	45	46	46	55
May	14	7	48	13	11	7	17
Jun	9	16	19	4	4	3	9
Jul	15	14	29	8	8	7	13
Aug	8	6	18	3	3	2	6
Sep	34	33	24	36	30	17	27
MAP	**947**	**793**	**800**	**572**	**546**	**536**	**693**
	847			**551**			

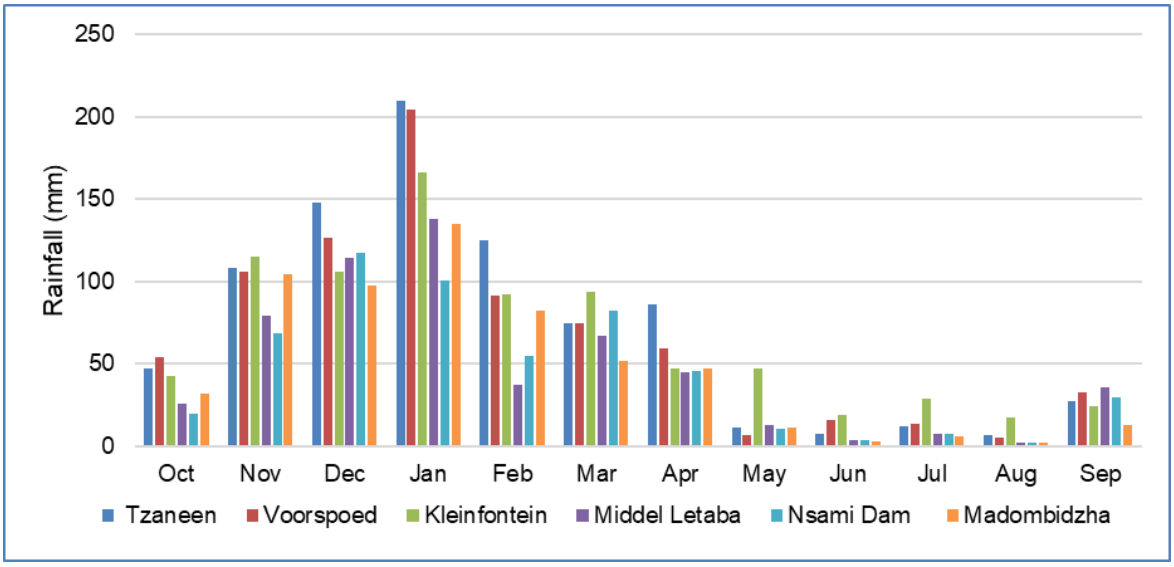

Figure 2-4: Mean monthly rainfall from 2007 to 2016.

2.3.3 Temperature

The study area is cold during June and July with the average monthly minimum and maximum temperatures of 6.8˚C to 23.8˚C, respectively. During the Summer, the temperature reaches a minimum and maximum of 14.1˚C and 29.0˚C, respectively in the highveld areas. The Lowveld summer months (September to March) temperatures range from a minimum of 13.8 ˚C to a maximum of 29.5 ˚C. The high temperature results in a very high rate of evapotranspiration. Table 2-4 presents the summary of the mean monthly minimum and maximum temperatures and is displayed in Figure 2-5.

Table 2-4: Mean monthly temperatures.

Highveld			Lowveld	
Months	Tzaneen		Madombidzha	
	Min	Max	Min	Max
Oct	14.05	27.82	15.22	29.29
Nov	15.75	27.98	16.38	28.92
Dec	17.62	28.75	18.03	29.43
Jan	18.31	28.72	18.19	28.98
Feb	18.12	29.02	18.12	29.45
Mar	16.86	28.53	16.89	29.01
Apr	14.06	25.94	13.77	26.63
May	10.75	25.25	9.94	25.82
Jun	8.02	23.58	6.97	23.84
Jul	7.60	22.85	6.76	22.88
Aug	9.02	25.46	8.94	25.57
Sep	11.82	27.89	12.46	28.66

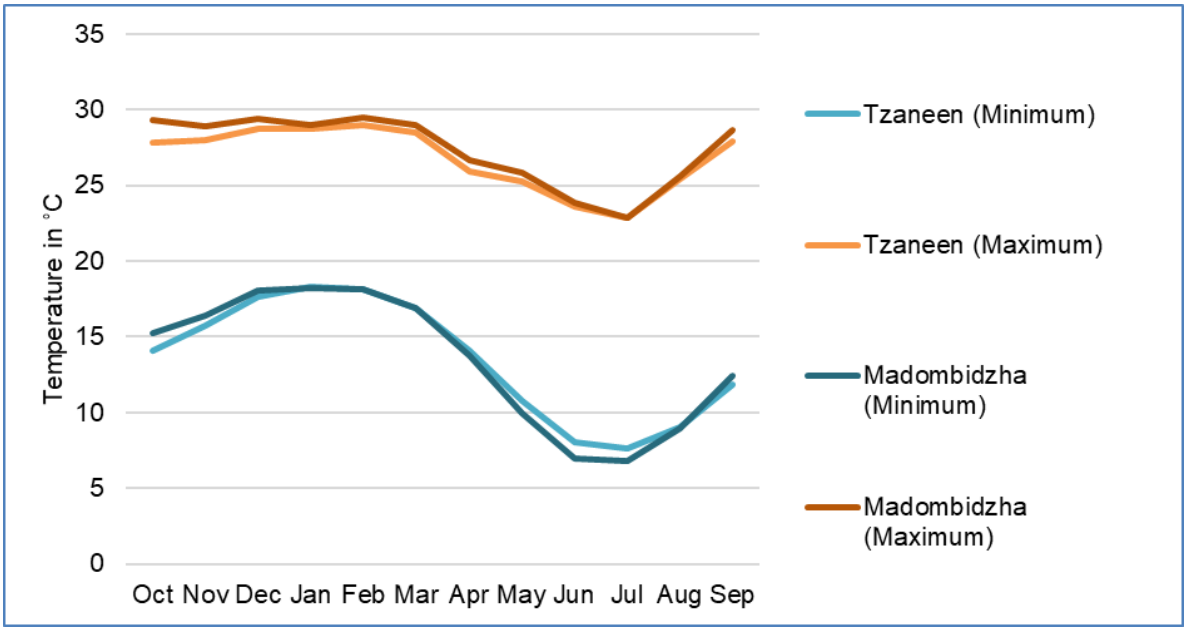

Figure 2-5: Mean monthly minimum and maximum temperatures.

2.3.4 Evapotranspiration

Evapotranspiration is the main process through which water is lost from a hydrologic system (Schulze, 1995). Allen *et al.* (1998) indicate that the rate of evapotranspiration, among other factors depends on the root depth, density, water availability, plant physiology, and the length of the pathway from adsorption in the roots to evaporation in the leaves. The evapotranspiration rate is expressed using two terms, namely, reference evapotranspiration (formerly known as potential evapotranspiration) and actual evapotranspiration (Allen *et al.*, 1998). The reference evapotranspiration (ET_0) was introduced by Penman (1956) to replace potential evapotranspiration (PET), and the concept of PET is no longer being used as ET0 has replaced it. ET_0 describes the atmosphere's evaporating ability at a certain place and time of the year and ignores the crop traits and soil conditions. It is defined as the evaporative demand of the atmosphere (De Silva, 1999). When there is an unlimited water supply, ET_0 happens, and actual evapotranspiration (ET_a) represents the amount of water evaporated from the soil. The Food and Agricultural Organisation (FAO56) describes the reference evapotranspiration (ET_0) based on parameters such as temperature, relative humidity, precipitation, and wind speed. ET_0 was estimated for each day of the month using the Penman-Montheith Method (Allen *et al.*, 1998) as outlined by the Food and Agricultural Organisation (FAO56).

Despite the fact that Summer (September to March) is the season with the most rainfall, the reference evapotranspiration (ET_0) values in the study area are often high due to high temperatures (Table 2-5). The actual evapotranspiration (ET_a) was calculated using the coefficient 0.75 that represents the bush and woodlands that largely cover the study area. Table 2-6 shows that ETa increases with rainfall and is hence higher during the Summer months compared to the Winter months.

Table 2-5: Mean monthly Reference Evapotranspiration (ET_0).

Months	Middle Letaba Dam	Nsami Dam	Madombidzha	Mean ET_0
Oct	110	130	122	121
Nov	118	125	111	118
Dec	118	122	123	121
Jan	124	119	117	120
Feb	119	114	113	115
Mar	123	124	114	120
Apr	93	95	86	95
May	80	84	80	81
Jun	77	77	59	71
Jul	74	75	92	80
Aug	89	78	85	84
Sep	114	116	109	113
Annual PET	**1240**	**1258**	**1211**	**1236**

Table 2-6: Mean monthly actual evapotranspiration (ETa).

Months	Middle Letaba Dam	Nsami Dam	Madombidzha	Mean ET_a
Oct	83	97	92	108
Nov	88	94	83	107
Dec	88	91	92	109
Jan	93	89	88	109
Feb	89	86	85	104
Mar	93	93	85	109
Apr	70	72	65	83
May	60	63	60	73
Jun	58	58	45	66
Jul	55	56	69	71
Aug	67	58	64	75
Sep	86	87	82	102
Annual ETa	**930**	**943**	**908**	**1116**

2.3.5 Runoff

Stormflow, base flow, and seepage all contribute to runoff, which is defined as the amount of water draining from a specific catchment (Schulze, 1995). It is an important constituent of the water budget that contains the extra precipitation that does not infiltrate and flows along the surface to rivers, lakes or the ocean.

Precipitation and watershed characteristics have a big impact on runoff. Precipitation characteristics include the intensity of the rainfall, duration, and frequency, while watershed features include terrain, geology, vegetation cover, and soil type (Tripathi and Singh, 1998). The mean annual runoff for all the Quaternary catchments within the study area was estimated and found to be ranging between 11.29 Mm^3/a and 28.20 Mm^3/a (DWA, 2015), resulting in a total of 164.47 Mm^3/a.

Due to the impact of long-term groundwater abstraction, the mean annual runoff was reduced to a total of 145.17 Mm^3/a with Quaternary catchments B82B and B82C being the most highly impacted (DWA, 2015).

Available data from the river gauging stations (B8H071, B8H033, and B8E008) indicate that runoff in the study area is extremely seasonal and varied, with intermittent flow in several of the streams and rivers. Most rivers only flow during the rainy season (December to April) or after high rainfall events. Runoff in the study area is largely influenced by the number of small dams and the high abstraction rate of water directly from the river in the catchment upstream of the Middle Letaba Dam.

2.4 Physiography

2.4.1 Land cover and use

The study area is dominated by rural settlements and is generally covered by natural grasses, with medium to high cultivated areas (Figure 2-6). Small-scale agriculture (livestock grazing and dryland cultivation of sweet potatoes, beans, maize, and sorghum) is also popular in the communities. According to Khwashaba (2018), the land is generally degraded in most parts of the settlement areas in the Mopani District Municipality. The degraded land is assumed to have caused by the interaction between the ecosystem and human activities through grazing, ploughing, and other agricultural practices.

Land degradation often diminishes the soil's ability to hold water, leading to an increased surface runoff where most of the water flows into the surface water bodies and, thus, reducing groundwater recharge (Döll and Florke, 2005). The occurrence of shrubs and trees are associated with the availability of deeper soil moisture for more extensive root systems.

Generally, the rock outcrop areas are only sparsely vegetated, with a greater abundance of shrubs and trees occurring along river channels and the edge of scree slopes surrounding mountains. There are numerous small-scale gold mines in the Greenstone belt areas in the Giyani and surrounding villages.

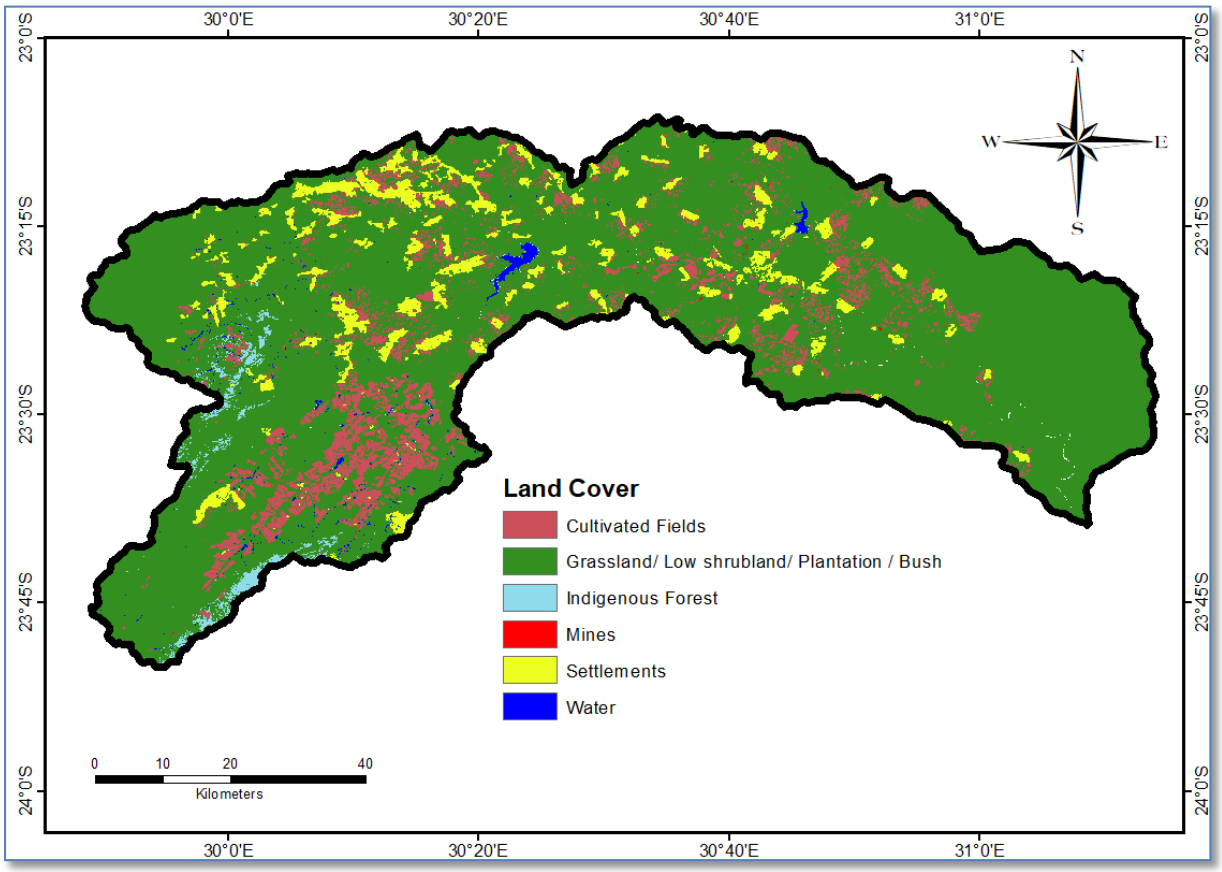

Figure 2-6: Land cover map of the Klein Letaba River catchment.

2.4.2 Soils

Soils in the study area were assessed to understand the hydraulic conductivity of different soil types (Figure 2-7). Hydraulic conductivity is an important hydrogeological parameter that together with other parameters controls the flow of water in the unsaturated zone and groundwater recharge. These soils are generally formed due to the long exposure to weathering and erosion of the igneous and metamorphic rocks that are found within the study area. The soils are generally shallow and rocky, overlying an impeding hard rock or weathered saprolite layer of the parent rock.

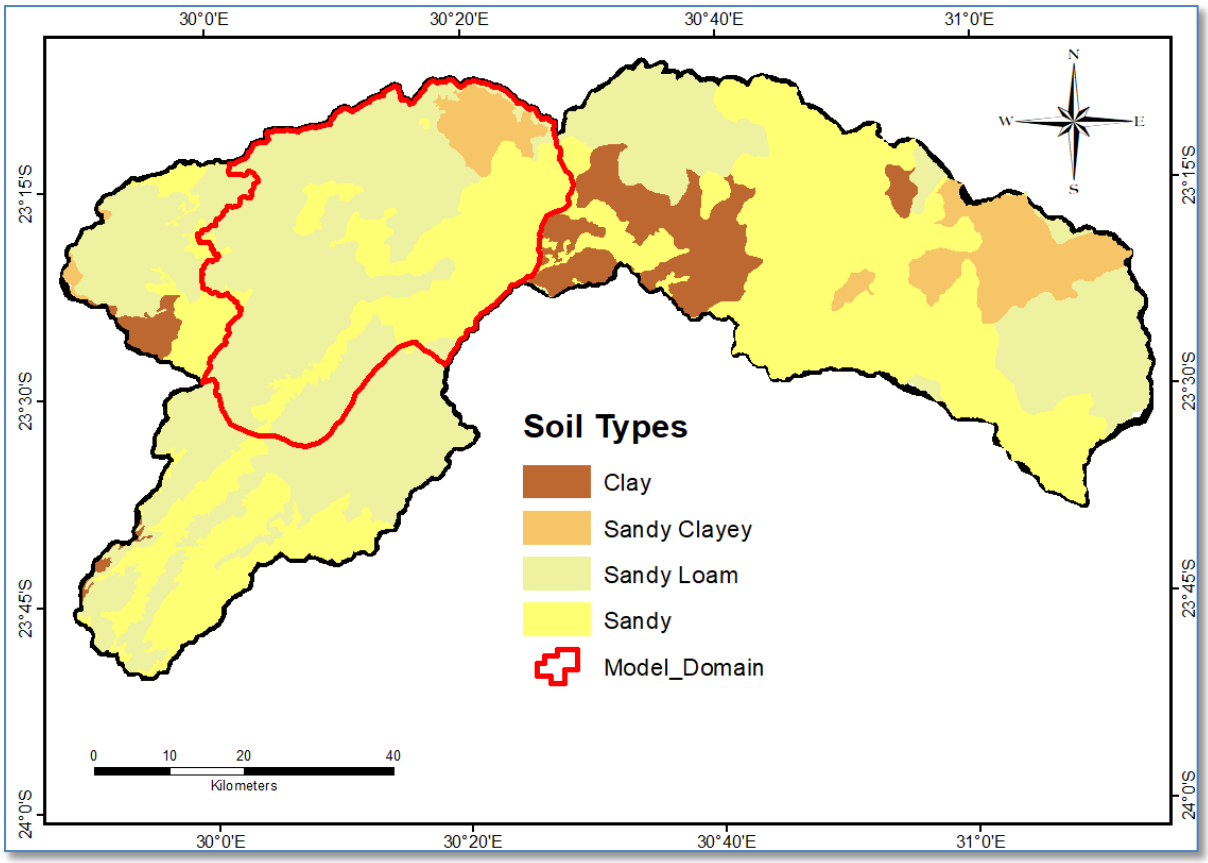

Figure 2-7: Soil cover map of Klein Letaba River catchment.

Soil type expresses the grain size distribution consisting of clay, silt, and sand content (Dippenaar *et al.,* 2010). Based on the regional soil data, the study area is characterised by soils with sandy to loam texture.

These soils are categorised as having high hydraulic conductivity that naturally allows water to percolate through them quickly. However, the presence of medium averaged clay content (0-30 %) in the soils may cause some moderate water holding capacity. A sporadic occurrence of slightly high average clay content (30 to 52 %) was noted in a few areas in the research area. Based on the field observations, soil derived from the Goudplaats Houtriver gneisses and granites forms light brown quartz-rich sandy soils, while soil derived from the greenstone belt rocks weather to form dark reddish-brown soils.

2.4.3 Vegetation

The study area is located within the Savanna Biome (Low and Rebelo, 1998). The Savana Biome grows in hot, seasonally dry climatic conditions and is characterised by rolling grassland scattered with shrubs and isolated trees (Smith, 1996). This vegetation type varies across the study area, from the Lowveld rugged mopaneveld occurring on uneven plains with significant steep hills and slopes to the cathedral mopane bushveld trees ranging between 10-15 m tall, often with some shrubs of approximately 2-3 m tall (Environomics, 2009). Lowveld rugged mopaneveld often consists of dense shrubland with sparse ground cover and occasional trees. Cultivation and other built-up areas have already modified about 20% of the land. As a result, vegetation occurring outside the protected areas is placed under strain due to the high density of rural human populations and agricultural activities.

The soils where this vegetation grows are generally porous, with rapid drainage. The climatic and soil conditions in this environment also create high evaporative demand, with the result that most savannas are in water deficit for a large part of the year, including the wet seasons (Scholes and Walker, 1993).

2.5 Water Resources

Water is supplied from surface and groundwater through several water schemes to many communities residing in the Greater Giyani and Greater Letaba local municipalities in the Mopani District, and Makhado and Collins Tshabane Local Municipalities in the Vhembe District Municipality. According to Mopani District Municipality (2020), the agricultural sector uses the greatest portion of the available water source estimated to be 70 %, leaving 30 % for the other water users. The Middle Letaba and Nsami Dams are the two main dams in the study area that supply water for irrigation and domestic water in Mopani and Vhembe District Municipalities (MDM, 2020).

2.6 Geological Setting

2.6.1 Regional Geology

The geology of the study area consists of the Archean basement rocks that make up the Kaapvaal Craton and Limpopo metamorphic Complex. These rocks constitute some of the oldest preserved material on the earth's surface and are characterised by the abundance of granites, gneisses, and greenstone belts. According to de Wit *et al.* (1992), the Kaapvaal craton grew through the process of initial extension of the continental lithosphere from the mantle, followed by the tectonic accretion of crustal fragments to produce distinct granite-greenstone subdomains. Accretion along the northern edge of the expanding craton is believed to have formed deformational structures within the basement lithologies that could subsequently impact the groundwater flow.

The northern part of the Kaapvaal craton underwent magmatic activities during early Neoarchean times, including during the emplacement of post-tectonic granitoids in the Pietersburg and Murchison areas (Poujol *et al*., 2003). Limpopo Mobile Belt (LMB) is made up of three primary crustal zones that run parallel to one another in an ENE orientation, separated by notable shear zones from adjacent cratons (van Reenen *et al*., 1992, Chinoda *et al*., 2009). The three zones are the Southern Marginal Zone (SMZ), the Central Zone (CZ), and the Northern Marginal Zone (NMZ).

The present research area is located within SMZ as indicated by the red circle in Figure 2-8. The SMZ is comprised of granite-greenstone cratonic rocks altered by a Neoarchean high-grade tectonic-metamorphic event (Belyanin *et al.,* 2012). To the south of the SMZ, the Hout River Shear Zone (HRSZ) separates granites and greenstone rocks of the Kaapvaal Craton from the high-grade granulite facies of the SMZ (Van Reenen *et al.,* 1990). Towards the north, the Northern Shear Zone separates the Zimbabwe Craton from the granulite rocks of the Northern Marginal Zone (Van Reenen *et al.,* 1990).

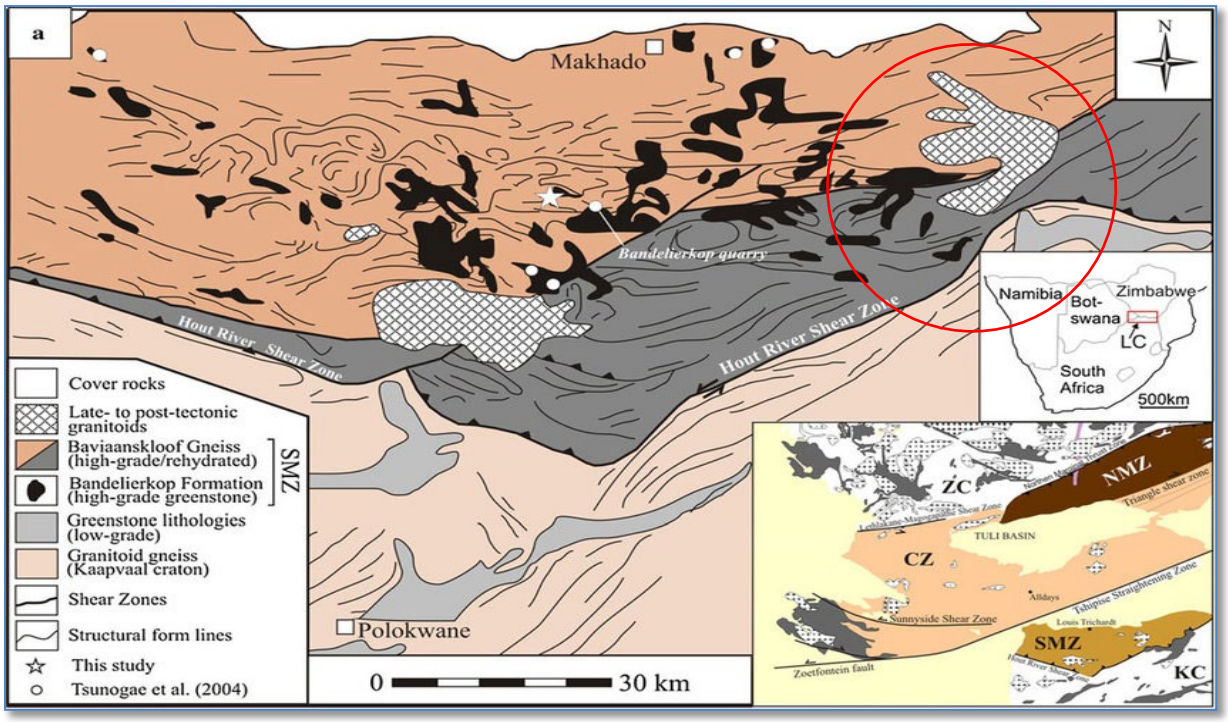

Figure 2-8: Generalised geological map of the Southern Marginal Zone of the Limpopo Complex (LC), Belyanin *et al*., (2012). The Klein Letaba River catchment falls within the red circled area.

2.6.2 Local Geology

The Archean Basement Rocks, which include gneisses, greenstone belts, and granitic intrusions, dominate the study area. The distribution of the rocks occurring in the study area is depicted in Figure 2-9. A summary of the geology of the study area is discussed below.

2.6.2.1 *Archean Gneisses*

The study area is underlain by Goudplaats-Hout River gneisses, comprised of a diverse range of granitoid gneisses of various types and compositions. The gneissic bodies vary from homogeneous to weakly stratified, from light grey to dark grey, and from medium-grained to pegmatoidal varieties (Brandl, 1987; Anhaeusser, 1992; Brandl and Kröner, 1993). Generally, these gneisses typically form flat surfaces with very poor exposures, mainly exposed in river beds and eroded stream gullies, where outcrop is typically weathered. The gneisses are light to dark grey when fresh and typically light yellow when weathered forming yellow to white sandy soil. Due to its ability to weather extensively, this rock creates a conducive environment for an aquifer to have a high hydraulic conductivity (Morrice *et al*., 1997).

Groundwater accumulates in the unconsolidated weathered material and seeps into fractures in the bedrock (Taylor and Howard, 1999).

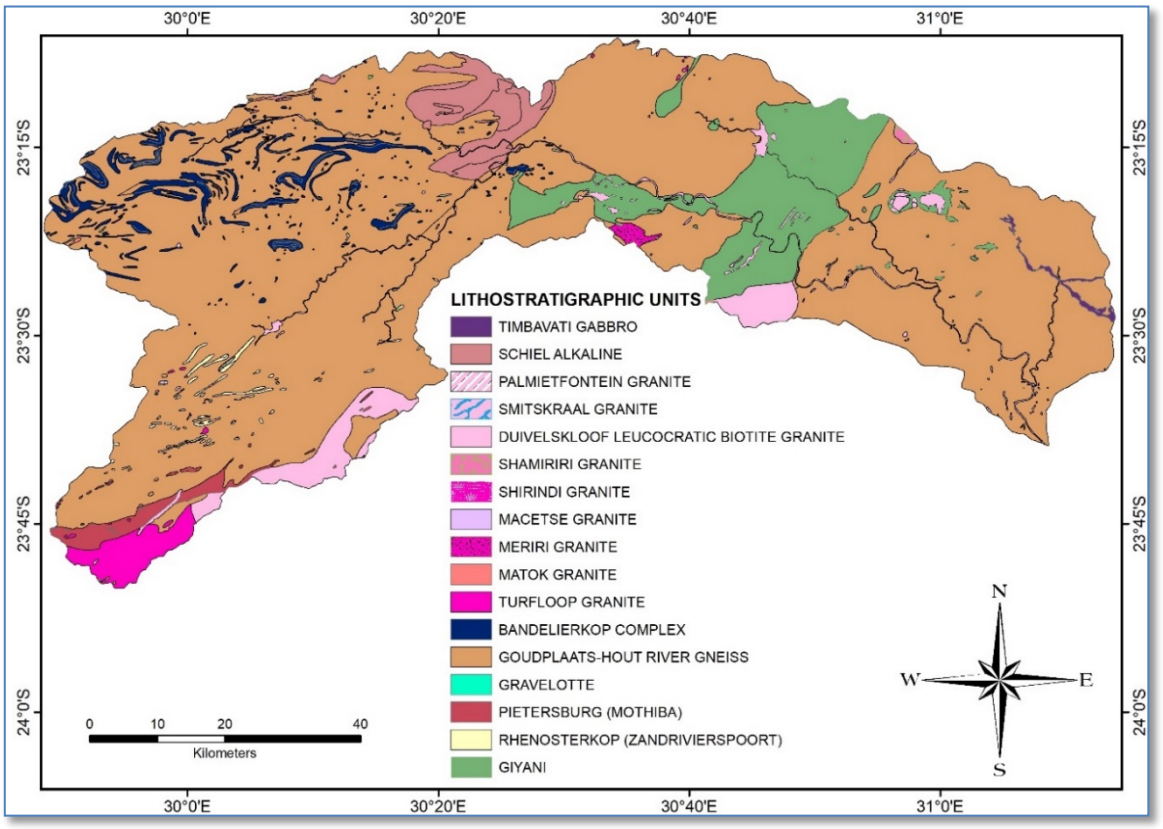

Figure 2-9: Regional-scale geological map of the study area (Data Source: Council for Geoscience).

2.6.2.2 *Archean Greenstone Belt*

The Greenstone Belts are known to represent the oldest volcano-sedimentary sequences preserved on the earth's crust (Madisha, 1996). Their origin, spatial and temporal relationships are still being debated (Brandl *et al.,* 2006). However, the available information based on Robb *et al.,* (2006), indicates that these rock units are of Paleo to Mesoarchean age (approximately 3 200 Ma). They consist mainly of extrusive mafic and, to a limited extent, ultramafic and felsic rocks. There are also occurrences of iron formation, felsic schists, and metasediments, though generally rare (SACS, 1980).

The Greenstone Belts in the study area are the Pietersburg (Mothiba Formation), Rhenosterkop, Giyani, and Murchison (Gravelotte) Groups. These rocks are generally fine-grained, porous and may have high transmissivity rate as well as specific storage capacity (Barrat, 2018) due to the presence of the bedding planes, foliations, and fractures associated with the contact zones between different lithologies, faults, and shear zones.

2.6.2.3 Granite Intrusions

The study area has eleven different types of granitic rocks. The younger unfoliated granite intrusions occur in the form of batholiths and plutons. These granitic intrusions create distinguished topographic highs that are visible in different localities within the study area. These types of rocks have high silica content (53 to 65%), creating a very hard rock composite (Monroe *et al*., 2007). Fractures within these rock types cause groundwater to be under pressure and may contain high hydraulic conductivity (Buchanan *et al*., 1999).

2.7 Structural Settings

2.7.1 Regional Structures

The study area is part of the Limpopo Metamorphic Complex's (LMC) Southern Marginal Zone, which is poly-metamorphic and highly deformed terrain that is part of the Archean crust that separates the Kaapvaal craton in the south from the Zimbabwean craton to the north (Figure 2-10). According to Smit *et al.,* (1992), the SMZ went through four stages of deformation, which formed significant structural fabrics with NE-SW orientation and Neoarchean granite intrusions of different ages.

- The initial D_1 event formed the crustal wedges, foliation, and isoclinal folds within the granite-greenstone rocks leading to the formation of the north-dipping regional schistosity and a sequence of ENE-WSW and E-W trending, north-dipping oblique to reversely rotated shear zones,

- D_2 event is related to the creation of significant shear zones separating the three LMB terranes. This event formed the HRSZ lineament along the southern limit of the SMZ,
- D_3 event is associated with the intrusion of regionally extensive biotite granites attributed to the last stages of the Limpopo Orogeny, a period of regional extension following the amalgamation between the Kaapvaal and Zimbabwe cratons. This event formed the shear zones within the LMB terranes, resulting in multiple shear zones such as Annaskraal, Petronella, and Matok Shear Zones, and
- D_4 event resulted in the re-activation of the pre-existing shear zones in a strike-slip movement which is discordant with the older shear zones and other structures within the SMZ.

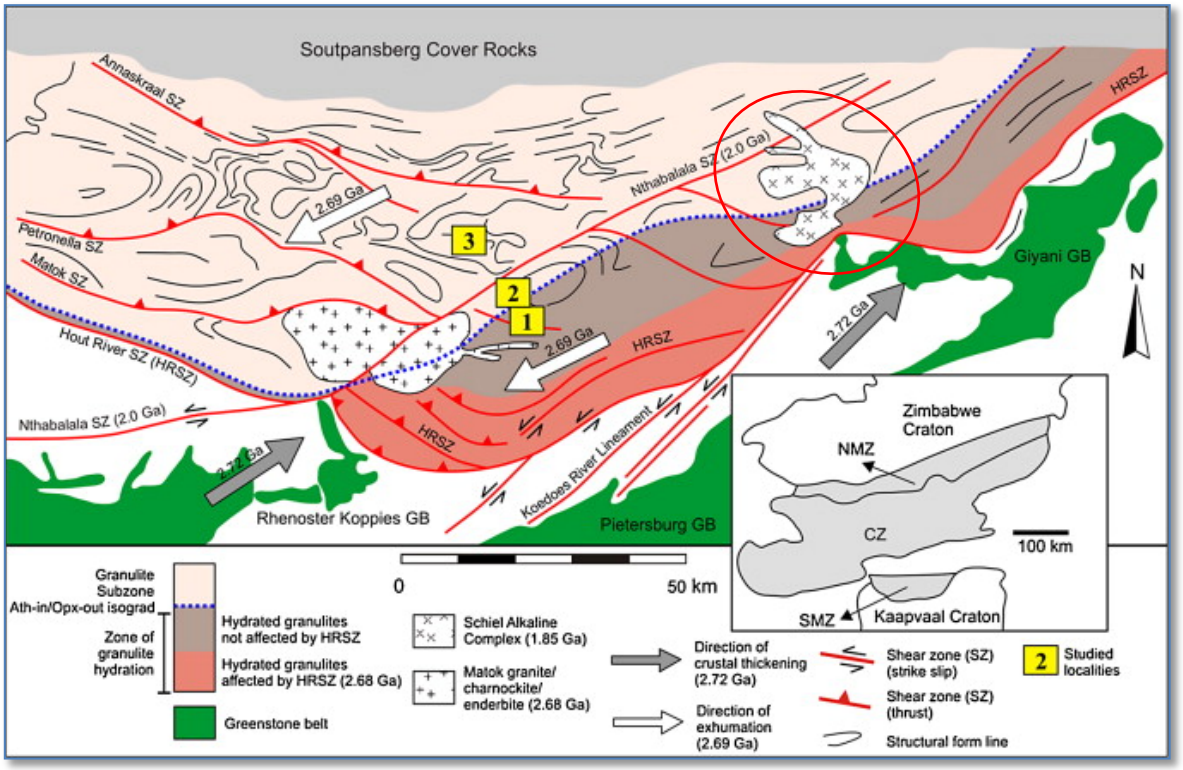

Figure 2-10: Regional geological structures (after Dubinina *et al.*, 2015). The study area is circled in red.

Dubinina *et al.,* (2015), further established metamorphic isograd increasing from north to south across the Greenstone belt (Figure 2-10). This variation trend of metamorphic

grade is possibly believed to be attributed to the HRSZ passing through the Giyani greenstone belt. This is best exposed along with the northern contact of the Giyani Greenstone Belt, and the contact of the HRSZ (McCourt and van Reenen, 1992).

2.7.2 Local Structures

Regional airborne magnetic data and medium-resolution Advanced Spaceborne Thermal Emission and Reflectance Radiometer (ASTER) mission from the Council for Geoscience and the Department of Water and Sanitation, respectively were employed to synthesise geological structures of the study area.

2.7.2.1 Aeromagnetic Data Interpretation

The total magnetic intensity map of the study area (Figure 2-11) is based on the regional airborne magnetic data, generated and processed by the Council for Geoscience (CGS). According to Magaia (2009), the processing of aeromagnetic data involves the removal of diurnal variations and corrections for the IGRF model of the Earth in the data set. This also included leveling and interpolation of the line data to study the effect of height differences on the recorded magnetic field.

The aeromagnetic data received from CGS was plotted on ArcGIS to study the magnetic intensity of the rocks in the study area. The magnetic intensity of the area ranges from -153.9 nT to 374.3 nT. Most of the linear high magnetic anomalies are the expression of the outline of NE-SW trending dolerite dykes and related rocks. Areas of low magnetic intensity (-153.9 nT) indicate weakly magnetised felsic rocks, dykes with high remnant magnetism, felsic dykes such as pegmatites, and mafic dykes with low magnetic susceptibility.

2.7.2.2 ASTER Lineament data Interpretation

ASTER data is good for lineament analysis because of their substantial spectral resolution, high spatial resolution, ability to derive DEMs, and affordable prices of acquiring the satellite imagery (Sander, 2007). The mapping and interpretation of lineaments is conducted by geological remote sensing consultants on behalf of the DWA Limpopo regional office (Holland, 2011). The processed ASTER DEM consisting of an enhanced image, normalized difference vegetation index (NDVI) image, and hill-shaded relief image were visually interpreted using ArcGIS to extract lineaments

through on-screen digitizing (Mkali, 2020). The extracted lineaments were used to generate lineament density, lineament intersection map and rose diagram (Figure 2-12). The lineament / fracture analyses indicated that the area has numerous long and short fractures whose structural trends are mainly in the north-east direction.

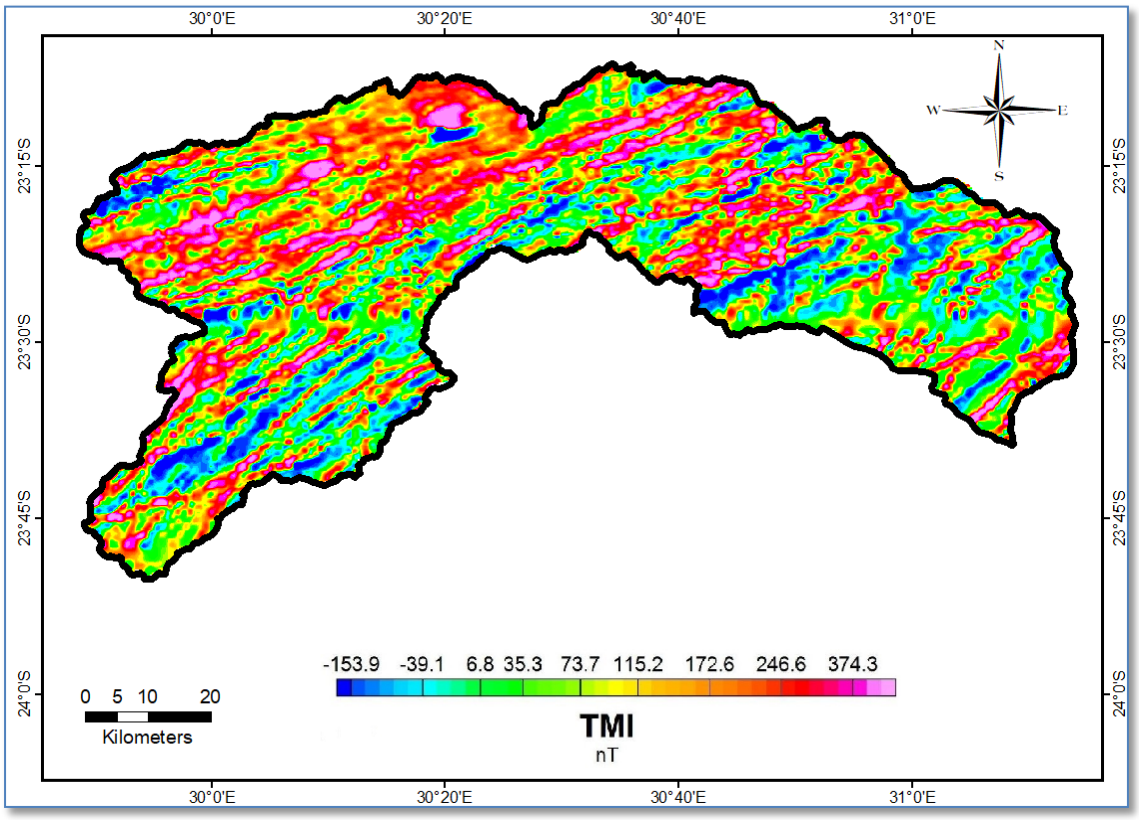

Figure 2-11: Map showing electromagnetic data of the study area.

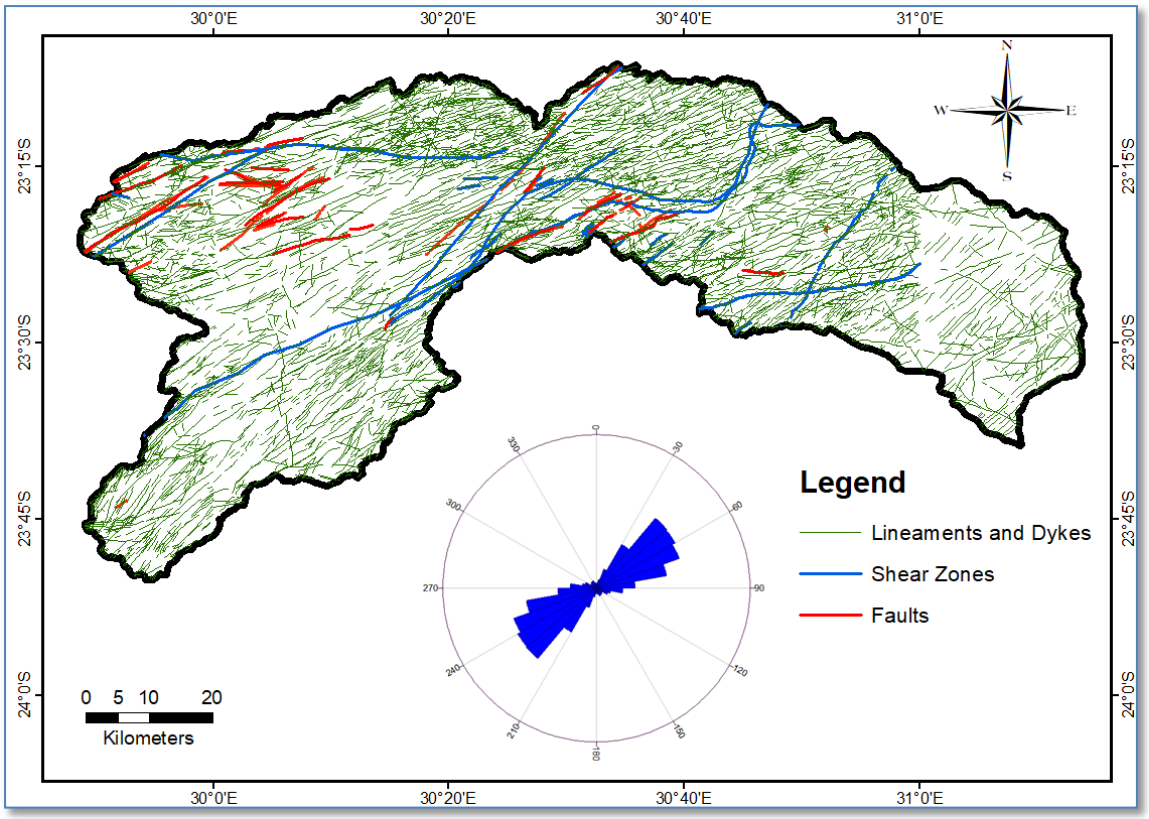

Figure 2-12: Map showing the distribution of geological structures and rose diagram.

2.7.2.2.1 Dykes

The dykes occur in the form of swarms with the dominant trend towards the NE-SW direction. The frequency and orientation of dykes in the study area form distinctive structural features. The largely NE-trending dykes and associated aeromagnetic lineaments have the same age and orientation as the 2 700 Ma Ventersdorp rift structures, but also feature similar NE-trending Karoo-age dolerite dykes (Uken and Watkeys, 1997). During this time, the northeastern Kaapvaal Craton expanded from NW-SE such that zones of weakness were created perpendicular to this orientation, allowing dykes emplacement (Stettler *et al.,* 1989).

The dolerite dykes are fundamentally important in limiting groundwater flow by acting as barriers to groundwater flows or accumulating groundwater along their strike. Based on the current neotectonic stress-strain regime (NE-SW tension and NW-SE compression), the youngest dolerite dykes in the study area are generally closed (not fractured) and known to have poor groundwater potential (Witthüser *et al*., 2011). Figure 2-13 (A and B) display dolerite dykes cutting across the gneisses.

Figure 2-13: (A and B) Dolerite dykes cutting across the Gneisses.

2.7.2.2.2 Faults, Joints, Lineaments, and Shear Zones

The study area is characterised by a series of discrete shear zones, faults, lineaments (that include the Hout River Shear Zone, Pietersburg Lwaji Shear Zone, Annaskraal Shear Zone, N'tabalala Shear Zone, Soutpansberg Faults and Kudoes River Lineament) (Figure 2-12 and Figure 2-14).

These geological structures were formed from multiple deformational events that have affected the SMZ and are believed to be open under the current neo-tectonic stress regime (Witthüser *et al*., 2011). The interconnectivity and periodicity of these structures influence groundwater flow. Numerous fault zones and joints are occurring along major regional shear zones. Due to the NE-SW trending neotectonic tension, Bird *et al.,* (2006), suggest that the NW-SE striking joints (fractures) are open and assumed to be favorable for groundwater flow.

Based on field observations and information obtained from borehole logs, some of the mapped lineaments are related to the lithological contacts, quartz and pegmatite veins, fractures, faults, and shear zones. It is evident that many rivers tend to follow regional geological structures (that are Kudoes River Lineament, Hout River Shear Zones, Annaskraal Shear zones, and other fault zones in the area). Figure 2-14 (A-F) shows the occurrence of fracturing and jointing.

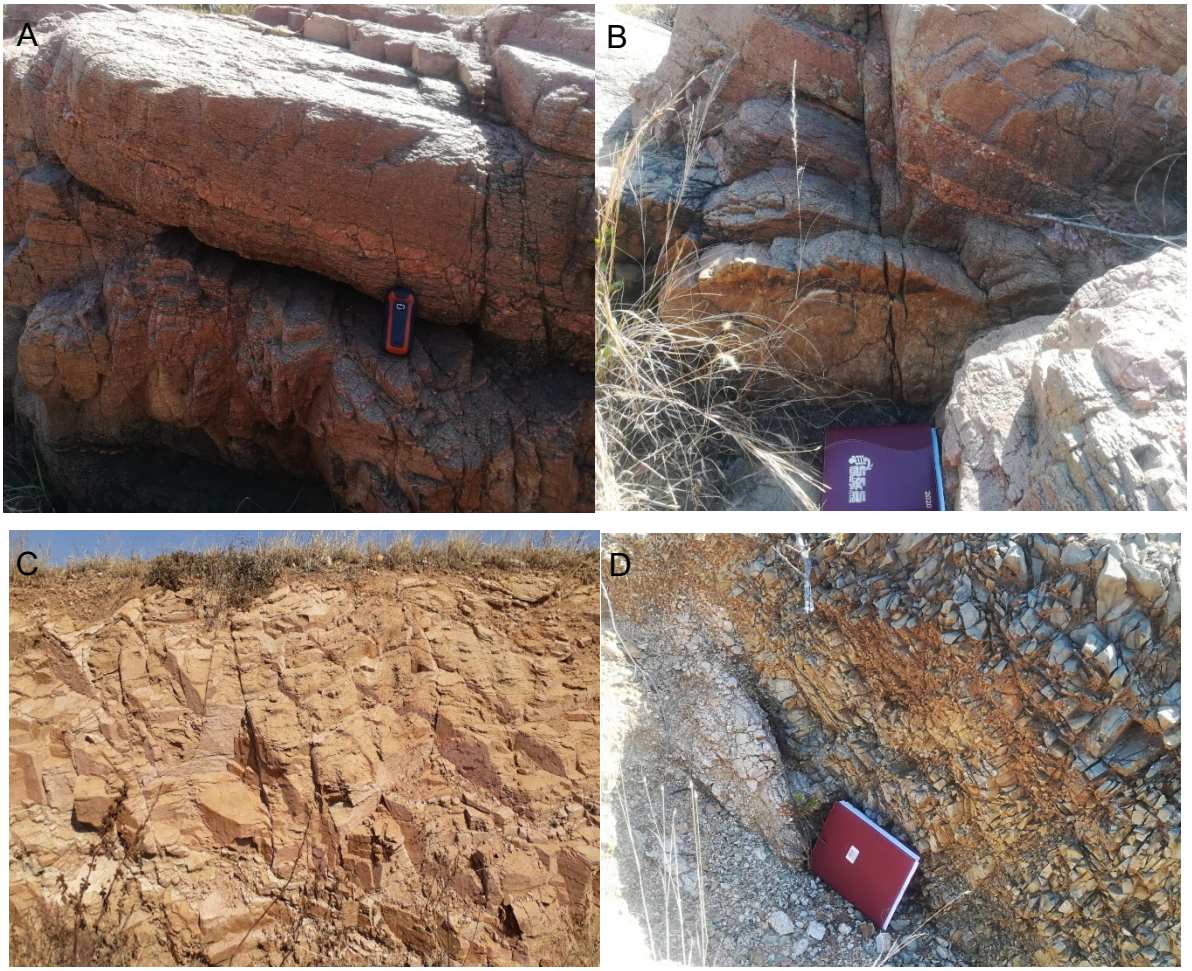

Figure 2-14: (A-D) Faulted, jointed, foliated and weathered gneisses and dolerite dykes in the study area.

2.8 Hydrogeological Settings

The tectonic evolution of the study area has contributed to the formation of major geological structures that are favourable for the development of composite aquifers of weathered and underlying fractured layers. According to Holland (2011), weathering depth in the lowveld region rarely exceeds 30m but increases to 45m further east with the borehole yields decreasing away from the escarpments. A series of shear zones created a network of fracture systems, increasing the permeability of the country rocks and, thus, increasing borehole productivity. Intrusions of the younger granites have also created fractures along with the contact with the host rocks, therefore increasing the water-bearing properties (Vegter, 2003).

2.8.1 Aquifer Systems

The aquifers in this area are mostly semi-confined to confined (Du Toit, 2001). The unconsolidated weathered zone is described as moderately permeable, whereas the consolidated fractured bedrock is considered a fractured porous media with regional groundwater flow occurring within the major interconnected fractured systems (Holland, 2011). A thin saprolite layer with minor water strikes overlies the major water-bearing fractured aquifer in the weathered zone (Holland, 2011). Based on lithological information obtained from borehole logs, the area between the lower boundary of the weathered zone and the higher boundary of the fractured zone has proven to have the highest permeability and storage capacity resulting in high groundwater yields.

According to Du Toit and van Lelyveld (2006), aquifer systems in the study area are categorised into four modes of groundwater occurrence with borehole yields ranging from <0.1 to > 5 l/s:

- Aquifers associated with alluvial deposits, occurring along river channels and consisting mainly of sand and gravel,
- Shallow highly weathered (regolith) and unconfined aquifer, consisting of a prolonged in situ chemically and mechanically weathered profile. These types of aquifers are associated with in situ bedrocks such as weathered granite and gneisses,
- Highly fractured (semi-confined/confined) aquifer, consisting of fractures with variable orientations. These aquifers correspond to highly fractured volcanic and intrusive rocks of Greenstone Belts and the surrounding granite gneisses, and
- Deep less fractured (fresh) confined aquifer, believed to be associated with the regional geological structures that are entirely tectonic in origin.

Nel *et al*., (2014) indicated that the fractured and intergranular aquifers exhibit transmissivity values ranging from 0.5 m^2/day to 150 m^2/day. The transmissivity of different rock types occurring in the study area was investigated by Holland (2011), and the following transmissivity values were documented:

- Schiel Complex with the highest transmissivity of 42 m^2/day,
- Greenstone Belt with a moderately high transmissivity of 37 m^2/day,
- Goudplaats Gneiss with moderate transmissivity of 24 m^2/day,and
- Bandelierkop complex with the lowest transmissivity value of 16 m^2/day.

Based on the transmissivity classification (Table 2-7) of Krasny (1992), the values that were obtained from the four lithological units occurring in the study area are categorised as intermediate, suggesting that groundwater in the study area is suitable for local and small community supplies. The values further show that groundwater resource in this region would be developed and used sustainably if boreholes were to be abstracted as per specified yield recommendations by the qualified hydrogeologists based on the proper aquifer test results supported by a proper monitoring and management plan.

Du Toit and Van Lelyveld (2006) adopted the classification of the aquifer system from UNESCO (1983) hydrogeological maps to suit the hydrogeological circumstances and groundwater occurrences of South Africa (Mukheli, 2018). This classification simply differentiates the occurrence of groundwater based on whether the interstices are primary or secondary.

Table 2-7 Classification of aquifer transmissivity (after Krasny, 1992).

Transmissivity Values (m^2/day)	**Classification of Transmissivity Magnitude**	**Groundwater Abstraction Potential**
> 1000	Very High	Abstraction of regional scale
100 -1000	High	Abstraction of sub regional scale
10-100	Intermediate	Abstraction for local scale (small communities)
1-10	Low	Minimal abstractions for domestic purposes
<1	Very low	Minor abstraction

Following Orpen (1994) approach, the borehole yields are classified into five (5) categories as noted below:

- High yielding: > 5 l/s; suitable for water delivery in cities and rural areas, industries, or large-scale irrigation,

- Moderately high yielding: 2-5 l/s; suitable for urban and rural water supply, to small towns, industry, or small-scale irrigation,
- Moderately low yielding: 0.5-2 l/s; suitable for residential and livestock watering supply to rural settlements, hospitals, and health facilities, as well as small-scale irrigation in community vegetable gardens,
- Low yielding: 0.1-0.5 l/s; recommended used for single-family households, private and government institutions (250 persons), or livestock drinking. Hand, submersible, or windpumps are commonly used in this set of boreholes, and
- Very low yielding: 0.0-0.1 l/s; ideal for domestic supply to small single homesteads. Suitable for hand pump installations only.

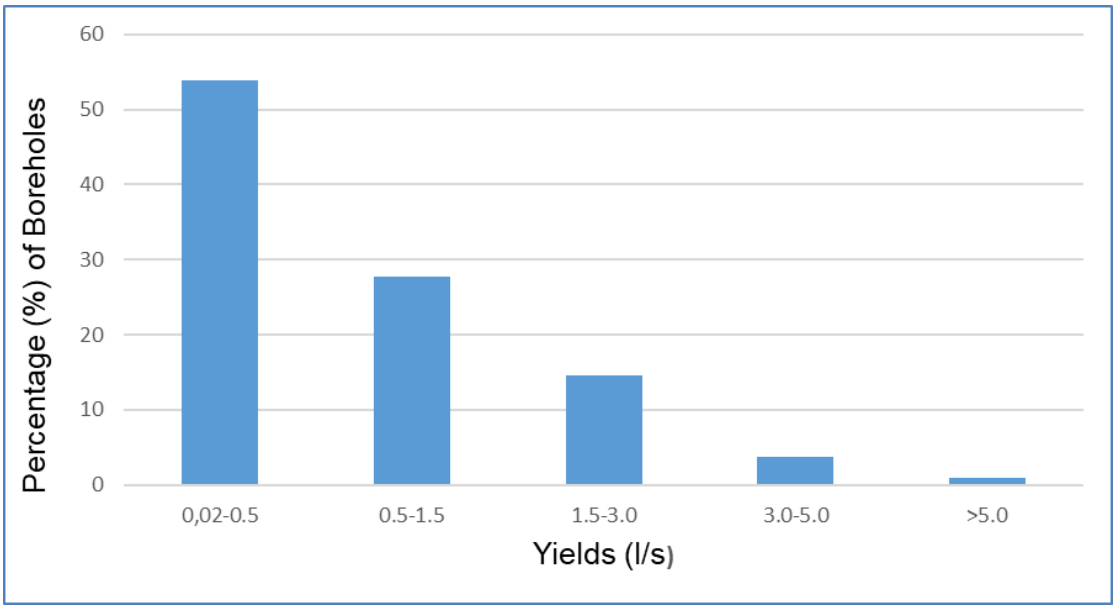

Figure 2-15: Distribution of borehole yields in the study area.

Based on the total number of 891 borehole yields records (determined from aquifer pumping test) from GRIP database, the study area is generally characterised by low (varying between 0.02 to 0.5 l/s) to moderately low (varying between 0.5 to 1.5 l/s) yielding boreholes (Figure 2-15). About 53% of the boreholes in the study area are classified as low-yielding while 28% are considered moderate. Boreholes that are suitable for small-scale urban and rural water supply account for only 14.6 % with only 1% of the boreholes suitable for large-scale urban and rural water supply. The borehole yields are highly variable within a short distance, even within the same rock type.

CHAPTER 3 : LITERATURE REVIEW

3.1 Introduction

The literature study is important as it enables us to identify a knowledge gap where there is a need to address key problems related to groundwater. A review of prior studies that are relevant to the present research study is presented. These include the following aspects;

- hydrogeological characteristics and aquifer types within the study area,
- hydrochemical characteristics,
- impact of climate change on groundwater resources,
- impacts of anthropogenic factors, and
- groundwater recharge.

3.2 Hydrogeological characteristics of the crystalline basement aquifers

Aquifer characterisation forms a fundamental aspect in terms of establishing a conceptual understanding of the hydrogeological systems and it defines the important geological, structural, chemical and hydraulic parameters that control the occurrence of groundwater (Tessema *et al.,* 2014). Furthermore, aquifer characterisation provides a foundation for groundwater flow modelling to assess the groundwater resource.

Numerous studies have been conducted on hydrogeological characteristics of the crystalline basement rock aquifers in different climatic settings (Dewandel *et al*., 2006 and 2011; Holland., 2011; Lachassagne *et al*., 2011, 2014b and 2021; Tessema *et al*., 2014; Witthüser *et al*., 2011). Most of these studies focused on understanding the aquifer parameters and providing knowledge on the geological structures that control the occurrence and movement of groundwater to ensure efficient exploration and sustainable development of groundwater resources. The current study intended to use a combination of the hydrogeological characterisation and modelling approach to understand the groundwater flow dynamics and quantify the impacts of climate change and anthropogenic factors to assess the extent of vulnerability on groundwater resources.

To determine the hydrogeological characteristics that control the groundwater flow in the crystalline basement aquifers, Dewandel *et al.,* 2006 and 2011; Holland 2011; Lachassagne *et al.,* 2011, 2014b and 2021; Marechal *et. al.,* 2004;) developed the general conceptual model of the crystalline rock aquifer which occurs in Africa, India, North and South America, Australia and Europe. Their findings indicate that the hydraulic conductivity of these aquifers depends on secondary fracture permeability and weathering processes.

Hydraulic conductivity values (Table 3-1) of geological materials vary significantly (Davis, 1969; Freeze and Cherry, 1979 and Fitts, 2002). This is mainly due to the differences in aquifer thickness, the influence of the clay material and fracture connectivity, among many other variables. Weathered aquifers of igneous and metamorphic rocks are generally characterised by the presence of sandy-clay materials which tend to influence the hydraulic conductivity of these rocks (Dewandel *et al*., 2006).

Table 3-1: General representative of the hydraulic conductivity values for different geological materials.

Geological material and locations	**Hydraulic conductivity (m^2/s)**	**Source**
Gravel	10^{-1} to 100	Fitts, 2002
Silty Sand	10^{-5} to 10^{-1}	
Silt	10^{-7} to 10^{-3}	
Weathered Granites, Uganda	$5x10^{-7}$ to $8x10^{-6}$	Taylor and Howard (2000)
Fractured Granites, Uganda	$3x10^{-7}$ to $4x10^{-5}$	
Weathered Igneous and Metamorphic rocks, Africa	$2x10^{-7}$ to $4x10^{-5}$	Wright (1992)
Weathered Igneous and metamorphic rocks, Africa	up to 10^{-6}	Jones (1985)
Fractured igneous and metamorphic rocks, Africa	up to 10^{-4}	
Weathered Igneous and Metamorphic rocks, Malawi	$9x10^{-7}$ to $8x10^{-6}$	McFarlane (1992)
Fractured Granite Victoria Province	$3x10^{-6}$	Houston and Lewis (1988)

In similar rock types, the hydraulic conductivity of the fractured aquifers is mainly controlled by the interconnectedness and frequency of the fractures. The representative hydraulic conductivities values for various unconsolidated and consolidated geological materials which are similar to those occurring in the research area are shown in Table 3-1. Hydraulic conductivities of the weathered and fractured aquifers generally range between 10^{-7} m/s to 10^{-6} m/s and 10^{-6} m/s to 10^{-4} m/s, respectively.

On a global scale, constraints in sustainable development and management of crystalline basement aquifers for water supply include the frequent high failure rate (i.e. 10-40%) of boreholes yields, low storage capacity and low recharge rates (Wright and Burgess, 1992). The study conducted by Vassolo *et al.*, 2019 indicated that weathering of the basement rocks forms the composite aquifer which is underlain by a fractured aquifer, and overlaid by a shallow saprolite aquifer. Similarly, Yidana *et al.* 2013 conceptualised the spatial distribution of key hydraulic parameters of the crystalline aquifer in southwestern Ghana to provide the basis for characterising the hydrogeology of the area for the large-scale development of groundwater resources. The results from the study show that aquifer heterogeneities, coupled possibly with topographical trends, have resulted in the development of five prominent groundwater flow paths in the area (Yidana *et al.* 2013). The methodologies and materials applied in the studies outlined in this section for hydrogeological characterisation are similar to the current study.

A study conducted by Witthüser *et al.*, 2011 in the Limpopo plateau indicated that hydrogeological characteristics of the weathered zone are characterised by low primary porosity and groundwater movement and storage mainly occur in fractures, faults, weathered zones and other secondary features that enhance the aquifer potential. Holland (2011) determined the hydraulic conductivities of different lithological units of the crystalline basement rock aquifers covering a large area of 63500 km^2 (Limpopo Plateau and Letaba Lowveld regions) which included the current study area. The findings of the study by Holland (2011) were used in the current research study.

Ebrahim *et al.,* 2019 used an integrated hydrogeological modelling approach to understand the recharge and groundwater flow processes to inform water use and management in the Hout River Catchment, Limpopo Province. The results indicated that groundwater resource relied on low, highly variable recharge and storage making the the groundwater resource systems more vulnerable to climate and anthropogenic factors. The hydrogeological characterisation and modelling approach are significant for understanding spatio-temporal variability in key parameters required for managing the groundwater resource sustainably (Ebrahim *et al.,* 2019). The previous local studies provided the basis for the hydrogeological characterisation of the impact of climate and anthropogenic factors to be undertaken in the current study.

3.4 Impacts of Climate Change

Climate change refers to long-term shifts in regional or global climatic conditions which is partly caused by the atmospheric composition of carbon dioxide and other greenhouse gases, according to the Intergovernmental Panel on Climate Change (IPCC, 2007). Since 1800, human activities have been the main driver of climate change, primarily due to the burning of fossil fuels like coal, oil and gas (United Nations, 2023). In South Africa, carbon content in the atmosphere places the country as the number 12 contributor to worldwide CO_2 emissions (EDF, 2015).

The country is often referred to as the 30th driest country in the world (DWA, 2013), based on its average annual rainfall of 500 mm compared to the global average annual rainfall of 860 mm (Botai *et al*., 2018). It is located in a region with increasing levels of water scarcity and water quality challenges, aggravated by population increase and issues of social and economic development (Dennis and Dennis, 2011).

According to Kusangaya et al., (2014), the country is likely to experience a decrease in rainfall intensity and most likely, it will experience longer spells of dry periods due to climate change. These extreme climatic events are causing devastating impacts on the limited water resource in rivers and dams which are strongly dependent on rainfall which varies significantly from season to season.

The Limpopo Province is highly prone to the effects of climate change. In this province, many rural communities mainly rely on water for food production, mining and other related economic development sectors.

Rainfall is highly variable and characterised by slightly normal to below-average rainfall patterns. The SAWS (2023) recorded eleven (11) drought periods between 1921 and 2023 with six (6) of these recorded within the last 3 decades (1989 to 2023) (Figure 3-1). The latter drought periods were recorded in 1992, 1994, 2002, 2003, 2005 and 2015. Within a similar period, only three wet seasons were reported and the events occurred during 1996, 2000 and 2021. According to Reason and Keibel (2004), 25% of the rainfall received during the year 2000 resulted from natural climatic cycles (i.e. tropical cyclone Eline). This cyclone made the year 2000 the wettest year on record in Southern Africa since 1976 (Reason and Keilbel, 2004).

The study conducted by Maponya (2013) revealed that Limpopo Province is amongst the worst regions affected by drought in recent years, which resulted in a drastic decline in dam levels to 50% as compared to 84% full in the 1980s. The irrigation schemes and many of the unemployed local people rely on the limited surface water resources (i.e., dams and rivers) for crop production and fishing to support their families and for the supply to the markets.

The analytical results of the locally downscaled climate for the Mopani area suggest a clear warming trend that will become more severe by 2050 if global mitigation measures fail (Brodrick *et al.*, 2014). The annual maximum temperature is expected to rise by 1 to 3°C, while the minimum temperature will rise by 2°C. Rainfall changes are temporal and spatial in variability, and projections are less clear. The long-term future is expected to be drier towards the northern part of the district than in the south. Khwashaba (2018) projected an increase of 50 to 100 mm of rainfall in some areas of the Mopani District.

Tshiala and Olwoch (2010) determined the effects of climate change on tomato production in the Limpopo Province, with the results indicating a negative correlation between temperature and tomato production. Tomato is one of the many agricultural products that contribute significantly to the local economy. The expected problems of water supply in the Mopani District will affect the agricultural sector which is the main contributor not only to the local but to the provincial economy. Planners and decision-makers must evaluate the potential consequences of climate change on the water resources and develop policies to maintain the long-term viability of water supplies; thus, food security (Mukheibir, 2007).

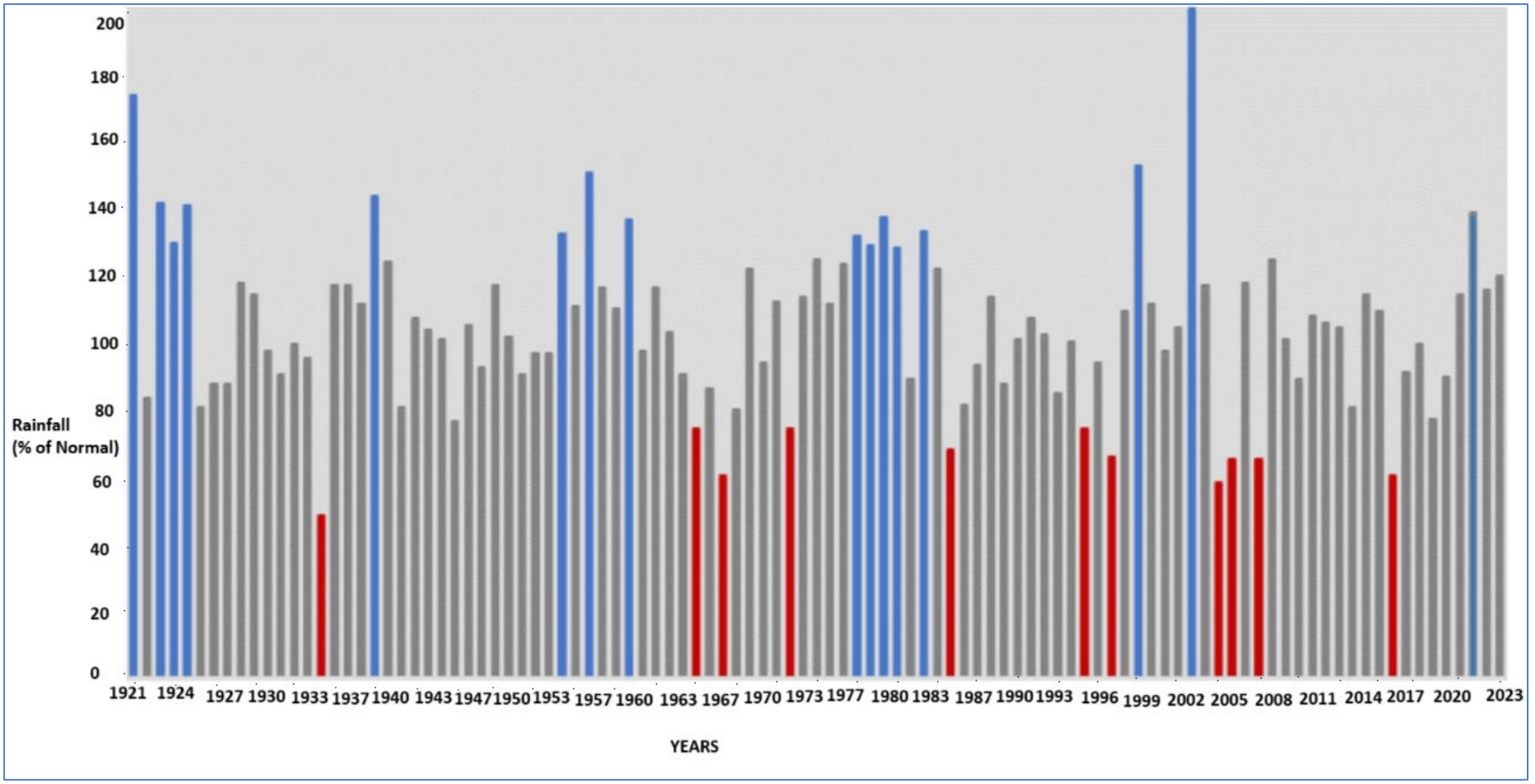

Figure 3-1: Limpopo annual rainfall data for the period 1921 to 2023 with red bars indicating dry years (<75% of normal rainfall) and blue bars indicating wet years (>125 %) of normal rainfall, (SAWS, 2023).

3.5 Impacts of anthropogenic factors

There was balance in the aquifer systems in terms of recharge and discharge prior to large-scale anthropogenic activities in many locations, and natural groundwater quality was generally good (IAH, 2016). However, in recent years, rapid population growth, increasing food demand, land-use change and other socio-economic factors are a threat to the availability and quality of water resource. These are considered the main factors that affect the capacity to optimally manage groundwater resources (Clifton *et al.,* 2010).

The Limpopo Province is among many areas in South Africa with poor water quality mainly related to the excessive levels of fluoride and nitrates (Tredoux *et al*., 2001; Tredoux *and* Talma*,* 2006; Holland, 2011; DWA, 2015). These contaminants are of great concern for water consumption due to their impacts on human health. In many rural communities of Limpopo Province, high concentrations of nitrates in groundwater are generally known to be associated with anthropogenic factors such as pit latrines, agricultural effluent from fertilisers, wastewater treatment, improper waste disposal and livestock concentration at watering stations near boreholes. Arsenic (As) concentration was found to be above the prescribed drinking limit and this was observed mainly in boreholes located within the rocks of the Greenstone Belt.

Groundwater in the study area is highly sensitive to nitrate contaminants due to the presence of a thin and highly weathered layer that allows fast movement of water into the underlying highly fractured aquifers (Holland, 2011).

The historical GRIP database, with a total number of 612 borehole records, was used to assess and characterise groundwater hydrochemistry in the Klein Letaba River catchment. The results indicate that the quality of water is dominantly compromised as a result of the elevated levels of nitrates. As shown in Figure 3-2, the high concentrations of nitrates are distributed across the study area from the Highveld to the Lowveld regions. However, this high elevated nitrate seems to be widespread amongst the settlements. To a limited extent, high concentrations of chloride, sodium, fluoride, electrical conductivity, total dissolved solids and total hardness were also detected in groundwater. Of the 612 boreholes, only 5 were found to have fluoride with

high excessive levels whilst < 30 and < 20 boreholes were found to have elevated concentrations of chloride and sodium, respectively.

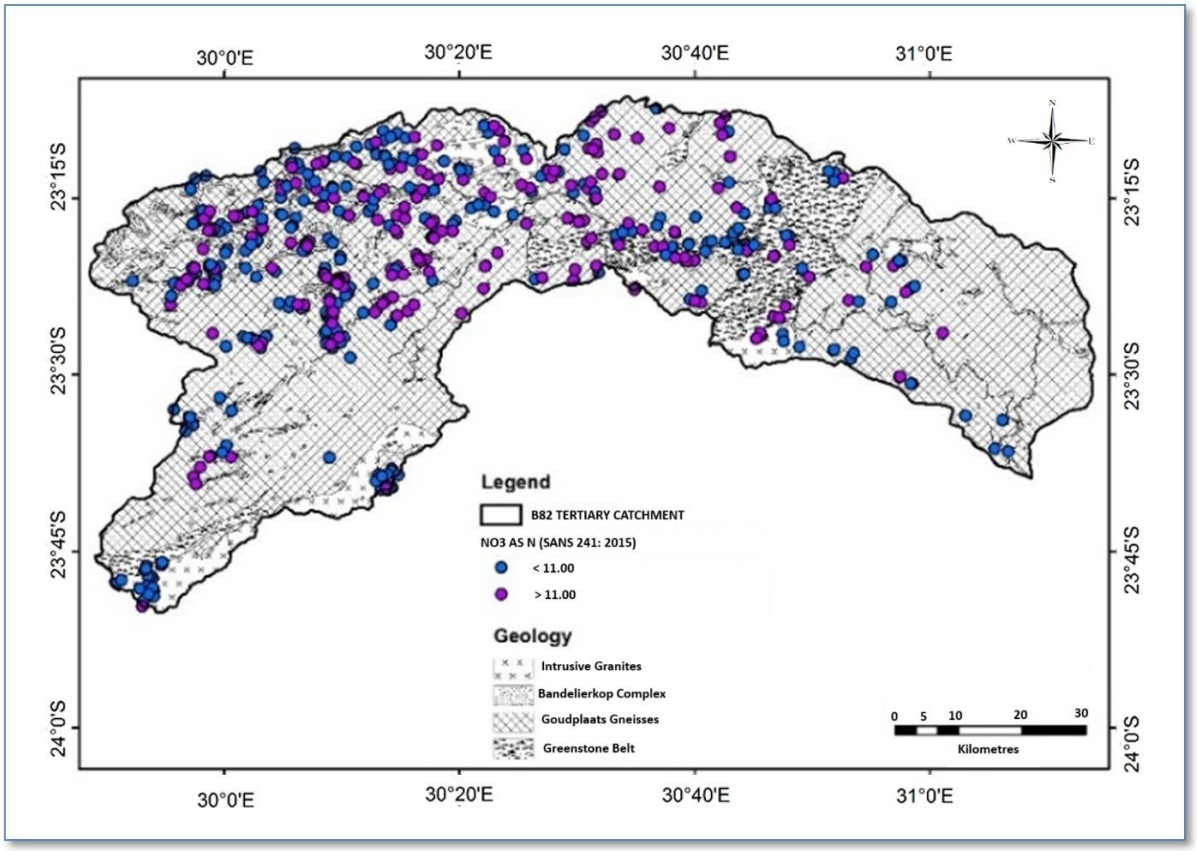

Figure 3-2: Map showing the concentrations of Nitrate in the study area.

The study conducted by Cai *et al.,* (2017), indicated that there is significant water use for irrigation in the Limpopo Province. Groundwater is used to irrigate 27% of the agricultural land, surface water 26%, conjunctive use (using both groundwater and surface water) is 10%, and rainfall contributes 37% of the water used for irrigating agricultural land (Figure 3-3).

Agriculture is one of the most important economic sectors in the study area, contributing approximately 17% to the Gross Domestic Product, (GGLM IDP, 2024). This sector comprises small-scale commercial farming where fruits (i.e., bananas and mangoes) and vegetables (i.e., maize, cabbage, butternuts, beetroots, etc.) are grown mostly on community schemes in tribal land and in irrigation schemes. The other small-scale agricultural activities include livestock farming.

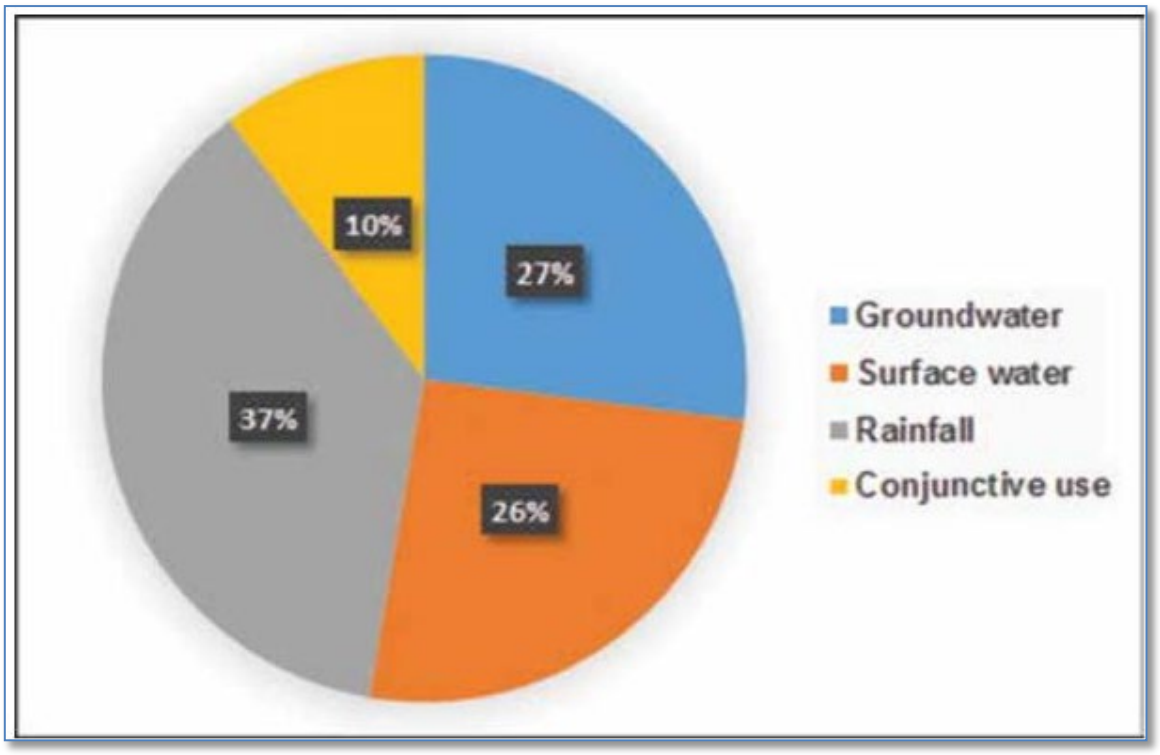

Figure 3-3: Different sources of water used for agricultural purposes in the Limpopo Province (after Cai *et al*., 2017).

A long-term groundwater abstraction of 80 Mm^3/a in the Letaba area is believed to be impacting heavily on the Middle Letaba in the catchments B82B and B82C which are currently over-utilised and runoff has decreased by nearly 40% (DWA, 2015). The study further indicates the depletion of base flow by 10% in the Letaba area.

The study conducted by DWS (2015), estimated that a total of about 114 million m^3 per annum of water is used in Klein Letaba River catchment. This total abstraction is made of 97.561 million m^3 per annum from surface water resources and 16.862 million m^3 per annum from groundwater resources. Based on the Water Use Authorisation and Registration Management System (WARMS), an additional 7.239 million m^3 per annum is abstracted mainly for irrigational purposes. Although groundwater is extensively developed in the study area, the users are not monitoring water levels during abstractions, hence there exists no information on the records of the volumes or water levels during abstraction.

3.6 Groundwater Recharge

One of the processes that influence groundwater level fluctuation is groundwater recharge, which is a hydrologic process by which aquifers are replenished (Todd and Mays, 2005). It can occur in both natural and man-made induced phenomenon (Sophocleous, 2004). This process generally involves a three-dimensional movement of water into the aquifer either in an downward, upward, and/ or lateral orientation (Lerner *et al*.,1990).

In a semi-arid region like Limpopo Province, groundwater aquifers rely on indirect and localised recharge (De Vries and Simmers, 2002), which occurs in a downward flow through the subsurface area until it reaches the groundwater table. In this region, direct recharge is significantly important for aquifer replenishment only during heavy rainfall or flood events (Van Wyk, 2010). However, due to below-average rainfall and high evapotranspiration rates, a considerable amount of rain returns to the atmosphere before reaching the aquifer (Xu and Beekman, 2003).

Based on a thinner weathered zone and flat topography, rainfall recharge is expected to reach the aquifer/water table quickly (Fetter, 2001). However, the rate of groundwater recharge may be hampered by the intensity of rainfall, clay content in the weathered layer, non-vegetated areas, isolated trees and shrubs that characterise most of the study area (Scanlon *et al.* 2002).

Recharge is generally low in the study area ranging between 10 to 15 mm/a in the Lowveld and 15 to 25 mm/a in the Highveld regions (DWS, 2015). The high recharge in the Highveld regions (Soutpansberg and Magoebaskloof mountains) is characterised by steep slopes. Along these steep slopes, recharge is discharged rapidly in the form of springs providing baseflow to the rivers (DWS, 2015). These resources are not available for exploitation by the regional aquifers that occur in the low elevated areas, hence a large fraction of recharge cannot be directly exploited through boreholes.

The study conducted by Cavé e*t al*., (2003) indicates that a 20% reduction in mean annual rainfall volumes might result in an 80% reduction in recharge for areas receiving less than 500 mm rainfall per annum.

These results infer those small variations in rainfall could lead to substantial changes in recharge and, therefore, dire consequences for groundwater-dependent communities (Woldeamlak, 2007). Understanding the groundwater flow mechanisms and factors that are influencing groundwater recharge is critical in the selection of suitable recharge estimation methods. Multiple recharge estimation methods should be employed, given the inherent difficulties that make recharge estimation complicated (Adams *et al*., 2004 Simmers, 1996).

Different techniques of recharge estimations for the semi-arid conditions of South Africa are outlined by Van Tonder and Xu (2000) and Xu and Beekman (2003). The following methods are recommended to be more reliable; Chloride Mass Balance (CMB), Groundwater Modelling, Water Table Fluctuations (WTF), Saturated Volume Fluctuation (SVF) and extended model for aquifer Recharge and moisture Transport through unsaturated hard rock (EARTH). Abiye (2016) suggests that CMB, SVF and WFT are good and can provide reasonably accurate recharge estimation results, as these methods consider the aquifer properties. Previous recharge estimation techniques in the study area (Klein Letaba River catchment) indicate that recharge varies across the study area, in that high from the western Highveld areas decreasing towards the eastern Lowveld areas.

The overall results of this section provided the foundation of knowledge on the research topic and available water resources in the study area. Furthermore, this has indicated that the available groundwater information in the study area is fairly old and would require comprehensive fieldwork to collect new information, gain familiarity with the study area and the settings.

CHAPTER 4 : MATERIALS AND METHODS

4.1 Introduction

This chapter presents research materials and methods that are used in this study. The compilation of existing relevant data is a prerequisite for groundwater flow modelling. In areas where there is inadequate existing data or poor data quality, the filling of missing datasets through fieldwork is very important. The hydrogeological characterisation and modelling approach followed in this research study allowed a better understanding of how water interacts with the surface and sub-surface environments at different geographic locations of the crystalline basement rock aquifers. Crystalline basement aquifers have complex hydrogeological properties, the methods and materials used complemented each other enabling determination of groundwater flow direction and extent vulnerability.

In the following sections, the steps that were implemented to pre-process various datasets and the procedures used to develop the conceptual and numerical model of groundwater flow are presented.

4.2 Desktop Review

A detailed literature review was conducted, which helped to define the primary research problem. In addition, the desktop study was carried out concurrently with a compilation of existing data. These include a compilation of 1:250 000 scale geological map, 1:50 000 topographical and aeromagnetic data. Most of the regional scale hydrogeological maps were obtained from the Department of Water and Sanitation. These maps were used to understand the regional and local geology, as well as the hydrogeological conditions of the study area. The 1: 50 000 scale Advanced Space Borne Thermal Emission and Reflectance Radiometer (ASTER) images were obtained from the Department of Water and Sanitation, and the data were used together with aeromagnetic data to generate the lineament map of the study area.

Climate data which include, rainfall, temperature and evapotranspiration were obtained from the South African Weather Services (SAWS), Agricultural Research Council (ARC) and the Department of Water and Sanitation.

In addition, ARC also provided soil data. The 30 m resolution digital elevation model (DEM) data was obtained from the United States of Geological Surveys.

All the data compiled were used to generate thematic maps and a hydrogeological database of the study area using ArcGIS software.

4.3. Fieldwork

Site visits were undertaken in areas where various water sources were supplying the communities, health facilities and schools. This also included areas where there could be a potential impact from the land use (i.e. mines and farming activities). Furthermore, areas located on the outskirts but within the study boundary were also visited. Hydrocensus was conducted on the boreholes and surface water bodies were selected for sampling. This was done to assess the local conditions, access to sampling points and to record basic site information (i.e., water levels, depths, etc.).

4.3.1 Sampling

Water samples were collected from both active and inactive boreholes and shafts, dams, ponds and major rivers. Active boreholes were sampled from the outlets and standpipes. Submersible pump and/or plastic bailers were used to sample shafts and boreholes (Figure 4-1A).

Prior to sampling, static water levels from the boreholes were measured. This was followed by purging water from the borehole by pumping and this allowed to remove suspended particles and introduce fresh water from the aquifer into the borehole so that a representative sample is collected. Before collecting water samples, bottles were rinsed three times with the water to be sampled, and then filled with water.

Physicochemical parameters including electrical conductivity (EC), pH, temperature (T˚) and dissolved oxygen (DO) were measured on-site using multi-meter probes designed for the in situ water quality analysis. Water sample analysis included, major ions, trace elements and environmental isotopes ($\delta^{2}H$, $\delta^{18}O$ and $\delta^{3}H$). Samples for isotopes and chemistry were transported to iThemba Labs in Johannesburg and Waterlab in Pretoria, respectively.

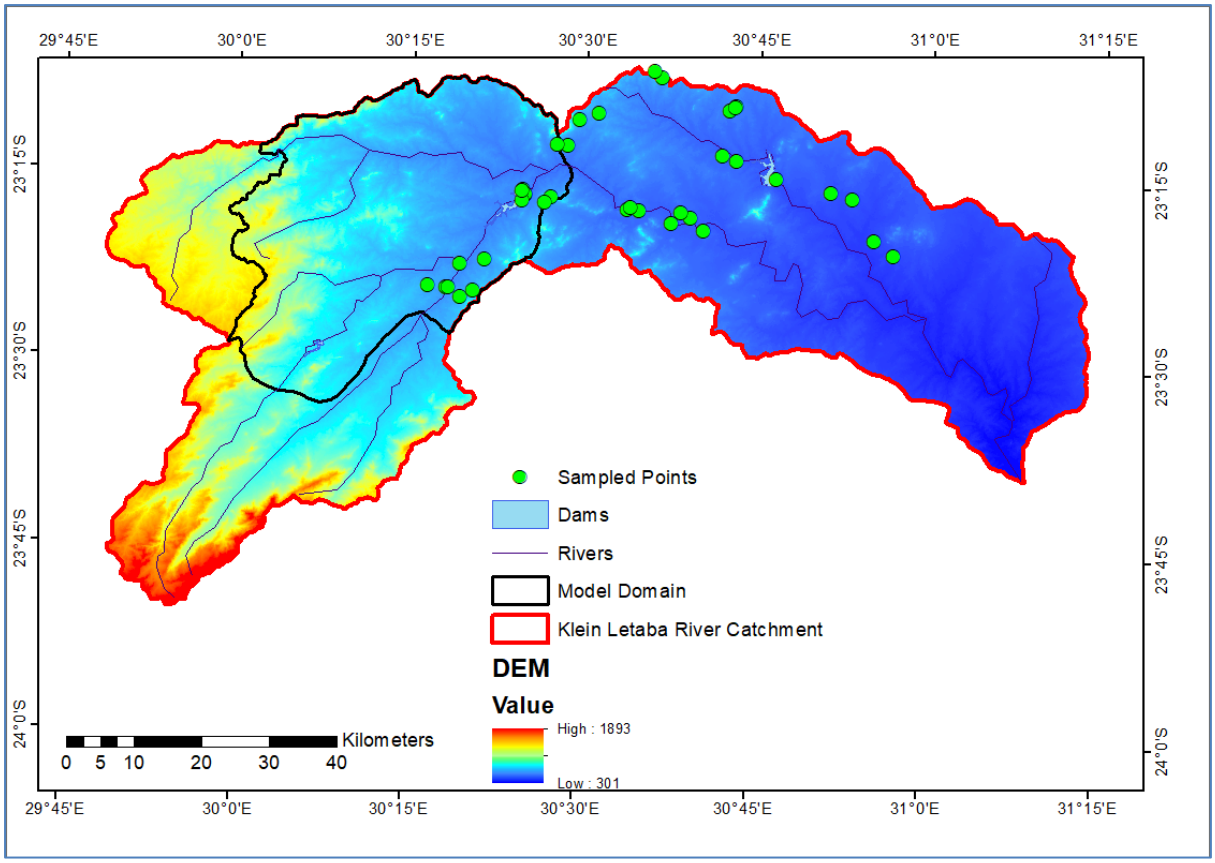

Figure 4-1A: Map showing locations of the sampled points

4.4 Laboratory analysis

Hydrochemical and environmental isotopes data provide information about the source, evolution and quality of the water (Tessema *et al.,* 2014). Major cations and trace metals were analysed using an Inductively Coupled Plasma Atomic Emission Spectrometer (ICP-AES) and Mass Spectrometer (ICP-MS), respectively. Major anions were analysed using Ion Chromatography (IC).

Stable isotope ratios of ^{18}O and ^{2}H were analysed using a Los Gatos Research (LGR) Liquid Water Isotope Analyser-model 45-EP. The analytical precision for this equipment is approximately 0.5‰ for $\delta^{18}O$ and 1.5‰ for $\delta^{2}H$.

The relationship between the standard and the isotopic ratios is expressed as parts per 1000 deviation from the Vienna Standard Mean Ocean Water (V-SMOW):

$$\delta^{18}O = \left(\frac{\left({}^{18}O / {}^{16}O \right)_{Sample}}{\left({}^{18}O / {}^{16}O \right)_{Standard}} - 1 \right) 1000$$

Where $(^{18}O/^{16}O)_{sample}$ and $(^{18}O/^{16}O)_{standard}$ are the heavy oxygen isotope ratio in the water sample and the Vienna Standard Meteoric Ocean Water (VSMOW), respectively (Craig, 1961). Sampled water can be either enriched or depleted with respect to the standard sample.

4.5 Data Processing

This section presents the data processing techniques that were implemented to generate the results. These include the processing of borehole data and spatial datasets that are relevant for the construction of boundary conditions and MODFLOW layer groups.

4.5.1 Borehole data

The borehole logs obtained from the NGA database were rearranged in excel sheet and only boreholes considered to have adequate information (i.e., borehole depth, comprehensive logging details and other related borehole attributes) were considered for further processing and input into the LogPlot to build the conceptual model of MODFLOW Layer Groups.

4.5.2 Groundwater level data

Groundwater levels obtained from the Department of Water and Sanitation database and the borehole elevations extracted from the Digital Elevation Model (DEM) were used to establish the relationship between the groundwater level and borehole elevation. The GIS ArcMap 10.8.1 was used to extract the elevations and interpolate (Kriging) the groundwater levels. The data was further processed using Golden Surfer 9 software to construct a water level contour map and groundwater flow directions.

Groundwater level data from the observation boreholes was used to investigate the long term trends in and evaluate the response in relation to the climate changes (i.e., rainfall, temperature and evapotranspiration).

4.5.3 Aquifer test data

The Flow Characteristics FC Method (Van Tonder *et al*., 2001) was employed to assess pumping test data and determine the hydraulic parameters of the aquifers. The FC method uses the first and second-order derivatives that are interpreted from time drawdown data, available drawdown, boundary conditions and recharge to obtain sustainable borehole yields. The T and S properties are estimated in the FC method using the generalized Theis (1935) radial flow model. The meaning and use of these parameters are therefore confined to the estimation of the sustainable yield in the FC method.

4.5.4 Hydrochemical, environmental isotopes and radiogenic data

To evaluate the hydrochemistry of the water resource in the study area, a historical dataset with borehole records from the GRIP database and new datasets collected by the Council for Geoscience as well as data collected during the present study were used.

4.5.4.1 Hydrochemical data

The ion balance of the hydrochemical data was evaluated to verify the level of accuracy and reliability of the data prior to further processing. The chemical constituents measured were compared and classified according to various guidelines and standards (e.g., DWAF, 1996, WHO, 2011 and South African National Standards, SANS 241, 2015). These guidelines enable an assessment of the suitability of water for drinking purposes.

In addition, a Piper diagram (Piper, 1994) was used to characterise and evaluate water types as it demonstrates the correlations between the most essential dissolved elements in collected groundwater samples (Chandrasekar *et al*., 2014).

4.5.4.2 Stable isotopes (^{18}O and ^{2}H)

For the interpretation of the stable isotope data, the $\delta^{18}O$ and δD composition of the rainfall at the International Atomic Energy Agency (IAEA) station in Pretoria was utilised as the local meteoric water line (LMWL). Local Meteoric Water Line (LMWL) is determined from the best fit line of the locally averaged rainfall samples. Stable isotopes data of the research area were compared with the Pretorial Local Meteoric

Water Line (PLMWL) and Global Meteoric Water Line. Global Meteoric Water Line (GMWL) has been determined based on the global analyses of $\delta^{18}O$ and $\delta^{2}H$ in fresh waters from different localities and regional meteorological stations around the world (Craig, 1961). The GMWL is expressed as:

$\delta D = 8^{18}O + 10‰$

Where, the slope and intercept (deuterium excess d) of the straight line are 8 ‰ and 10 ‰, respectively. The variations in moisture at the source site (e.g., sea or ocean) and different paths of moisture account for deuterium excess (Clark and Fritz, 1997).

The $\delta^{18}O$ and $\delta^{2}H$ are attributed to the extent of evaporation, groundwater circulation, distance from the source, altitude, mixing of groundwater, rock-water interaction, etc., while d_{excess} reflects conditions of the moisture source which involves humidity, sea surface and air temperatures as well as wind speed (Dansgaard, 1964). D-excess is calculated from the Pretoria LWML equation, which is expressed as:

$D_{excess} = \delta D - 6.7\delta^{18}O$

4.5.4.3 Radiogenic isotopes (^{3}H)

Tritium (^{3}H) is a radioactive isotope of hydrogen with a half-life of 12.43 years (Fetter, 2001). This makes it to be suitable for being used in determining groundwater residence time in different aquifer systems. The age of groundwater has important implications for water resource management.

Tritium originates from a nuclear reaction between atmospheric nitrogen and thermal neutrons (Libby, 1946). It is also found in the subsurface as a result of a spontaneous breakdown of Uranium (U), Thorium (Th) and Lithium (Li) as well as in nuclear reactors (Clark and Fritz, 1997).

The tritium concentrations in rainwater are exceedingly low, with a $^{3}H/^{1}H$ ratio of 10^{-18} (Clark and Fritz, 1997). In groundwater, tritium levels remain intact underground and are only affected by mixing with older water and radioactive decay (Weaver *et al*., 2007). The atmospheric concentration in Southern Africa was estimated at a value of 5 TU (Weaver *et al*., (1999). The value continued to decrease and a concentration of about 3 TU from rainwater was recorded in South Africa (Levin and Verhagen, 2013).

Tritium composition values for rainfall in Taaiboschgroet (Limpopo Province) were estimated at an average of 2.8 TU (Butler and Verhagen, 2013). For comparison purposes, semi-quantitative derived mean residence times (MRT) values suggested by Clark and Fritz (1997) and Weaver *et al*., (1999), shown in Table 4-1, were used in this study. Based on this classification, modern or mixed groundwater contains $^{3}H/H$ concentration greater than 0.5 TU, and values below that can be classified as old groundwater. The mean residence time (MRT) or recharge period of the groundwater in the study area was determined by comparing its ^{3}H content with those of present-day rainfall. Measurable ^{3}H in boreholes indicates recharge, while 0.2 TU would indicate low or no recharge of that aquifer (Levin and Verhagen, 2013).

Table 4-1: Semi-quantitative derived MRT from groundwater tritium values (Sources: Clark and Fritz, 1997 and Weaver *et al*., 1999).

Mean Residence Time (MRT)	Tritium values (TU) (Clark and Fritz, 1997)	Tritium values (TU) (Weaver *et al*., 1999)
Groundwater recharged before 1952	<0.8	<0.5
Recharged before and after 1952 (Mixed groundwater)	0.8-4	0.5-5
Groundwater recharged after 1952	>4	5

4.5.5 Climate Data

Based on 10 years (from 2007 to 2016) of climate data, this study evaluate the temporal and spatial variation of rainfall, temperature, and evapotranspiration using statistical techniques and trend analysis.

The existence of outliers and missing values of hydrogeological data were carefully examined in the early stages of data inventory. Most of the extreme values in the upper range were identified from the rainfall data and these were mostly related to the floods and high rainy seasons. In the lower ranges, these values were generally linked to drought periods. These extreme values were not removed from the dataset as they were representative of the high rainfalls and droughts that occurred in the study area.

The descriptive statistical analysis was undertaken using IBM SPSS Statistics software and an excel spreadsheet to determine the measure of central tendency

(minimum, maximum, and mean) and dispersion (standard deviation and coefficient of variations). The monthly, annual, and seasonal variations are considered and this was divided into four seasons; Summer (from December to February), Autumn (March to May), Winter (June to August), and Spring (September to November).

Fluctuation analysis was carried out using the Coefficient of Variance (CV) which is calculated to evaluate the variability of rainfall and temperature in expressing the fluctuation of the climate elements. The coefficient of variance indicates whether the data is a normal or skewed distribution with respect to the central value, i.e., mean. The higher the value of CV, the greater the level of distribution around the mean. CV is expressed as the percentage ratio of the standard deviation to the mean (Achite et al., 2021 and Gummandi et al., 2018):

$$CV = \frac{\sigma}{\mu} X100$$

Where CV = coefficient of variation; σ is the standard deviation and μ is the mean.

4.6 Groundwater Flow Modelling

Groundwater flow model is a mathematical representation of groundwater flow through an aquifer, and is expressed in terms of a partial differential equation (McDonald and Harbaugh, 1988):

$$\frac{\partial}{\partial x} * \left(Kxx * \frac{\partial h}{\partial x}\right) + \frac{\partial}{\partial y} * \left(Kyy * \frac{\partial h}{\partial y}\right) + \frac{\partial}{\partial z} * \left(Kzz * \frac{\partial h}{\partial z}\right) \pm W = -Ss * \partial h/\partial t$$

Kxx, Kyy, and Kzz are values of hydraulic conductivity along the X, Y, and Z coordinate axes, which are assumed to be parallel to the major axes of hydraulic conductivity,

Where h is the hydraulic head, ±W is a volumetric flux per unit volume and represents sources (+) and/or sinks (-) of water, Ss is the specific storage of the porous material, while t is time.

The equation represents groundwater flow in a heterogeneous and anisotropic medium under non-equilibrium conditions (Pathak *et al.,* 2018). The equation is solved using analytical and numerical methods by applying initial and boundary conditions.

Numerical modelling approaches are known to be most suited for modelling complicated groundwater flow systems for which most of the analytical solutions are not able to provide the solution. The modular groundwater flow model (MODFLOW) simulates groundwater flow in aquifer systems using the finite difference (FD) method. It was created by the U.S. Geological Survey (USGS) and has been widely used for the solution of various hydrological and hydrogeological problems. The program was developed in the early 1980's (McDonald and Harbaugh, 1988 and Harbaugh and McDonald, 1996), and has continued to evolve, with the addition of numerous new packages and related applications for groundwater studies. It has become one of the preferred and industry standard modelling tools for simulating and quantifying groundwater and surface water interactions (Harbaugh *et al.,* 2000, Harbaugh, 2005).

Groundwater modelling was conducted to understand the flow and determine the water budget, which enables the formulation of effective use and management of groundwater resources.

In the study area, water is supplied from the surface and groundwater resources and the problems of water scarcity are mainly associated with the complex characteristics (i.e. heterogeneity) of the crystalline basement rock aquifers, limited rainfall, and high evapotranspiration rate. Because of the capabilities of MODFLOW in handling and simulating a wide range of hydrologic features such as rivers, streams, dams, boreholes, evapotranspiration, and recharge from precipitations, it is an ideal tool to accurately simulate groundwater flow.

4.6.1 Selection of modelling software codes

MODFLOW NWT along with its upstream weighted flow package (UPW) was chosen to simulate the groundwater flow. It utilises Newton's formulation and unstructured, asymmetric matrix solvers to solve the partial differential equation of groundwater flow expressed as a matrix equation (Niswonger *et al*., 2011). In addition, the ModelMuse graphical user interface was used for pre- and post-processing the results obtained from MODFLOW NWT.

The MODFLOW NWT is based on its capability to solve problems associated with drying and rewetting nonlinearities of the unconfined groundwater flow (Niswonger *et al*., 2011). If a cell is dry (that is, the head is below the cell bottom) and underlain by a

fully or partially saturated cell, its horizontal conductance will be 0 and the head in the dry cell can be calculated in terms of the sum of inflow to the cell from adjacent cells and external sources (Hunt and Feinstein, 2012).

4.6.2 Groundwater Recharge

Groundwater recharge is defined as a portion of total rainfall falling into a drainage basin that eventually reaches the water level in the saturated zone of an aquifer (Freeze and Cherry, 1979). For this study, recharge values were calculated using the Chloride Mass Balance (CMB) method.

4.6.2.1 Chloride Mass Balance

The Chloride Mass Balance (CMB) is the most commonly used technique for calculating recharge rates in fractured aquifer systems (Cook, 2003). The Chloride Mass Balance method was used because of the availability of data and due to its limitations, the results were compared with the recharge estimates from other methods (i.e. saturated volume fluctuations and cumulative rainfall departures) as well as the recharge from the published articles. The Chloride Mass Balance method assumes that chloride acts conservatively, is solely sourced from precipitation, and that groundwater has returned to steady-state conditions following any land-use changes (e.g., vegetation clearing; Leaney et al., 2011).

The recharge of groundwater is estimated based on the following equation (Witthüser *et al.,* 2011):

$$Rr = \frac{TDxMAP}{Clgw}$$

R_r = total recharge (mm/a)

TD= total atmospheric chloride deposition (mg/l)

Cl_{gw} = mean annual chloride in groundwater (mg/l)

MAP= mean annual precipitation (mm/a)

The total atmospheric chloride deposition (TD) is based on the average concentration of 0.69 mg/l determined by Holland (2011) in the Letaba Catchment area. The mean

monthly rainfall received over the model domain area varies between 800 mm/a to 570 mm/a based on the 10 years (2007 to 2016). For this reason, mean annual precipitation was calculated from the three rainfall stations (Kleinfontein, Voorsped, and Middle Letaba) that are located in the area selected for modelling. Chloride in groundwater (Cl_{gw}) was determined from boreholes located in the vicinity of rainfall monitoring stations.

For comparison purposes, other methods including the published groundwater recharge map and reviewed reports were considered. The study by DWS (2015) estimated mean annual aquifer recharge across the Highveld areas varies from 15 mm/a to 25 mm/a, while in the Lowveld the recharge varies from 10 to15 mm/a. Makonto (2013), estimated the mean annual recharge of 15.38 mm/a of 837 mm MAP for the Middle Letaba catchment.

4.6.2.2 Recharge (RCH) Package

The purpose of the RCH package is to simulate spatially or arealy distributed recharge to the groundwater system. Groundwater recharge is usually expressed as a percentage of rainfall infiltrating the groundwater system as a spatially uniform recharge rate across the water (McDonald and Harbaugh, 1988; Anderson and Woessener, 1992).

In this study, the upper unit has been determined to be the top 35 m in the entire model area. This is the part where most of the weathering and fracturing has occurred and the material may be unconsolidated to a large extent, especially in the top 2 m where both the recharge process and evapotranspiration process actively take place. The recharge rate for the model domain was derived from monthly rainfall using the chloride mass balance, “Qualified guesses” methods, and previous studies described in section 4.5.2.1 and section 3.6, respectively. The recharge rate was applied consistently to the entire upper surface of the model and applied at a constant rate for the duration of each stress period using the MODLFOW ‘RCH’ package. The recharge rate calculated for the model represents effective recharge that reaches the aquifer after the interception losses and evapotranspiration have been taken into consideration.

4.6.2.3 Surface Runoff

Surface runoff forms an integral part of the water balance estimation. This consists of runoff from the catchment where the study area is situated as well as upstream catchments. There are no gauging stations upstream of the study area to monitor runoff from the high recharge areas. This creates uncertainties in the data due to the heavy abstraction of surface water taking place upstream of the study area.

For this purpose, the mean annual runoff estimated by the Department of Water Affairs (DWA, 2015) was used for water budget estimation.

4.6.3 Water resource abstractions

Water is exploited from both surface and groundwater resources to meet the needs of the community and agriculture. Community water supplies are through dispersed boreholes operated by different Water Services Authorities.

The Rural Water Supply Schemes (RWSS) cut across the different catchment and municipal boundaries. Most of the water users do not comply in terms of monitoring the water abstraction volumes, therefore it is difficult to access water level and discharge rate monitoring data. The water balance estimates are calculated using abstraction volumes reported by the water resource regulator (Department of Water and Sanitation).

4.6.4 Development of Hydrogeological Conceptual Model

4.6.4.1 Selection of Model Domain

The model domain covers 2 Quaternary catchments of the Klein Letaba River catchment and has a total surface area of 1551 sq. km (Figure 4-1) with the topographic height ranging between 1271 and 459 meters above mean sea level (a.m.s.l.). The groundwater flow boundaries of the model were chosen after consideration of hydrogeological, hydrological, geological, structural, and digital elevation data. The model boundaries are coincident with the watershed divide determined by surface water runoff and topographic relief.

The surface water flows in the study area follow a topographic gradient from the southwest to the northeast (Figure 4-1).

The hydraulic head distribution indicates that the movement of groundwater also follows topography with its flow direction largely mimicking the surface water flows. This was confirmed using the hydrochemical data from boreholes located along the Middle Letaba River from the high elevated recharge area to the low elevated discharge area.

The development of a conceptual model is generally a simplified and pictorial representation of the hydrogeological system (European Commission, 2003). This simplification is introduced as a set of assumptions that relate to and not limited to the following:

- The Geometry of the aquifer boundaries,
- Groundwater flow regime in the aquifer,
- Sources and sinks, and
- Inflow and outflow boundary conditions that express the interactions with its surrounding environment.

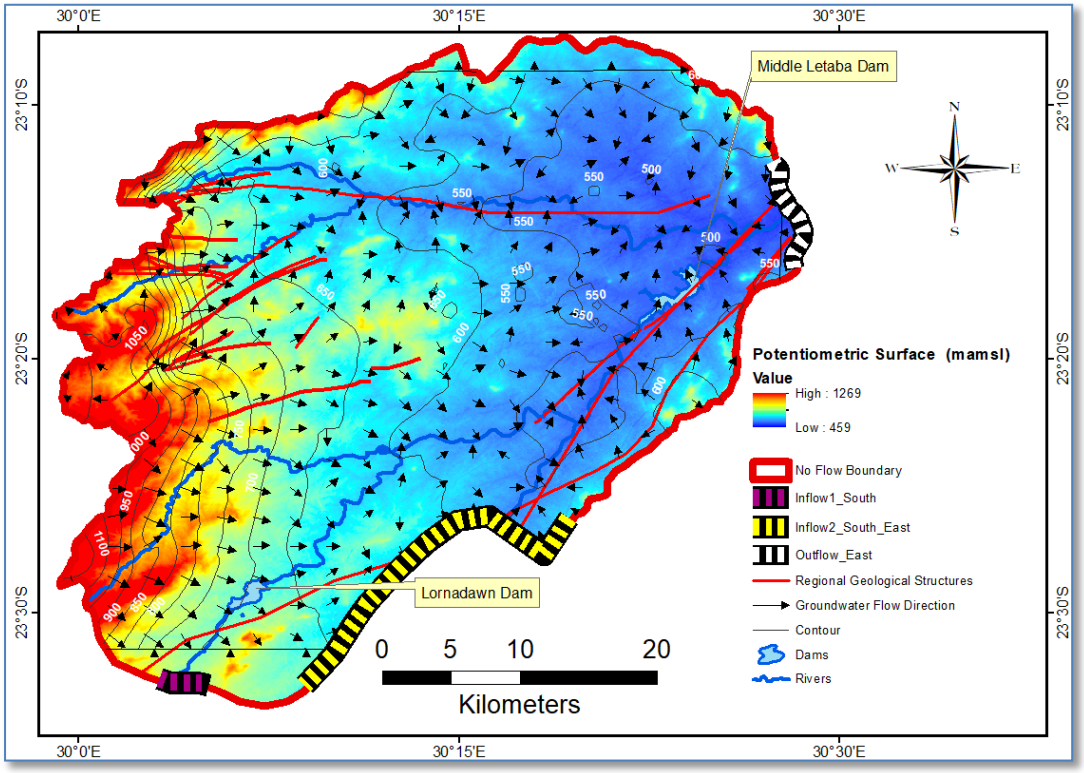

Figure 4-2B: Map showing the model domain, groundwater flow directions, regional geological structures and flow boundaries.

Two inflow boundaries with lengths of 3 418 m and 25 838 m were selected in the south and south eastern part of the model, respectively. These inflows represent areas where surface water enters the mode domain area.

Outflow boundary with a length of 8 640 m was selected in the eastern part of the model representing an area where water exit the model domain. The length of the inflows and outflow boundaries are based on the contrast or the comparison of land surface elevation and piezometric surface. The source of inflow into the Middle and Little Letaba Rivers arises from high tropical mountain areas where rainfall is abundant during the Summer months. Mosukodutsi, Soeketse, and Lebjwelebore are the three minor rivers in the model domain area feeding into the perennial Middle and Little Letaba rivers. There are two dams within the model domain, these are the Middle Letaba and Lorna Dawn dam.

4.6.4.2 Groundwater flow boundaries

Considering the structural and geological dynamics, groundwater flow in the studied area is complicated and is assumed to be controlled by the hydraulic potential gradient and hydraulic conductivities in the weathered zone and fractured bedrock (Holland, 2011). The study area is dissected by a series of discrete shear zones, faults, lineaments, and dolerite dykes. These geological structures were formed from multiple deformation events that have affected the SMZ and are believed to be open under the current neo-tectonic stress regime (Holland, 2011). Groundwater flow in the study area is highly affected by the presence and orientation of these geological structures.

Groundwater flow directions were constrained using hydrochemical and environmental isotope data, and also used to build a conceptual model of groundwater flow. In addition, topographic data, topographic elevations and depth to groundwater level were used to support the construction of the conceptual model. The hydraulic head data were used to develop the groundwater level contour map for the model domain area, which enabled the determination of the groundwater flow direction, recharge, and discharge areas (Figure 4-1). Results suggest that groundwater flow direction is from the west and south west (high recharge and mountainous areas) to the east and north east (flat, low-lying areas).

However, local flow conditions were observed, particularly around the Middle Letaba dam and areas where major shear zones occur along the rivers. Local groundwater flow vectors were observed to feed into the dams, rivers, and shear zones.

A total of fifteen groundwater samples were selected in the proximity of the Middle Letaba River, in the direction of the groundwater flow. Ratios of Na/HO_3, EC/TDS, Ca/Mg and Ca+Mg/Na+K (Figure 4-2) were used to confirm the inflow and outflow boundaries. The results indicate that the ratios of Na/HO3 and EC/TDS are low at the southwest inflow area while the ratio of Ca/Mg and Ca+Mg/Na+K are high. As the distance increases towards the downstream side, the Na/HO_3 and EC/TDS ratios increase, while Ca/Mg and Ca+Mg/Na+K decrease towards the discharge area in the northeastern part of the model domain. According to Simonic (2000), groundwater TDS/EC ratios in South Africa vary from <6 in the southwest to >8 in the northeast (Simonic, 2000).

The higher values at the outflow boundary can be explained by the longer periods water takes to travel through from the high recharge area at the inflow boundary in the southwest, which allows longer contact with the aquifer. Another hypothesis could be a deep discharge from underlying aquifers (Toth, 1999). On the other hand, by considering the samples in the direction of the groundwater flow up to the proximity of the Middle Letaba River, salt contents show an increment.

This phenomenon was further confirmed by the isotope samples taken from surface water bodies which show evaporation enrichment of both deuterium (δ^2H) and oxygen-18 ($\delta^{18}O$) at a distance away from the high elevated recharge area upstream of the Middle Letaba River to the low elevated discharge area downstream of the Middle Letaba dam.

Deuterium excess was observed to be decreasing with distance from the high to low elevated areas. Therefore, a no-flow boundary was applied along the outline of the study area except for areas where the rivers enter and exit the model domain. The Middle and Little Letaba are the only two perennial rivers in the model domain.

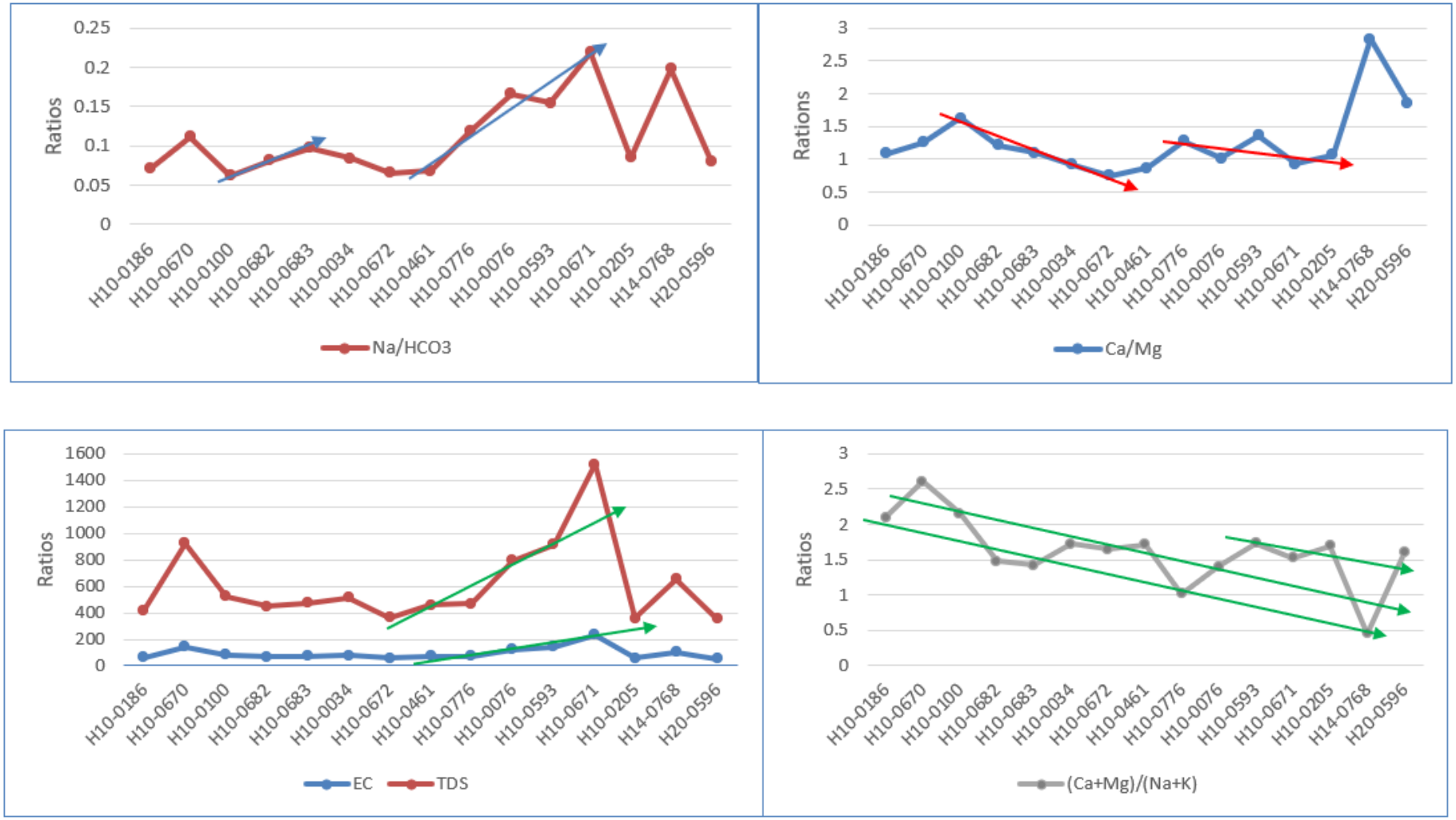

Figure 4-3: Ratios of Na/HCO3, EC, TDS, Ca/Mg and Ca+Mg/Na+K.

4.6.4.3 Hydrostratigraphic Units

Hydrostratigraphic Units (HSU) are defined as a body of rocks differentiated and characterised by porosity and permeability (Seaber, 1988). The flow and storage of water are determined by the connection of the openings in the rocks.

The hydrostratigraphic unit of the study area was developed by analysing the spatial and vertical distribution of the lithologies and water strikes as recorded on the borehole logs (Figure 4-3). Borehole log data with adequate information such as borehole depth, weathering, fractured zones, and water strikes were used to construct the conceptual model of MODFLOW Layer Groups.

A total number of 23 boreholes were used to identify the hydraulic properties. Stratigraphically, the model domain is underlain by 6 geological units consisting of Greenstone Belts of the Giyani Group and Rhenosterkop Formation, Goudplaats Gneisses, Bandelierkop Granulite Complex, and Granites of the Schiel Complex and Palmietfontein Formation (Figure 4-4). These rocks were grouped and reclassified into 4 rock units consisting of Greenstone Belt, Gneisses, Bandelierkop Complex, and Granites based on their similarity in hydraulic properties. The drill hole data provides the depth of water strike, which mostly occurs within the weathered and fractured layers.

The top and bottom of these layers were defined to determine the thickness of each layer. The results indicate that weathered and fractured layers rarely exceed 35 m bgl and 72 m bgl, respectively. However, water strikes that were recorded deeper than 70m were inferred as deeply fractured aquifer systems, which are assumed to be associated with the regional geological structures that are entirely tectonic in origin. The weathered zone consists of saprolite material which tends to have clay and sand due to frequent water table fluctuations and it is characterised by low yields (< 0.1 l/s). The fractured zone is characterised by a high density and interconnected fracture network with high yields of up to 5 l/s.

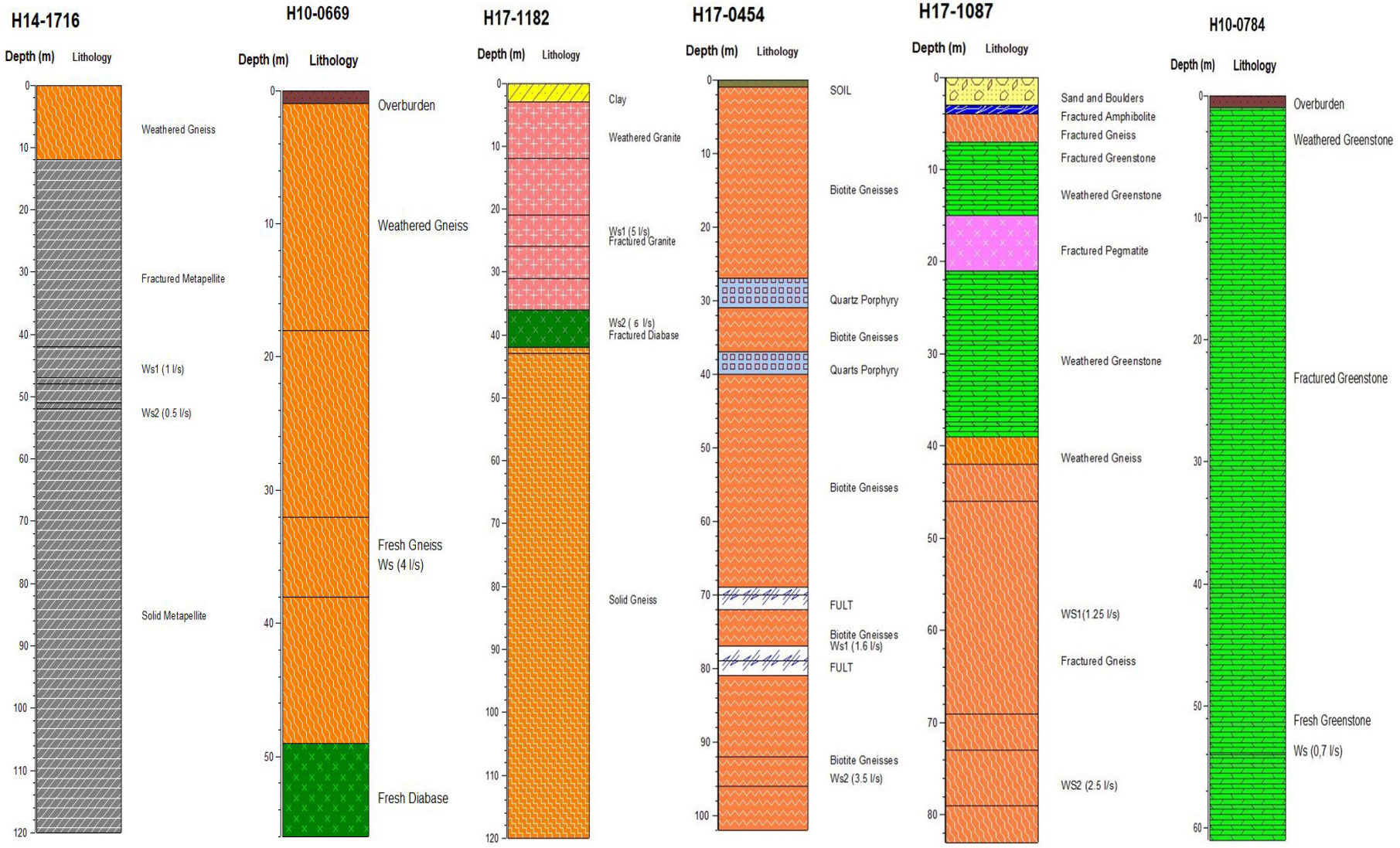

Figure 4-4: Selected borehole logs representing lithological units occurring in the Model domain area.

A total of 3 layers are considered to represent the aquifer system (Figure 4-5).

- Layer 1: Topsoil cover and extends up to a depth of 2m,
- Layer 2: Weathered layer of up to 35 m (average thickness of 33m), and
- Layer 3: Fractured layer of up to 72 m (average thickness of 37m).

Soil cover and weathered zone were defined as unconfined while the fractured zone was classified as confined. Due to the irregular distribution of the lithological units in the model domain area, borehole representation in the granites, Bandelierkop Complex and Greenstone Belt lithologies are very limited.

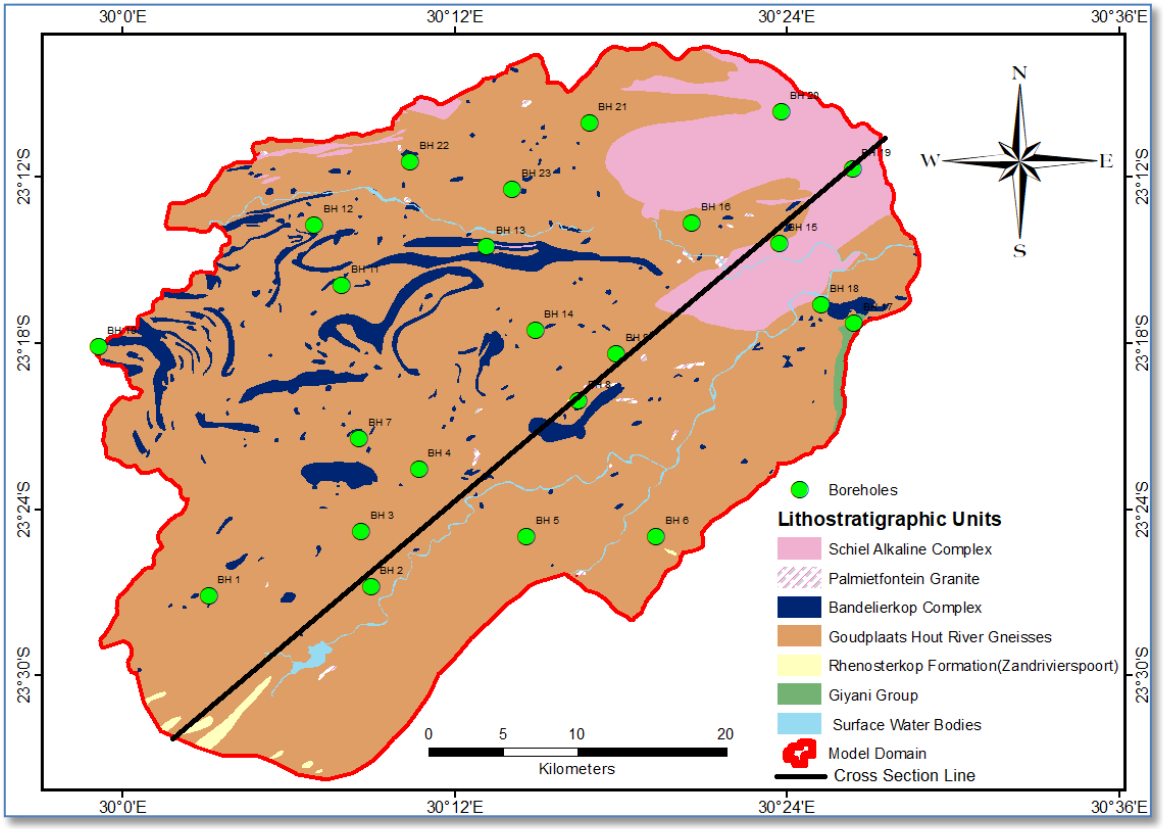

Figure 4-5: Geology and distribution of boreholes used to develop hydrostratigraphic units and cross-section line for the Model Domain Area.

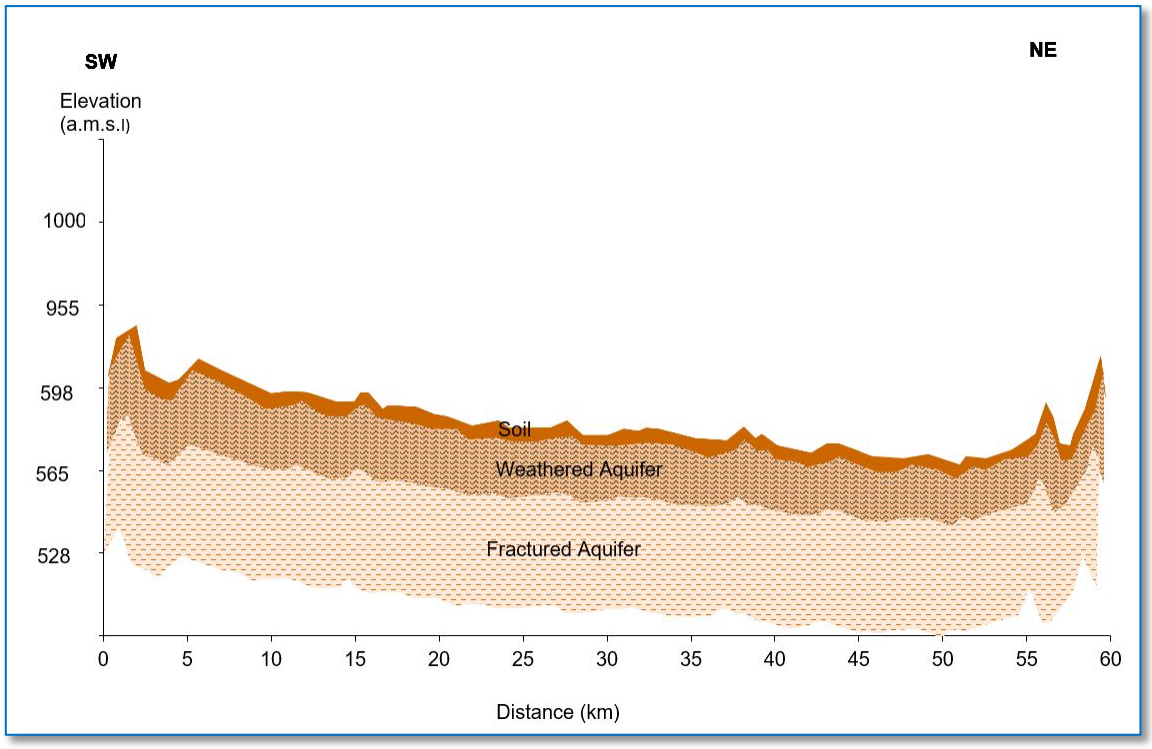

Figure 4-6: Hydrogeological cross-section of the model domain from the southwest to the northeast.

4.6.4.4 Hydraulic Conductivity

Borehole yield data were grouped according to 4 main rock units representing the two aquifers. The data was processed, and basic statistical parameters such as minimum, maximum, average, and median yields were determined corresponding to each lithological unit (Table 4-2 and Table 4-3). Borehole data with full pumping test records were analysed using the Flow Characteristics (FC) method to determine hydraulic properties such as transmissivity and storativity (Table 4-4 and Table 4-5). The results indicate that yields and transmissivity values vary significantly in boreholes within the same rock unit. The average transmissivity values were compared with the regional transmissivity values of the study conducted by Holland (2011). A significant difference was observed with regard to the transmissivity values of the Bandelierkop Complex and the granites, which could be attributed to the fact that Holland covered a large area of 63500 km^2 (Limpopo Plateau and Letaba Lowveld), which incorporated a wider range of transmissivity values from two different catchment areas. Bandelierkop Complex in the Limpopo Plateau is commonly known to be high yielding as compared to the one in the Lowveld region (study area).

The transmissivity values of the Goudplaats gneisses and the Greenstone Belt (Table 4-3) are within the same range, whilst granites were found to have the highest transmissivity values.

Four hydraulic conductivity zones were determined for the model domain based on the geological and hydraulic properties. The distribution of the hydraulic conductivity zones is depicted in Figure 4-6. The 1st layer (soil) is assigned horizontal hydraulic conductivity (HK) values in the ranges of 1E-4 m/s (Makonto, 2013), Table 4-6. The upper weathered zone of granitic gneisses is known to have high porosity and low hydraulic conductivity (due to clay-rich material) ranging between 1E-07 and 1E-06 m/s (Dewandel *et al.*, 2006; Taylor and Howard, 2000; McFarlane, 1992 and Jones, 1985). The 2nd layer (weathered zone or the first aquifer) was therefore assigned with horizontal hydraulic conductivity values of 1E-7 m/s in all geological units. The lower fractured unit or the second aquifer has been proven by numerous researchers and available datasets to have high permeability and; thus, high borehole productivity in terms of groundwater supply.

Table 4-2: Basic statistical analysis of borehole yields for Granites (left) and Greenstone Belt (right).

Geological Units	Yields over 24 duty cycle (l/s)	No. of Boreholes	Percentage
Granites	**>5**	0	0%
	2–5	8	19.5%
	1–2	5	12.2%
	0.5–1	9	22%
	0.1–0.5	12	29.3%
	<0.1	7	17.1%
Total		**41**	**100.00%**
Max	5 ℓ/s		
Min	0.02 ℓ/s		
Average	1.12 ℓ/s		
Median	0.6 ℓ/s		

Geological Units	Yields over 24 duty cycle (l/s)	No. of Boreholes	Percentage
Greenstone Belt	**>5**	0	0%
	2–5	11	12.6%
	1–2	30	34.5%
	0.5–1	14	16.1%
	0.1–0.5	24	27.6%
	<0.1	8	9.2%
Total		**87**	**100.00%**
Maximum	5 ℓ/s		
Minimum	0.02 ℓ/s		
Average	1.14 ℓ/s		
Median	0.8 ℓ/s		

Table 4-3: Basic statistical analysis of borehole yields for Bandelierkop Complex (left) and Goudplats Hout River Gneiss (right).

Geological Units	Yields over 24 duty cycle	No. of Boreholes	Percentage
Bandelierkop Complex	**>5**	0	0%
	2–5	0	0%
	1–2	4	15.4%
	0.5–1	7	27%
	0.1–0.5	12	46.2%
	<0.1	3	11.5%
Total		**26**	**100.00%**
Max	2 ℓ/s		
Min	0.02 ℓ/s		
Average	0.55 ℓ/s		
Median	0.32 ℓ/s		

Geological Units	Yields over 24 duty cycle	No. of Boreholes	Percentage
Goudplaats Hout River Gneiss	**>5**	6	1.2%
	2–5	63	12.9%
	1–2	114	23.5%
	0.5–1	106	21.9%
	0.1–0.5	173	35.7%
	<0.1	23	4.7%
Total		**485**	**100.00%**
Maximum	9 ℓ/s		
Minimum	0.03 ℓ/s		
Average	1.06 ℓ/s		
Median	0.6 ℓ/s		

Table 4-4: Basic statistical analysis of borehole Transmissivity (m^2/day) and Storativity for Granites (left) and Greenstone Belt (right).

Geological Units	Items	Yields over 24 Hrs Duty Cycle	Transmissivity (m2/d)	Storativity
Granites	Total	7		
	Max	3.8	174.1	2.55E-03
	Min	0.4	6.3	2.01E-03
	Average	2.7	63.8	2.26E-03
	Median	3.5	50	2.21E-03

Geological Units	Items	Yields over 24 Hrs Duty Cycle	Transmissivity (m2/d)	Storativity
Greenstone Belt	Total	23		
	Maximum	2.13	95.4	2.35E-03
	Minimum	0.1	2	6.55E-08
	Average	0.97	26.2	8.54E-04
	Median	0.7	23.3	1.86E-06

Table 4-5: Basic statistical analysis of borehole Transmissivity (m^2/day) and Storativity for Bandelierkop Complex (left) and Goudplats Hout River Gneiss (right).

Geological Units	Items	Yields over 24 Hrs Duty Cycle	Transmissivity (m2/d)	Storativity
Bandelierkop Complex	Total	6		
	Max	1.6	40.2	3.30E-03
	Min	0.1	2	2.05E-03
	Average	0.58	10.5	2.53E-03
	Median	0.43	5	2.33E-03

Geological Units	Items	Yields over 24 Hrs Duty Cycle	Transmissivity (m2/d)	Storativity
Goudplaats Hout River Gneisses	Total	30		
	Maximum	5.96	176.2	1.44E-03
	Minimum	0.12	0.9	2.70E-03
	Average	1.5	32.6	2.27E-03
	Median	0.685	13.05	2.26E-03

Hydraulic conductivity values of the fractured crystalline basement rocks range between 1E-07 and 1E-04 m/s (Dewandel, 2012; Taylor and Howard, 2000; Houston and Lewis, 1988; Jones, 1985). The 3rd or bottom layer (fractured zone) was assigned with values in the order of 1E-5 m/s (granites), 1E-6 m/s (gneisses and greenstone belt), and 1E-7 m/s (Bandelierkop complex). The vertical hydraulic conductivity (KZ) for various lithological units was assumed to be 1/10th of the horizontal hydraulic conductivity (KH). Table 4-7 presents the hydraulic conductivities of different lithological units.

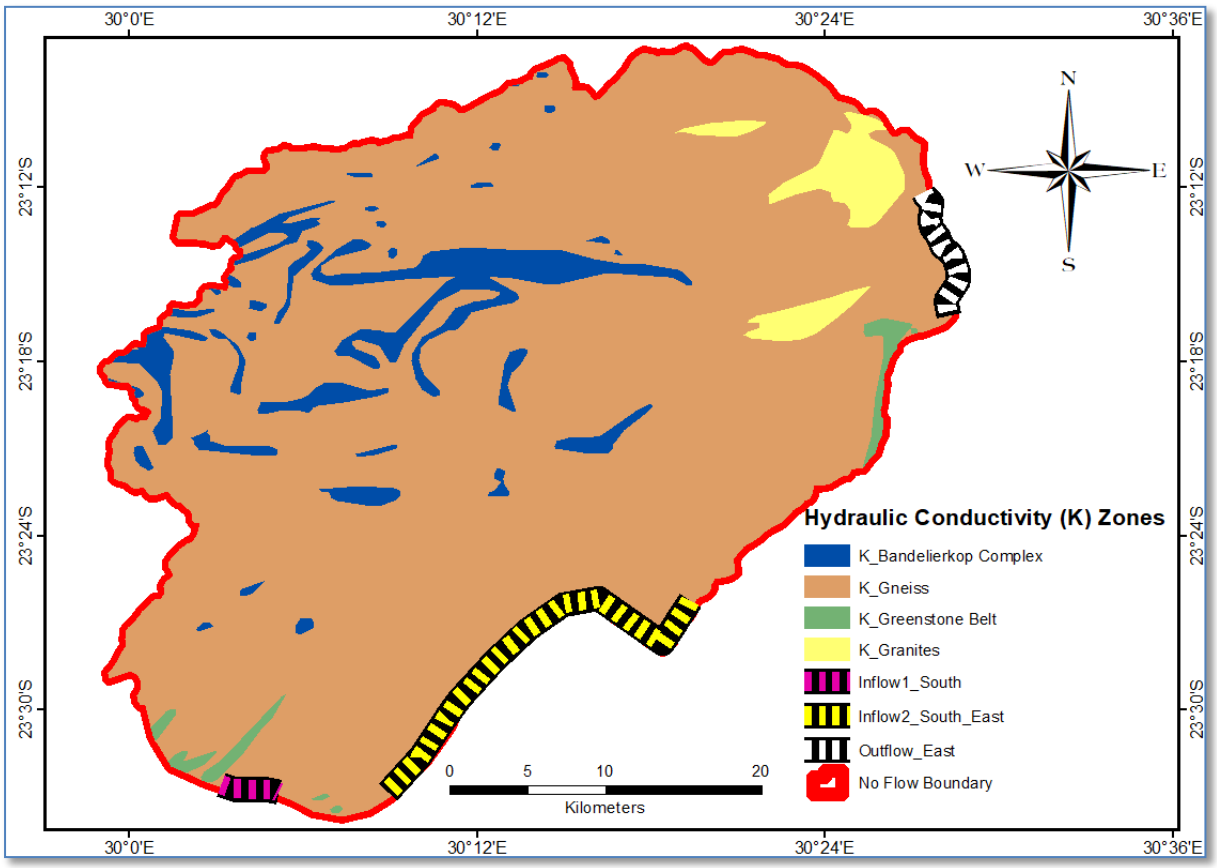

Figure 4-7: Map showing the distribution of the hydraulic conductive zones in the model domain area.

Table 4-6: Initial horizontal hydraulic conductivities (KH) for different soils occurring in the study area, unit: m/s.

Soils	KH_Layer1 (Soil)
Sandy Clayey	1.28E-04
Sandy Loam	1.85E-04
Sand	2.41E-04

Table 4-7: Initial horizontal hydraulic conductivities (KH) for different lithological units occurring in the study area, unit: m/s.

Lithological Units	KH_Layer2 (Weathered Zone)	KH_Layer3 (Fractured zone)
Intrusive Granites	1.00E-07	1.00E-05
Bandelierkop Complex	1.00E-07	1.00E-07
Goudplaats Gneiss	1.00E-07	1.00E-06
Greenstone Belt	1.00E-07	1.00E-06

4.6.4.5 Internal Stresses

4.6.4.5.1 River and Aquifer Interactions

Rivers and streams may interact with groundwater by either gaining or losing water from the aquifer through the riverbed. The study area is drained by two perennial rivers (Middle and Klein Letaba) and their non-perennial tributaries (Mosukodutsi, Soeketse, and Lebjelebore). Groundwater flow map of the area indicates that some tributaries of the main rivers seem to influence the underlying aquifer system where local flow conditions are observed. In areas where major shear zones occur along the rivers, local flow vectors (Figure 4-1) are observed to feed into these rivers. The River (RIV) Package was used to simulate the exchange between surface water (i.e., rivers or dams) and groundwater aquifers (McDonald and Harbaugh, 1988; Anderson and Woessner, 1992).

The RIV package uses the conductance of the streambed (CRIV) to account for the length (L) and width (W) of the river channel in the cell, the thickness of the riverbed sediments (M), and their vertical hydraulic conductivity (K). The Flow between the groundwater and the river in each cell was determined using the equation below (Langevin *et al.*, 2017):

$$CRIV = \frac{KLW}{M}$$

The rivers that fall within the model domain were added to the model using the RIV package to simulate the interaction between the rivers and aquifers. The rivers were imported as shapefiles using ModelMuse and converted to river objects which are readable by the MODFLOW. The gauging station (B8H014) located at Groot Letaba River was considered as an upstream gauging to estimate the river recharge into the model domain. From this station, the river recharge was estimated at 3.47E+10 m^3/a. Data recorded from gauging station B8H033 downstream of the model domain at Klein Letaba River indicate that the river discharge is at approximately 1.94E+10 m^3/a. The river stage and depths of the river bottom were determined and defined with respect to the surface topography. Hydraulic conductivity (K) = was assumed to be 1/100 of the hydraulic conductivity of the surrounding rocks (i.e. Goudplaats Hout River Gneiss). This assumption is based on the fact that riverbed often consists of fine to very fine sedimentary particles such as clay and siltstone beneath the sandy material. The hydraulic conductivity of such material is generally in the order of $1/10^{th}$ to $1/100^{th}$ lower than the surrounding rocks. The width of the river varies along the river course, and Google Earth Pro was used to trace the width of the river, and a polygon was created to determine the surface area of the river. Figure 4-7 shows the positions of the gauging stations where time-series data has been recorded and river polygons were traced to estimate the conductance of the river bottom.

4.6.4.5.2 Dam and Aquifer Interaction

The dams in the study area have a fundamental effect on water resource development and supplies in the Klein Letaba River catchment. For simulating the interaction between the Middle Letaba Dam and the surrounding aquifers, the general head boundary (GHB) was chosen to be the most suitable package as compared to the reservoir (RES) package.

GHB package offers the most generic tool to surface water and groundwater modelling based on its capabilities to account for surface water and subsurface fluxes in and out of the dam (EES, 2000). In addition, this package takes into cognisance the dam water level fluctuations which may occur due to climate change and the interaction with groundwater through the bottom of the dam.

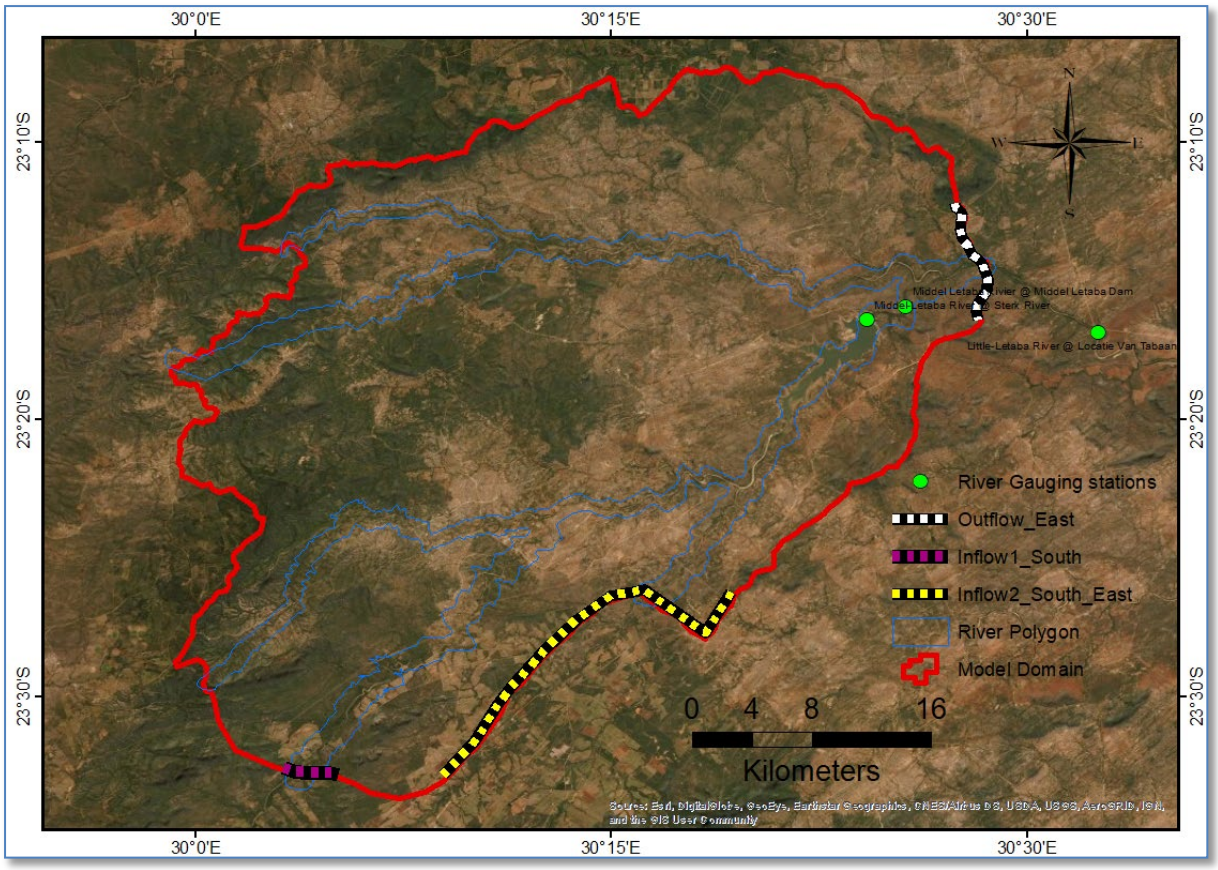

Figure 4-8: Google image showing river polygon, gauging stations, inflows and outflows boundaries.

The interaction of water between the dam and the surrounding aquifers is quantified by determining the conductance of the material that separates the dam and the aquifer. This was done by using the following formulation (Langevin *et al*., 2017):

$$Cb = \frac{KLW}{M}$$

The parameters used are the same as the ones for the river conductance described in section 4.6.4.51. Hydraulic conductivity (K) was assumed to be in the range between 1/100 of the hydraulic conductivity of the surrounding rocks. This assumption is based on the fact that the bottom of the dam often consists of fine to very fine sedimentary particles such as clay and siltstone. The hydraulic conductivity of such material is generally significantly lower than the surrounding rocks.

4.6.4.5.3 Borehole Abstractions

Boreholes are point sources that withdraw water from the model domain area. The significant withdrawal of the volume of water imposes huge stress on the groundwater system. The pumping rate (Q) in units of volume of water per time is specified. The groundwater abstraction boreholes drilled for community bulk water supply and agricultural purposes are simulated using the Well package. The abstraction rates from these boreholes range from 1.73E+02 m^3/day to 8.64E+02 m^3/day, with a total abstraction of 5.70E+03 m^3/a (Table 4-8). These boreholes are believed to be the ones imposing a significant amount of stress on the groundwater system. The rate of abstraction was specified for each of the boreholes. A negative value was applied for the estimated abstraction rate (Q) to indicate that it represents the withdrawal of water from the aquifer.

Table 4-8: Groundwater abstraction boreholes.

Bh ID	Water Use Sector	Latitude	Longitude	Abstraction Volumes (m^3/annum)	Abstraction Volumes (m^3/day)
BH 2	Agricultural Irrigation	-23.50975	30.09664	6.59E+04	1.73E+02
BH 5	Agricultural Irrigation	-23.21319	30.12340	8.00E+04	2.59E+02
BH 6	Agricultural Irrigation	-23.30558	30.29744	9.00E+04	2.59E+02
BH 7	Agricultural Irrigation	-23.45496	30.16581	9.12E+04	2.59E+02
BH 9	Agricultural Irrigation	-23.45653	30.18658	1.00E+05	2.59E+02
BH 10	Agricultural Irrigation	-23.52728	30.14697	1.01E+05	2.59E+02
BH 13	Agricultural Irrigation	-23.50339	30.15947	1.87E+05	5.18E+02
BH 14	Agricultural Irrigation	-23.15728	30.32636	2.00E+05	5.18E+02
BH 15	Agricultural Irrigation	-23.49153	30.13714	2.40E+05	6.91E+02
BH 16	Agricultural Irrigation	-23.13239	30.24561	2.77E+05	7.78E+02
BH 17	Water Supply Service	-23.19000	30.45000	3.04E+05	8.64E+02
BH 18	Agricultural Irrigation	-23.54425	30.07369	3.24E+05	8.64E+02
			Totals	**2.06E+06**	**5.70E+03**

4.6.4.6 External Stresses

4.6.4.6.1 Evapotranspiration (EVT) Package

The EVT package simulates the influence of plant transpiration and direct evaporation removing water from the groundwater system (McDonald and Harbaugh, 1988; Anderson and Woessener, 1992). Evapotranspiration was using FOA Penman-Montheith Method (Allen *et al.,* 1998) that expresses the reference evapotranspiration (ET_0), based on several parameters which include precipitation, temperature, relative humidity, and wind speed, among others. The actual evapotranspiration (ETa) was calculated as a function of the crop evapotranspiration coefficient and ETo. The vegetation coefficient (Kc) ratio of 0.75 corresponding to the woodland bush that largely covers the model area was applied to calculate ETa, which is given as (Allen *et al*., 1998):

ETa = ETo x Kc

The Evaporation package (EVT) was applied over the top of the model to simulate the amount of water lost from the aquifer system due to evaporation and transpiration processes.

4.6.4.6.2 General Head Boundaries

The general head boundaries (GHB) are the inflows in the south and an outflow located in the north eastern part of the model area. These boundaries were defined based on the hydraulic heads, hydrochemical, and stable isotope data as discussed in section 4.5.4.2. The flux across the GHB was calculated using the following equation (Langevin *et al.*, 2017);

$$Qb = Cb\ (Hsource - H)$$

$$Cb = \frac{Qb}{(Hsource - H)}$$

4.6.4.7 Water Balance Estimation

The water budget is essential for examining a hydrogeological system because it allows for the quantification of water flow in and out of the system (Anderson and Woessner, 1992).

The quantification of water balance components is important for the conceptualisation of the water resource systems and is used as first-hand information regarding the initial values of input parameters that are required for further numerical groundwater flow modelling (Weitz, 2016). Water balance estimation provides a basic structure for evaluating the hydrological behavior of a catchment and can also be used to identify changes in the water balance components (Zhang *et al.,* 1999).

Water balance involves estimating the volume of water entering and leaving the aquifer system in the model domain. It is based on the concept that enables the balance of the inflows and the outflows to and from the aquifer system, respectively. Inflows include groundwater recharge and river inflow into groundwater, while outflows include evapotranspiration, surface runoff, baseflow, and groundwater abstraction through pumping. Rainfall is the main source of recharge in the study area. The estimated parameters used for the water balance are based on the DWS (2015) estimates of the two Quaternary catchments of B82D and B82F, which largely cover the model domain. However, the river inflow is estimated using the flow rate recorded at the upstream gauging station (B8H014). The water balance equation can be expressed as;

Inflows – outflows = 0

Where,

Inflows = ($R_p + R_r$)

Outflows = ($E_a + R_s + G_WB_f + GW_{abs}$)

R_p = Estimated rainfall recharge; R_r = River Recharge; GwB_f = Base flow; E_a = Estimated evapotranspiration; R_s = Surface runoff; GW_{abs} = Groundwater Abstractions. The water balance results indicate that the study area exhibits a positive water balance with insignificant differences between the inflows and the outflows (Table 4-9).

Table 4-9: Water Balance for the model domain area.

Inflows (m^3/day)		Outflows (m^3/day)	
Rainfall recharge	3.37671E+04	Surface runoff	5.95068E+04
		Groundwater Base flow	7.73973E+03
River recharge	7.04160E+04	Evapotranspiration	2.60274E+04
		Groundwater Abstractions	1.00822E+04
Total Inflows	**1.04183E+05**	**Total Outflows**	**1.03356E+05**

4.6.5 Development of Numerical model

The conceptual model discussed in section 4.5.4.7 above will be translated into a numerical model based on MODFLOW NWT. MODFLOW NWT is the same version as MODFLOW 2005 but minimises the impacts of dry cells.

This was carried out by activating appropriate packages to simulate the flow dynamics (i.e. interaction of water between dams, rivers, and aquifers) and characterise the flow conditions in the study area. Input data files for each package were imported as shapefiles using ModelMuse and stored as the object which is directly readable by MODFLOW NWT.

4.6.5.1 Flow packages

MODFLOW-NWT along with its flow package, i.e., upstream weighting package (UPW) was used to characterise the groundwater flow conditions for the area. MODFLOW-NWT is described by Niswonger *et al*., (2011), as a Newton-Raphson formulation for MODFLOW-2005. It is a free-standing program that is used for solving problems involving drying and rewetting nonlinearities of the unconfined groundwater-flow equation (Niswonger *et al*.,2011).

According to Hunt and Feinstein (2012), MODFLOW-NWT provides vigorous management of dry cells, previously unavailable to a generation of MODFLOW versions (e.g., MODFLOW 2005).

This formulation solves the potential for unrealistic loss of recharge that can occur with dry cells. If a cell is dry (that is, the head is below the cell bottom) and underlain by a fully or partially saturated cell, its horizontal conductance will be 0 and the head in the dry cell can be calculated in terms of the sum of inflow to the cell from adjacent cells and external sources (Niswonger *et al*., 2011). The packages used include the Upstream Weighting Package (UPW) and Discretisation (DIS).

4.6.5.2 Layer Definition

The numerical model was defined as a three-layer model based on the Hydrostratigraphic Unit and local physical boundaries described in section 4.5.4. The 1st model layer consists of soil and the upper surface of the 1st layer was defined based on the topographic surface derived from the ASTER Digital Elevation Model. The lower surface of the top layer was determined from drilling log data obtained from boreholes drilled in the model domain area. The upper surface of the 2nd layer coincides with the lower surface of the 1st layer, which in turn is bounded above by the topographic surface. Depth from the surface to the bottom of the 2nd layer was determined by subtracting the lower boundary (determined from the borehole log) from the model top. This depth represents the bottom of the semi-confined layer. With the upper surface of the 3rd layer coinciding with the bottom surface of the 2nd layer, the lowest boundary of the model was defined by subtracting the model top from the bottom of layer 3 (determined from the borehole log). The bottom of 3rd layer represents the bottom of a confining layer or no-flow boundary condition.

4.6.5.3 Head Observations

The study area has a limited number of observation wells, a total of 5 were used for steady-state calibration (Table 4-10). Groundwater level monitoring in most of these boreholes is believed to have commenced between 2004 and 2006. In general, the groundwater level was constantly monitored, but there were a few instances where data was not recorded due to challenges such as failure or replacement of the level loggers. The selection of the observation boreholes was based on the availability of consistent monitoring data.

To keep the data consistent, model top data was extracted and applied as the borehole elevation data for each borehole.

Table 4-10: Observation head boreholes.

BH ID	Latitudes	Longitudes	X	Y	Water Level Observation (mamsl)	Screen Depth Elevation (mamsl)
BH 1	-23.20531	30.14028	207292	7430872	598	576
BH 2	-23.26800	30.38180	232151	7424394	511	500
BH 3	-23.46550	30.15652	209523	7402076	627	535
BH 4	-23.34400	29.99800	193039	7415210	959	951
BH 5	-23.24500	30.47400	241543	7427109	473	469

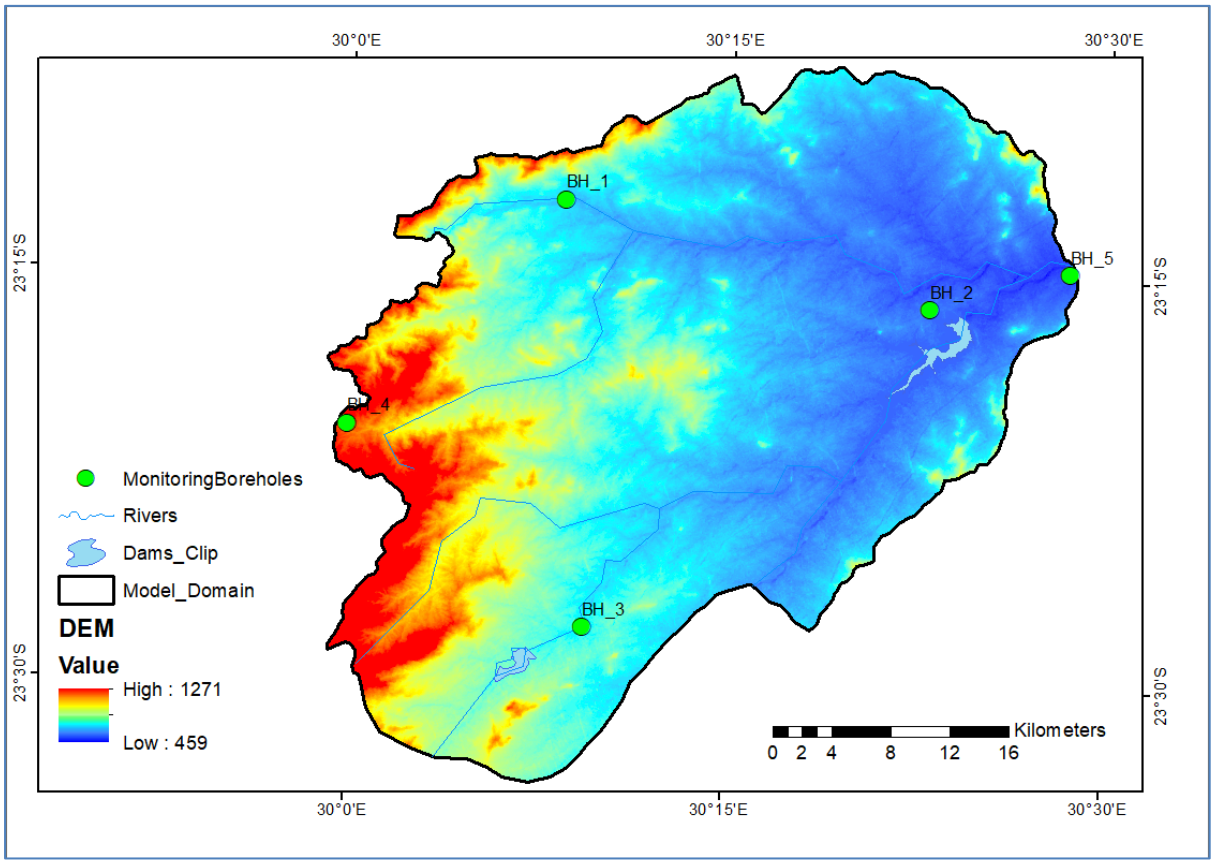

Figure 4-9 A: Model grids with rivers and refinements along the main dam.

4.6.5.4 Steady-state model

4.6.5.4.1 Grid Setting

The model domain covers an area of 1551 sq. km, and it was discretised with a regular grid of 100 m × 1 00 m mesh size, which consists of 610 rows and 634 columns (Figure 4-8B). The refinements with a grid cell size of 25 m X 25 m were done corresponding to the dam to improve the spatial resolution of the simulated head. Finally, a total of 155100 active cells are included in each model layer. This grid size was determined to be appropriate for the level of detail required for this study.

4.6.5.4.2 The solver used

MODFLOW NWT solver was utilised to solve the finite difference equations in each step of the MODFLOW stress period. A maximum number of outer iterations, flux tolerance, and head tolerance were set to 250, 0.06, and 0.0001, respectively. In addition, the optional simple model complexity was chosen, and this allowed the model run and convergence to be successful.

4.6.5.4.3 Sensitivity Analysis

Sensitivity analysis uses observation values (OBS) to determine the parameters that have major effects on the model output such as the simulated heads. In other words, it diagnoses the amount of error introduced into the simulated heads. It is the method of evaluating model input parameters to see how small changes in parameters affect model output (e.g., head and flows).

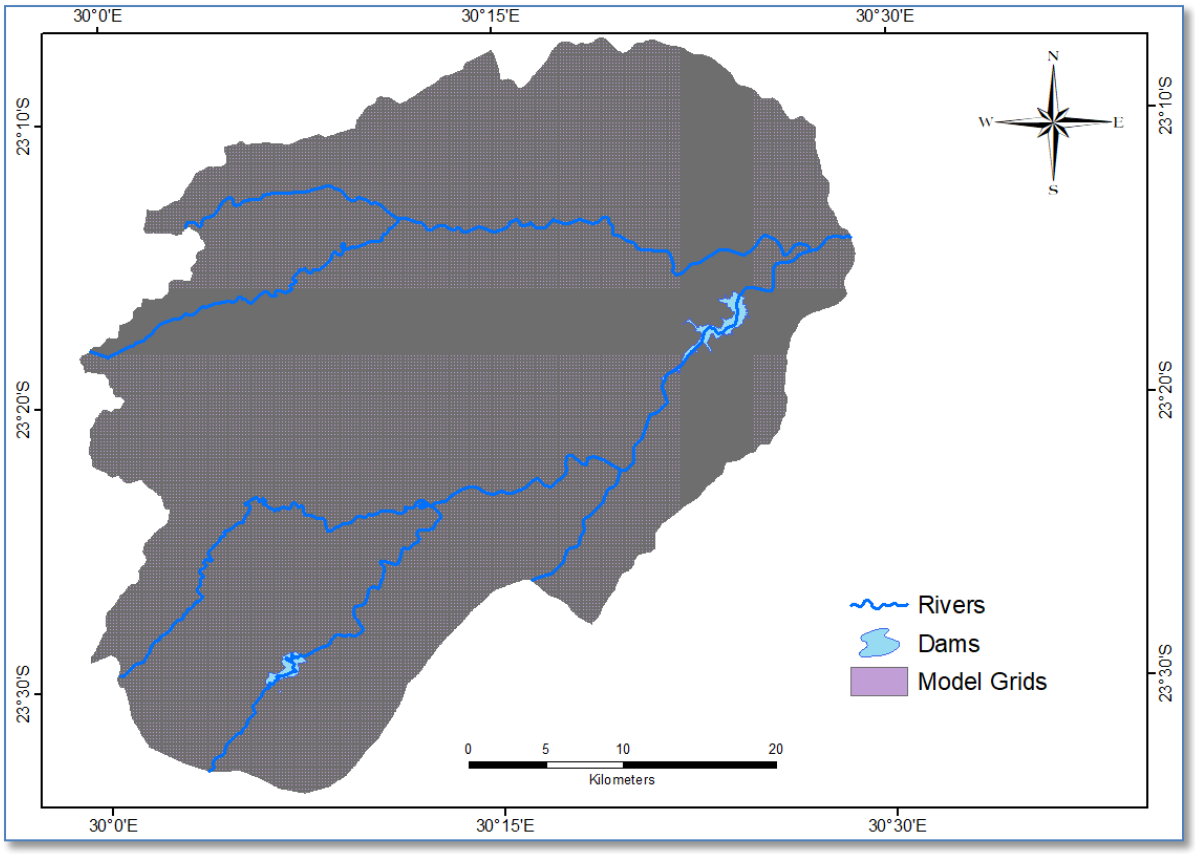

Figure 4-10B: Model grids with rivers and refinements along the main dam.

In this study, sensitivity analysis was carried out by changing parameters (e.g., hydraulic conductivity of different layers, recharge, evapotranspiration, conductance of the bottom of the dam, conductance of the riverbed, and abstraction of boreholes). Each of the parameters was adjusted by -25%; -50%; -75%; -95%; +25%; +50%; +75% and +95% and the corresponding RMS was used to evaluate the sensitivity of the model against parameter change.

Results are presented in Figure 4-9 and Table 4-11 (RMS vs % of the change in parameter). The results enabled the evaluation and identification of the parameters that make the model most sensitive.

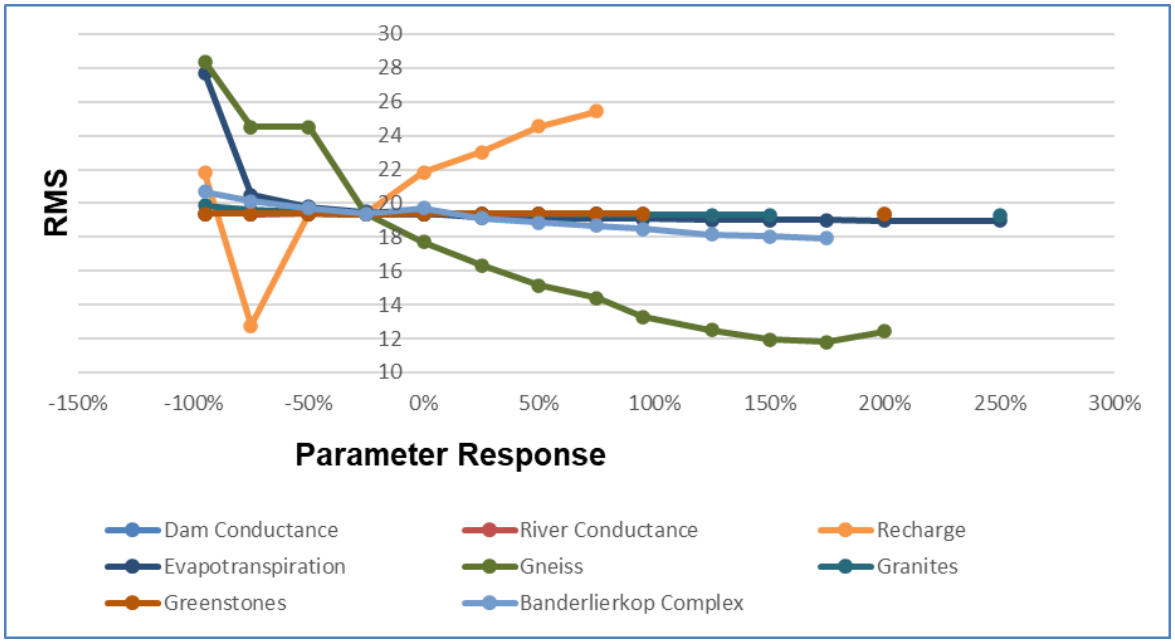

Figure 4-11: Results of sensitivity analysis of the model showing RMS vs % of change in parameters.

4.6.5.4.4 Steady State Model Calibration

Model calibration involves modifying the model's input parameters (e.g., hydraulic conductivity, borehole abstraction rates or recharge rate) and boundary conditions (head or flux) to obtain the level of fitness to the observed data (e.g., flow rate, hydraulic head, etc.) in a real groundwater system (Anderson *et al.*, 2015). Model calibration is usually a trial-and-error process involving the adjustment of model parameters to achieve a reasonable fit between predicted (model results) and observed (real-world) conditions. A successfully calibrated model is achieved by obtaining a set of parameters and boundary conditions that best fit the observed values within a reasonable error range (Anderson and Woessner, 1992).

In this study, the model calibration was conducted to reduce the error and indicate that the model is capable of producing field measurements heads and flows. This was done by reasonably adjusting parameter values (e.g., RCH, EVT, and K) one by one in a sequential manner within a pre-determined range of error criteria until the best fit is obtained between the simulated and the observed heads and flows. The level of the inconsistencies between the simulated and observed heads was evaluated using objective functions as summarised below.

Table 4-11: Results of sensitivity analysis showing RMS and % of change in parameters.

Response of Parameters (%)			Hydraulic Conductivities (m/s)						Root Mean Square (RMS)							
	RCH	EVT	Granite	Gneiss	Greenstone	Bandelierkop Complex	Dam	RIV	RCH	EVT	Granites	Gneiss	Green Stones	Banderlierkop Complex	Dam	RIV
-95%	5E-11	1.48E-09	5.00E-07	5.00E-08	5.00E-08	2.50E-08	2.30E-03	1.10E-03	ERROR	27.7	19.9	Error	Error	Error	19.4	19.3
-75%	2.5E-10	7.4E-09	2.50E-06	2.50E-07	2.50E-07	1.25E-07	1.15E-02	5.50E-03	21.8	20.5	19.6	28.4	19.4	20.7	19.4	19.4
-50%	5E-10	1.48E-08	5.00E-06	5.00E-07	5.00E-07	2.50E-07	2.30E-02	1.10E-02	12.8	19.8	19.5	24.5	19.4	20.1	19.4	19.4
-25%	7.5E-10	2.22E-08	7.50E-06	7.50E-07	7.50E-07	3.75E-07	3.45E-02	1.65E-02	19.4	19.5	19.4	24.5	19.4	19.7	19.4	19.4
0%	**1.00E-09**	**2.96E-08**	**1.00E-05**	**1.00E-06**	**1.00E-06**	**5.00E-07**	**4.60E-02**	**2.20E-02**	**19.4**	**19.4**	**19.4**	**19.4**	**19.4**	**19.4**	**19.4**	**19.4**
25%	1.25E-09	3.70E-08	1.25E-05	1.25E-06	1.25E-06	6.25E-07	5.75E-02	2.75E-02	21.8	19.2	19.4	17.7	19.4	19.7	19.4	19.4
50%	1.5E-09	4.44E-08	1.50E-05	1.50E-06	1.50E-06	7.50E-07	6.90E-02	3.30E-02	23.0	19.1	19.3	16.3	19.4	19.1	19.4	19.4
75%	1.8E-09	5.18E-08	1.75E-05	1.75E-06	1.75E-06	8.75E-07	8.05E-02	3.85E-02	24.6	19.1	19.3	15.2	19.4	18.9	19.4	19.4
95%	1.95E-09	5.77E-08	1.95E-05	1.95E-06	1.95E-06	9.75E-07	1.04E-01	4.29E-02	25.5	19.1	19.3	14.4	19.4	18.7	19.4	19.4
125%		6.66E-08	2.25E-05	2.25E-06	2.25E-06	1.13E-06				19.0	19.3	13.3	19.4	18.5		
150%		7.40E-08	2.50E-05	2.50E-06	2.50E-06	1.25E-06				19.0	19.3	12.5		18.2		
175%		8.14E-08	2.75E-05	2.75E-06	2.75E-06	1.38E-06				19.0		11.9		18.0		
200%		8.88E-08	3.00E-05	3.00E-06	3.00E-06	1.50E-06				19.0		11.8		17.9		
250%		1.00E-07	3.50E-05	3.50E-06	3.50E-06	1.75E-06				19.0	19.3	12.4	19.4	17.7		

4.6.5.4.5 Steady-state Error Estimation

The error quantification methods that are generally applied include mean error (ME), mean absolute error (MAE) and root mean squared error (RMS). A scatter plot of observed against simulated heads is another way of visual evaluation of the level of fit between the simulated and observed heads.

The root mean square error (RMS) provides the average of the square difference between the observed and simulated heads and can be expressed as (Aghlamand and Abbasi, 2019): $RMS = \left(\frac{1}{n}\sum_{i=1}^{n}(Obsei - Simi)^{0.5}\right)$

The mean absolute error (MAE) is the absolute value of the difference between the observed and simulated heads, which can be expressed as (Aghlamand and Abbasi, 2019): $MAE = \frac{1}{n}\left(\sum_{i=1}^{n}\left|Obsei - Simi\right|\right)$

The mean error (ME) is the average of the absolute non-squared error expressed as (Aghlamand and Abbasi, 2019): $ME = \frac{1}{n}\left(\sum_{i=1}^{n}\left(Obsei - Simi\right)\right)$

Where Obsei is the observed head and Simi is the simulated heads.

CHAPTER 5 : HYDROCHEMISTRY AND ENVIRONMENTAL ISOTOPES

5.1 Introduction

Hydrochemistry and environmental isotope data have a wide range of applications in hydrogeological studies. Both data sets enable us to comprehend the processes that occur in the hydrologic cycle. They provide valuable information about groundwater origin, flow direction, trace the source of water, the dynamics of interaction between groundwater and surface water (Ayuba *et al*., 2019; Zhou *et al*., 2017 and Kumar, 2013). Furthermore, hydrochemistry and environmental isotopes are important to constrain boundary conditions such as inflow and outflow boundaries of the conceptual model of groundwater flow (Demiroglu, 2017; Günay, 2006 and Deak, 1978, 1999).

In this study, the major ions and physical parameters of water were used to assess the chemical characteristics of water in the study area. In addition, these data sets were used to construct the conceptual model of groundwater flow, and understand the interaction between groundwater and surface water, thereby evaluating the impacts of these processes on the availability of a sustainable source of water in the area.

5.2 Hydrochemistry

The chemical properties of water are essential in determining its fitness for drinking and industrial use. When rainwater flows downward, before it reaches the saturated zone, it reacts with the surrounding rocks, and this process results in a change in the chemistry of infiltrating water along the flow path (Mazor, 2004). Thus, the composition of water provides information about the types of rocks the percolating water interacted, with and the length of time it resided along the flow path.

This process results in the enrichment or depletion of certain elements as water flows from one region to another allowing the chemical fingerprint to be used for the conceptualisation of groundwater flow mode (Mazor, 1991). To evaluate the hydrochemistry of the water resource in the study area, a historical dataset with borehole records from the GRIP database, and new datasets collected by the Council for Geoscience as well as data gathered during the present study were used.

Prior to further data processing, chemical data with values below detection limits were deleted. This was followed by the determination of ion balance to evaluate the reliability and validity of the hydrochemical data for the characterisation of the water quality in the area.

Hydrochemical data from the GRIP database was used to trace the groundwater flow path to ascertain the inflows and outflows boundaries (Figure 5-1). The results (see section 4.5.4 and Table 5-1), indicate that the ratios of Na/HO_3 and EC/TDS are low along the southwest inflow boundary, while the ratio of Ca+Mg/Na+K is high. As the distance increases towards the downstream, which is presumably the outflow boundary, the Na/HO_3 and EC/TDS ratios tend to increase, while Ca/Mg and Ca+Mg/Na+K decrease towards the discharge area in the northeastern part of the model domain. These results are consistent with the change in topographic elevation almost matching the groundwater level at the outflow boundary. Table 5-1 shows ratios of major ions and physical parameters used to ascertain the inflow and the outflow boundaries.

Electrical conductivity (EC) is generally associated with the presence of major ions and associated chemical species in groundwater (DWAF, 1996), which makes groundwater electrically conductive. EC indicates the amount of total dissolved salts (TDS) in water. The EC in the study area varies from 17 to 272 mS/m with a mean value of 77.14 mS/m. According to the SANS (2015), the recommended EC of water used for drinking purposes is ≤170 mS/m. EC values of water in the study area are below the recommended limit.

The total dissolved solids (TDS) is the measure of the amount of various inorganic salts dissolved in water (DWAF, 1996). In the model domain area, the TDS concentrations in the water vary from 112 to 1768 mg/l with an average of 501 mg/l. Of the 246 samples, 52 samples exceeded the recommended SANS 241 (2015) limit of ≤1200 mg/l. The ratio of EC to TDS is one of the key parameters that are used to define the inflow and outflow boundaries.

Table 5-1: The ratios of major ions and physical parameters.

Bh_No	Latitude	Longitude	Ca/ Mg	Na/ HCO3	(Ca+Mg)/ (Na+K)	EC	TDS
H10-0186	-23.46027	30.15333	1.08	0.07	2.10	64.40	418.60
H10-0670	-23.45636	30.15051	1.25	0.11	2.60	142.00	923.00
H10-0100	-23.45478	30.14419	1.63	0.06	2.15	80.50	523.25
H10-0682	-23.45341	30.16388	1.22	0.08	1.48	68.70	446.55
H10-0683	-23.45336	30.16452	1.10	0.10	1.42	72.60	471.90
H10-0034	-23.44669	30.16244	0.91	0.08	1.73	78.90	512.85
H10-0672	-23.44638	30.16969	0.75	0.07	1.65	55.80	362.70
H10-0461	-23.43619	30.15955	0.86	0.07	1.72	70.40	457.60
H10-0776	-23.45441	30.16286	1.28	0.12	1.02	72.20	469.30
H10-0076	-23.41133	30.19636	1.02	0.17	1.40	122.40	795.60
H10-0593	-23.41108	30.21327	1.37	0.16	1.74	141.00	916.50
H10-0671	-23.38891	30.23844	0.93	0.22	1.53	234.00	1521.0
H10-0205	-23.36580	30.29497	1.06	0.09	1.69	55.00	357.50
H14-0768	-23.27270	30.40875	2.83	0.20	0.45	100.20	651.30
H20-0596	-23.24060	30.43560	1.86	0.08	1.60	54.60	354.90

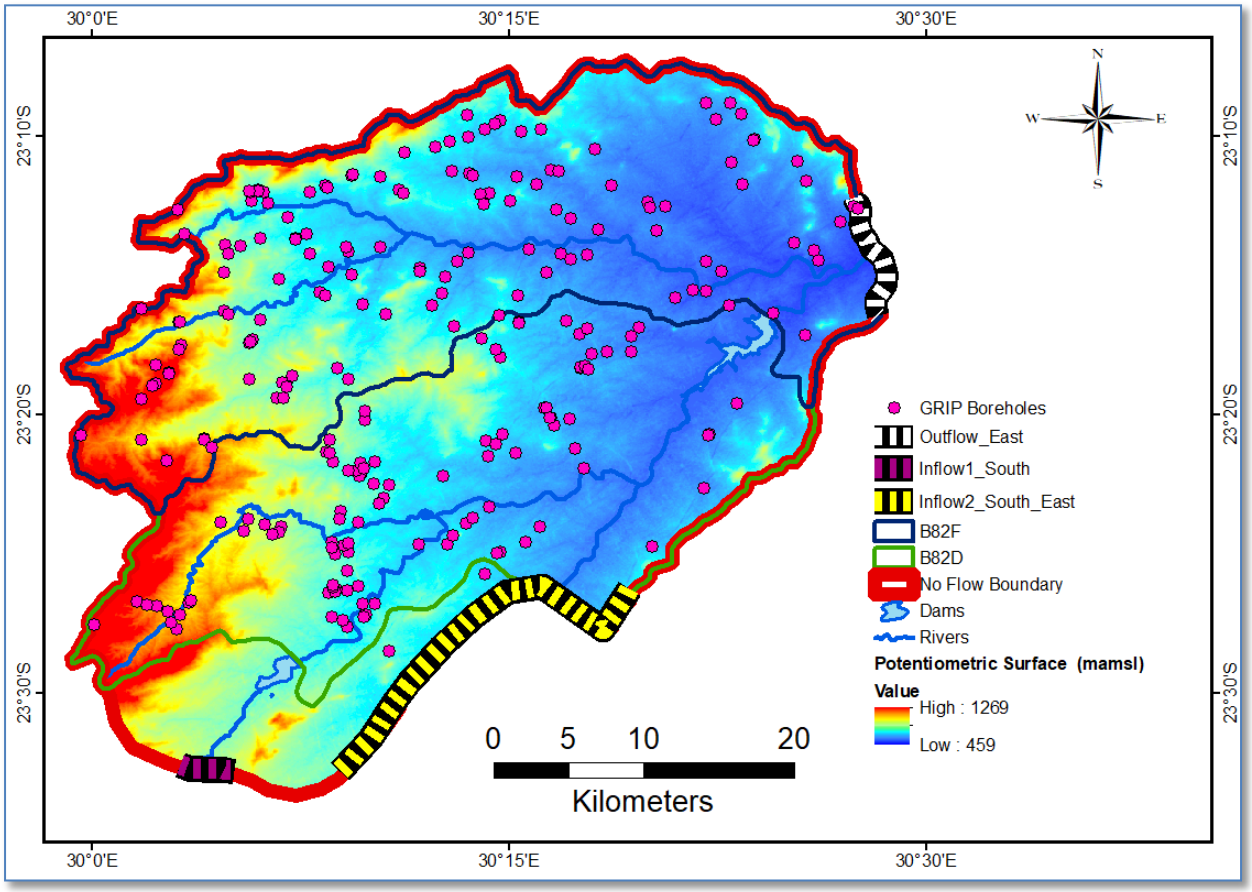

Figure 5-1: Map showing the location of boreholes used to constrain the inflow and outflow boundaries.

The ratio increases from south to north along the groundwater and surface water flow direction. This implies that the amount of dissolved chemicals in groundwater increases northward making groundwater more electrically conductive along the outflow than the inflow boundary.

As water flows from surface to subsurface, it undergoes continuous chemical reactions which give rise to the development of complex chemical composition, which varies from the surface to deep aquifers. Thus, the composition of groundwater emulates both the geochemistry of the watershed and the processes of rainfall and evapotranspiration (Harris, 2009). Figure 5-2A and B show the major ions composition of groundwater within the model domain dominantly composed of Mg-Ca-HCO_3. The results suggest that most of the aquifers are shallow and recently recharged water. These water types suggest that various processes control the groundwater chemistry as the water flows downward and laterally from one region to the other.

As the water flows from the southwest across the inflow to the outflow boundary, it gradually evolves in composition due to rock-water interaction, ion-exchange processes, and anthropogenic influences (Figure 5-3). As a result of these, the recharge zone situated in the southwestern part of the model domain is typically characterised by Mg- Ca-HO_3 water type, while the composition of groundwater across the outflow boundary exhibits Mg-Ca-Na-HCO_3-Cl, Mg-Ca-Na-HCO_3, Mg-Ca-HCO_3-Cl, and Na-HCO_3.

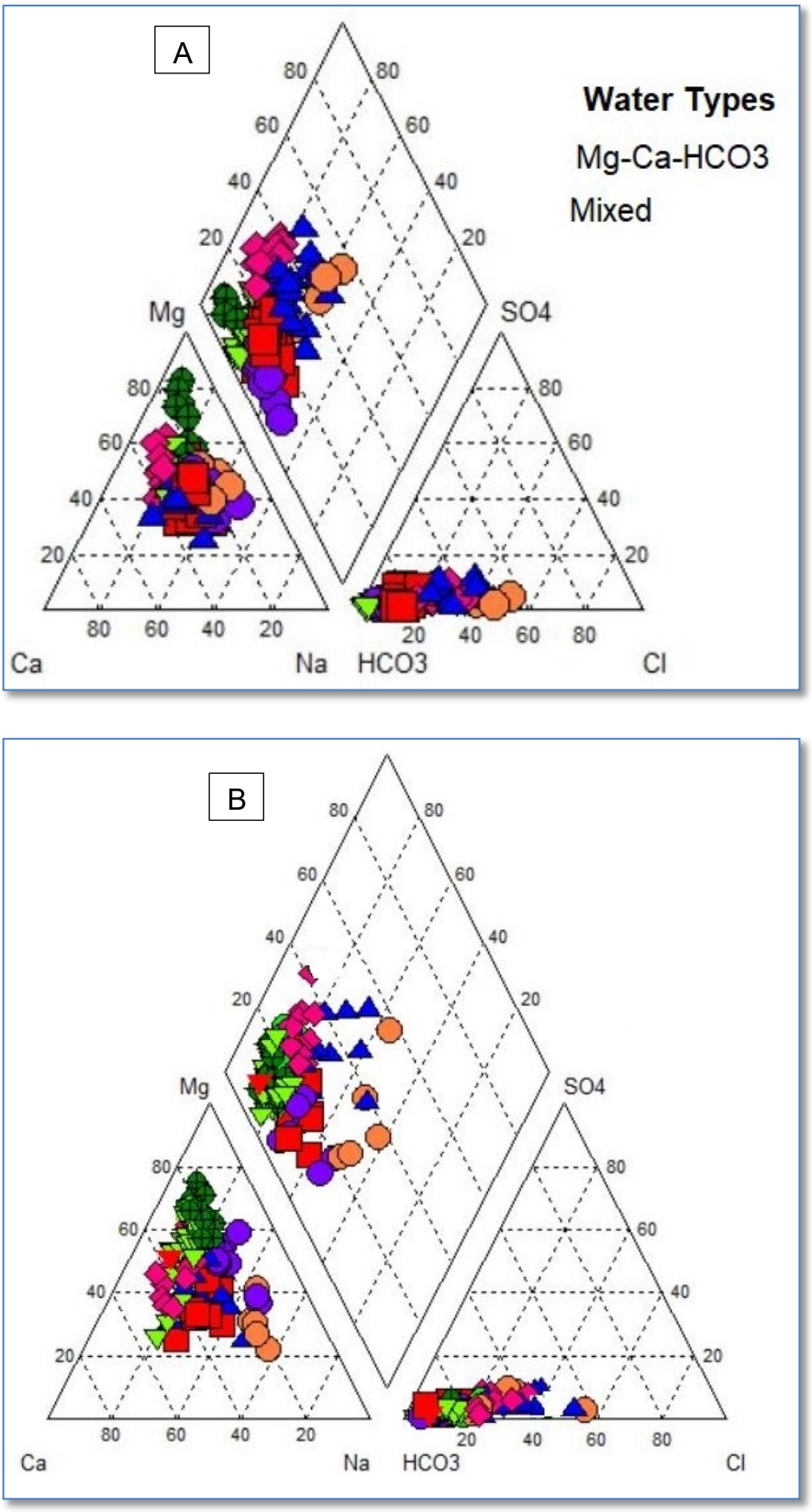

Figure 5-2: Piper diagrams showing hydrochemical characteristics of groundwater in (A) Quaternary catchment B82D and (B) Quaternary catchment B82F.

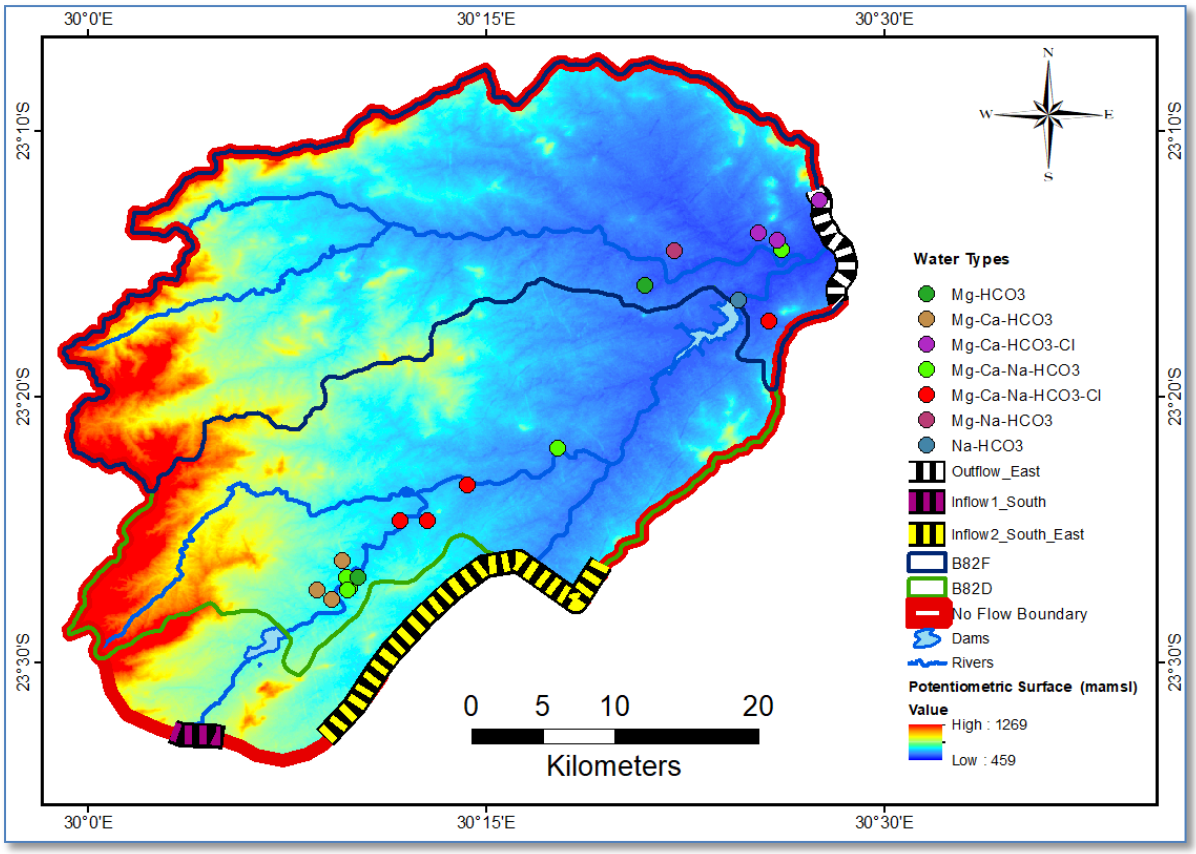

Figure 5-3: The distribution of the various water types across the inflows and outflows boundaries.

The comparison of the composition of water across the outflow boundary (Figure 5-4B) with the inflow boundary (Figure 5-4 A), suggests that ion exchange processes such as sorption and adsorption might have played a significant role in chemical changes as water flows from southwest (inflow) to northeast (outflow boundary). The hydrochemistry corresponding to the inflows and outflow boundaries is shown on Figure 5-4 A and Figure 5-4B.

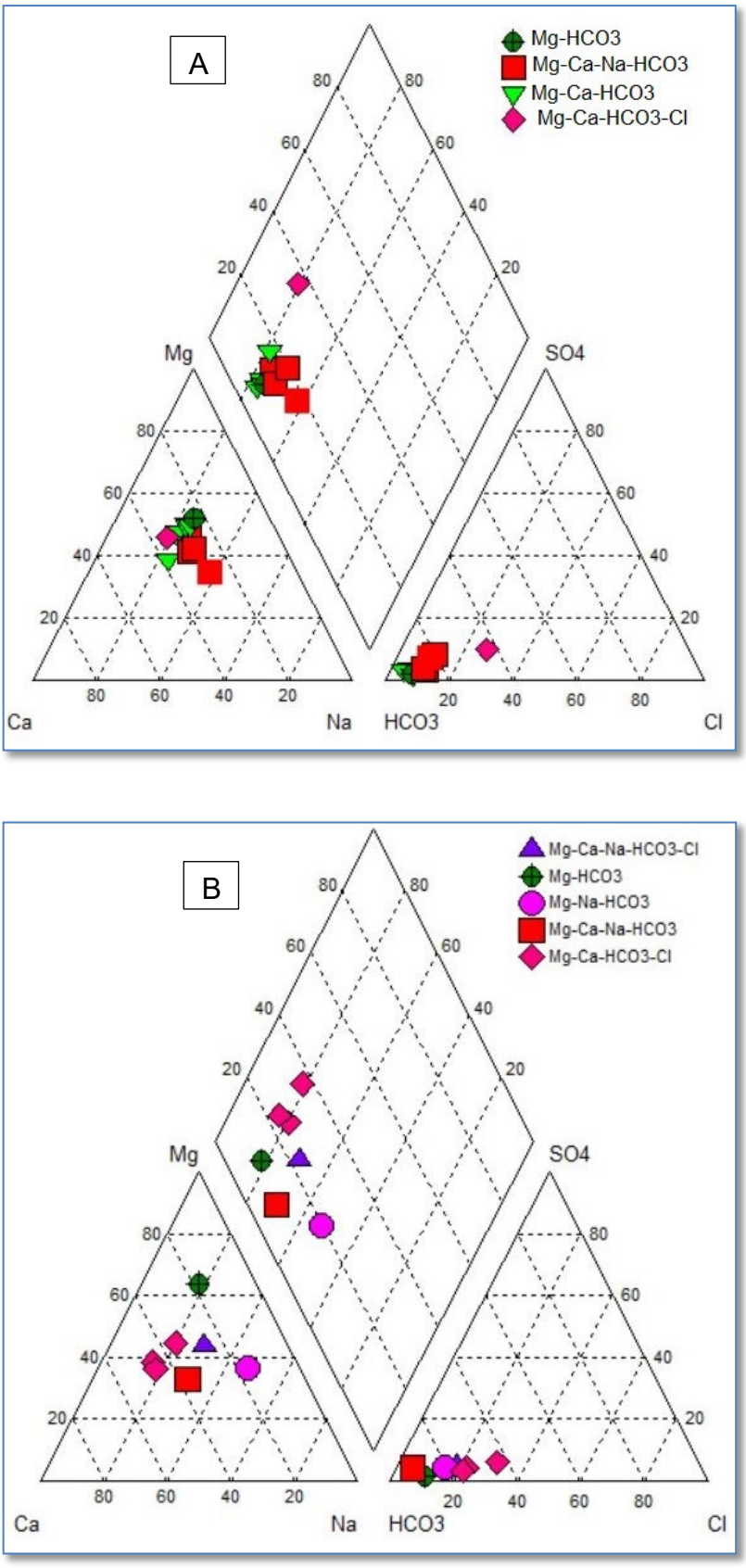

Figure 5-4: Piper diagrams showing hydrochemical characteristics and water types at the inflow (A) and outflow (B) boundaries.

5.3 Environmental Isotopes

5.3.1 Stable Isotopes of Water Molecule

Environmental isotopes of water molecule are widely used to trace the origin of water, and provide valuable information about the processes that are taking place in the hydrologic cycle (Kumar, 2013). The ^{18}O and ^{2}H isotopes are part of the water molecule, and they are heavier than the normal ^{16}O and ^{2}H isotopes.

The hydrological processes such as evaporation, condensation, and melting of ice, are among other processes that cause isotope fractionation, whereby stable isotopes are fractionated into heavy and light isotopes (Fetter, 2001). Thus, during the evaporation of seawater, the lighter isotopes of the water molecule are preferentially partitioned into the vapor phase, while the heavy isotopes remain in the residual seawater or any reservoir of water (Fetter, 2001 and Aggarwal *et al*., 2004, Weaver *et al*., 2007). The use of stable isotope ratios of water molecules provides an insight into the hydrological processes that take place at local to regional scale (Mazor, 2004).

The stable isotope data used in this study consists of 14 samples, out of which are 12 water samples from boreholes and 2 surface water samples collected across the model domain area. These data sets were used to investigate the sources and movement of water within the study area (Table 5-2). The results of $\delta^{2}H$ versus $\delta^{18}O$ were plotted and compared with the Pretoria Local Meteoric Water Line (PLMWL) and Global Meteoric Water Line (GMWL) as shown in (Figure 5-5). The PLMWL was generated based on the $\delta^{18}O$ and $\delta^{2}H$ composition of the rainfall at the International Atomic Energy Agency (IAEA) station which is situated in Pretoria. Based on the periodically recorded data at this station, the relationship between ^{18}O and ^{2}H ratios can be expressed in terms of the following equation:

$$\delta^{2}H = 6.7\ \delta^{18}O + 7.2\ ‰.$$

Following Craig (1961), on a global scale, the relationship between $\delta^{2}H$ and $\delta^{18}O$ in terrestrial water is linear, and can be expressed as:

$$\delta^{2}H = 8^{18}O + 10‰.$$

According to Craig (1961), the relationship between δ^2H and ^{18}O is linear and described as a Global Meteoric Water Line (GMWL). This relationship was established based on the global analyses of $\delta\ ^{18}O$ and δ^2H in terrestrial waters from different localities and regional meteorological stations around the globe (Craig, 1961). The GMWL is the basis or used as a standard reference for the interpretation of variation of stable isotope ratios resulting from fractionation during the processes of the hydrologic cycle.

In this study, both PLMWL and GMWL were plotted together with the results of the analysis of 14 water samples (Figure 5-5). The results show that the slope of PLMWL (6.7‰) is lower than the GMWL (8‰), indicating the influence of high evaporation resulting in more depletion of δ^2H values than $\delta\ ^{18}O$ ratios. Evaporation causes enrichment of $\delta\ ^{18}O$ and δ^2H (heavy isotopes) in rainfall resulting in a decrease in deuterium excess value (Wu, 2005).

The stable isotopes from the surface water and groundwater samples have shown different isotopic compositions with the mean values of $\delta^{18}O$ and δ^2H determined at –3.4‰ and -23.0‰ and -4.1‰ and -23.5‰, respectively (Figure 5-5). The results of surface water are showing enriched $\delta^{18}O$ and δ^2H composition (e.g., see MID-Let-DM and MID-Let-RIV samples on Table 5-2). This phenomenon is due to the surface water being exposed to solar radiation that fractionates the lighter isotopes while the residual surface water is enriched in heavier isotope ratios.

The results of groundwater samples show different isotopic compositions with some samples plotting above and below the GMWL. This suggests various processes controlling recharge mechanisms in the study area (Figure 5-5). Borehole H14-1459 is different from others, displaying highly enriched $\delta^{18}O$ and δ^2H isotopic composition (+0.07 ‰ and -0.04 ‰ of δ^2H and $\delta^{18}O$, respectively) suggesting the groundwater is directly recharged by the river. The water level (5.51 mbgl) indicates that the aquifer is probably shallow (e.g., an unconfined aquifer). The enrichment can be due to high evaporation.

The first group of groundwater samples (H14-0865, H14-1709, H14-1704, and H14-1691) are plotted below the GMWL and PLMWL. The average values of δ^2H and $\delta^{18}O$ for the four groundwater samples are -3.405‰ and -19.9 ‰, while the mean of the two surface water samples is -3.36 ‰ and -23.0‰, respectively.

The similarity in $\delta^{2}H$ and $\delta^{18}O$ values between the four borehole samples and the two surface water samples suggests that focused recharge from surface runoff where Middle and Klein Letaba Rivers recharge the underlying aquifers. Borehole sample H14-1709 shows a similar isotopic composition with sample MID-Let-Dam, suggesting an interaction between the two water sources.

The 2nd group of groundwater samples (Rtd-Bricks, Rtd-CLNC, H14-0861, Gidela SS, H14-1330, H14-1692 and H14-0231) are plotting below the lower segment of the PLMWL and GMWL, which suggests the effect of high evaporation under high humidity conditions. They are highly depleted $\delta^{18}O$ and $\delta^{2}H$ isotope ratios with respect to the VSMOW. As stated by Clark and Fritz (1997), their position relative to the PLMWL suggests recharge that occurred during colder climates in high humidity conditions. These boreholes suggest diffuse rainfall recharge through major geological structures (i.e., Kudoes River Lineament, Hout River, and Annaskraal shear zone).

Table 5-2: Stable isotope results from various water sources within the study area.

Site ID		Latitudes	Longitudes	Elevation (a.m.s.l)	Water Level (mbgl)	$\delta^{18}O$ (‰)	$\delta^{2}H$ (‰)
Groundwater							
	H14-1459	-23.27185	30.40906	502	5.59	0.07	-0.4
Group 1	H10-0865	-23.40365	30.30403	544	10.82	-3.96	-22.1
	H14-1709	-23.28772	30.44045	562	21.1	-3.09	-18.8
	H14-1704	-23.28027	30.45001	582	22.43	-2.66	-15.5
	H14-1691	-23.27874	30.41291	535	10.54	-3.91	-23.2
Group 2	Rotd-BRCK	-23.40446	30.30050	555	19	-5.3	-30.8
	Rotd-CLNC	-23.40148	30.27478	603	24.76	-5.01	-30
	H14-0861	-23.41739	30.32123	597	27.97	-5.32	-30.6
	Gidela S.S	-23.40717	30.33999	596	-	-4.97	-27.6
	H14-1330	-23.36563	30.35650	569	14.68	-4.87	-28.5
	H14-1692	-23.27769	30.41295	524	12.2	-5.07	-27.5
	H20-0231	-23.21175	30.47304	519	-	-4.64	-26.5
Surface water							
	MID-Let-DM	-23.28668	30.40803	530	-	-3.02	-20.6
	MID-Let-RIV	-23.3721	30.32079	540	-	-3.7	-25.4

As shown in Table 5-3 and Figure 5-6, the isotopic composition increases with distance from the high elevated inflow boundary (e.g., Mid-Let-RIV) to the low elevated outflow boundary (e.g., Mid-Let-Dam), which is consistent with enrichment of heavy isotopes due to evaporation and altitude effect.

Figure 5-6 further illustrate that groundwater samples in boreholes (Rtd BRKS, Rtd CLNC, Gidela SS, H14-0861 and H14-1330) located in the immediate vicinity of the inflow2 boundary are showing depleted $\delta^{18}O$ and $\delta^{2}H$ values compared to groundwater samples (H14-1459, H14-1709, H14-1704, H14-1691 located in the low elevated area towards the outflow boundary.

The d-excess is defined as a function of relative humidity above the ocean surface that indicates the conditions occurring during vapour production (Geyh, 2000), expressed as:

$D_{excess} = \delta 2H - 8\delta^{18}O$ (Dansgaard 1964).

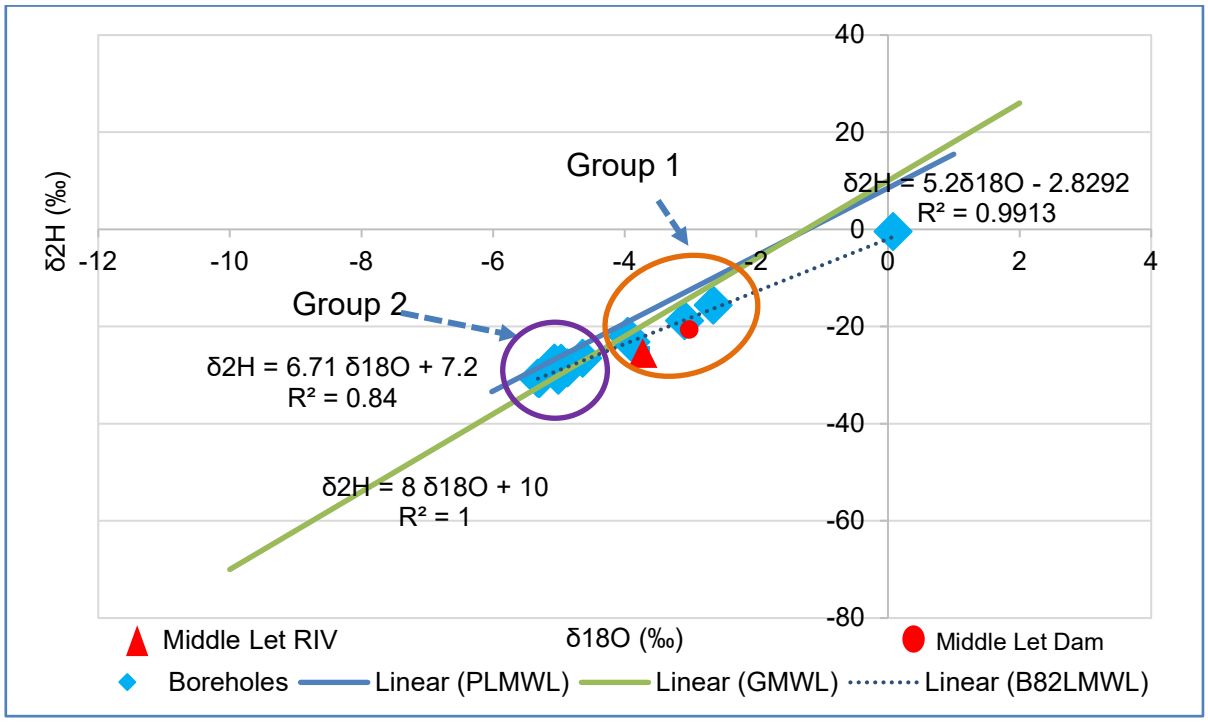

Figure 5-5: Relationship between $\delta^{18}O$ and $\delta^{2}H$ in water samples collected from various sites within the study area in relation to the PLMWL (IAEA, 2012) and GMWL (Craig, 1961).

Deuterium was calculated and found to be at ranges between -1.0‰ to 13.1 ‰ and 3.6 ‰ to 4.4 ‰ for groundwater and surface water samples, respectively (Table 5-3). The averaged d-excess for surface water and groundwater sources were determined at 4.0 ‰ and 8.3 ‰, respectively. The averaged d-excess value is lower than that of the GMWL (Dexcess =10), further indicating that the study area is generally receiving rainfall from a regional moisture source, possibly the Indian Ocean.

The plot of d-excess versus δ18O (Figure 5-7) suggests that the enrichment of δ18O resulted in a gradual decrease of d-excess, hence indicative of evaporative effects on both the groundwater and surface water systems.

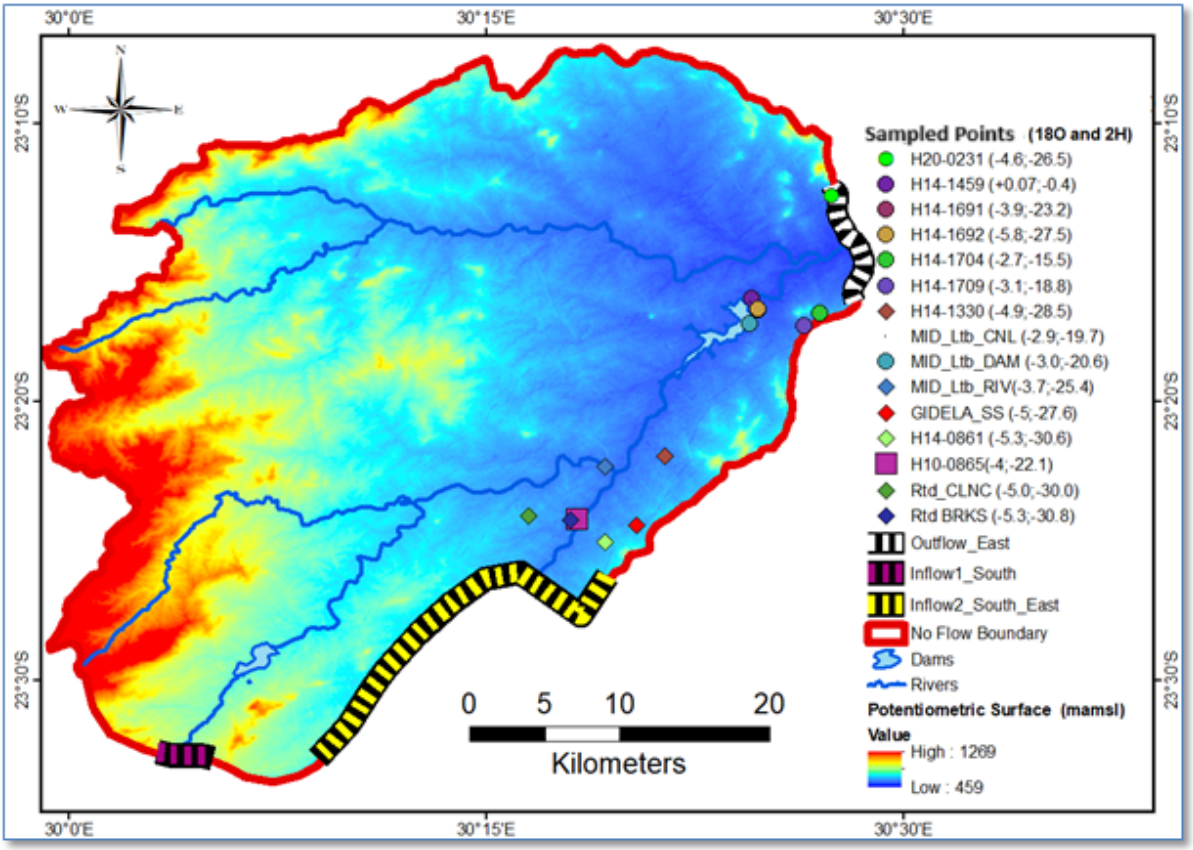

Figure 5-6: Map showing the distribution of $\delta^{18}O$ and $\delta^{2}H$ values used to support the inflows and outflow boundaries of the conceptual model of groundwater flow.

Table 5-3: Stable isotope values and d-excess.

Sample ID	$d^{18}O$	d D	D_Excess
H20-0231	-4.64	-26.5	10.6
H10-0865	-3.96	-22.1	9.6
H14-1330	-4.87	-28.5	10.5
Rtd CLNC	-5.01	-30.0	10.1
RTD BRCK	-5.30	-30.8	11.6
Gidela SS	-4.97	-27.6	12.1
H14-0861	-5.32	-30.6	12.0
H14-1709	-3.09	-18.8	5.9
H14-1704	-2.66	-15.5	5.7
H14-1459	+0.07	-0.4	-1.0
H14-1692	-5.07	-27.49	13.1
H14-1691	-3.91	-23.17	8.1
Mid Let Dam	-3.02	-20.6	3.6
Mid Let RIV	-3.7	-25.4	4.4

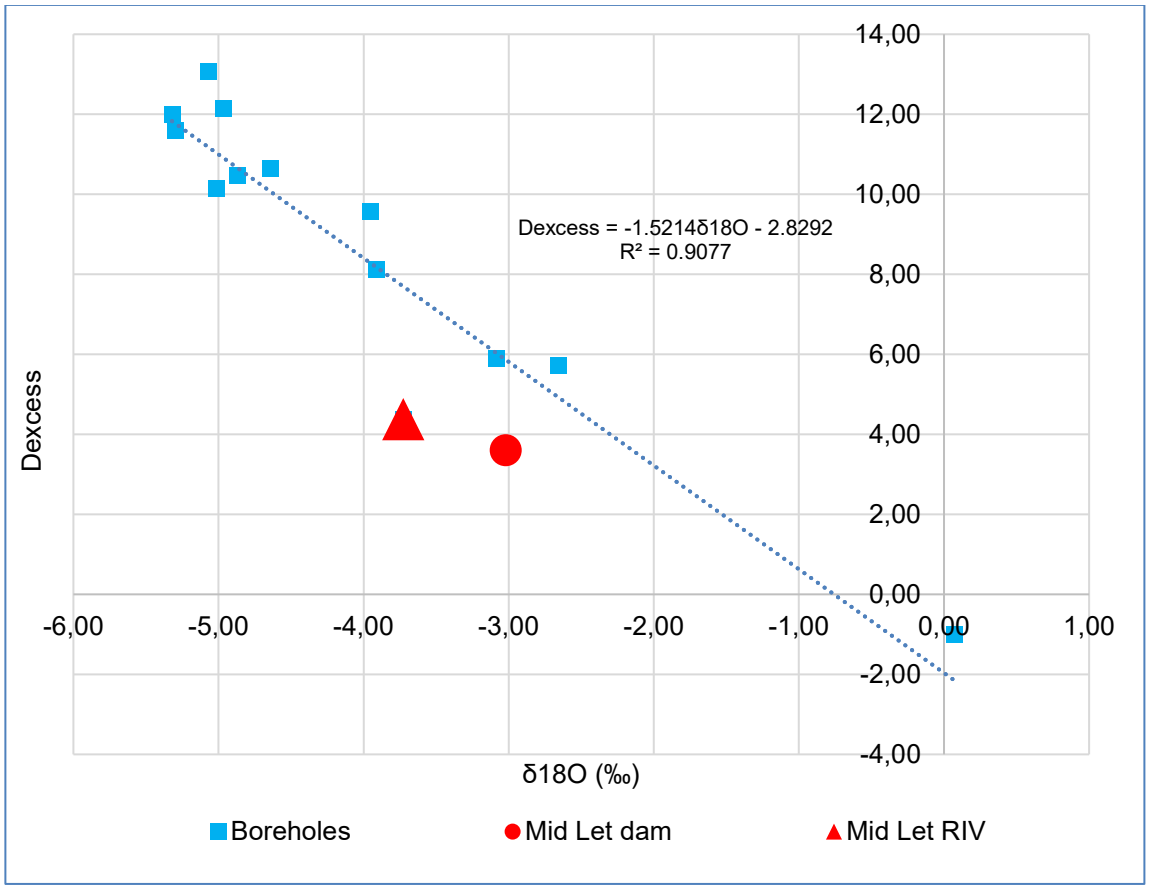

Figure 5-7: Plot of dexcess versus δ18O of groundwater and surface water samples.

5.3.2 Radiogenic isotopes (3H)

Tritium (^3H) is a radioactive isotope of hydrogen with a half-life of 12.43 years (Fetter, 2001). This makes it suitable for the estimation of the mean residence time (MRT) of the groundwater in an aquifer. The age of groundwater has important implications for water resource management. In the southern hemisphere, the tritium levels in rainfall are due to the effects of nuclear weapon tests during the 1950s to early 1960s (Abiye,2013), and due to natural tritium which varies from 3 to 5 TU. There was an increase in tritium composition in the atmosphere during the 1950s to maximum levels around 1965, and thereafter a decline to pre-bomb values of 2 to 3 TU. In South Africa, the current averaged tritium concentration in rainwater was determined at 3 TU (Abiye, 2013).

To obtain an understanding of the mean residence time (MRT) of the groundwater in the study area, sample results from 23 water sources consisting of 20 groundwater and 3 surface water samples located within the Klein Letaba River catchment were analysed (Table 5-4). The results indicate that low ^3H content in most of the groundwater samples varies from 0.2 to 1.9 TU, with an average of 0.8 TU. Surface water samples have ^3H values ranging between 0.9 TU to 2.1 TU with an average of 1.5 TU. According to Clack and Fritz (1997) classification, water samples with tritium concentrations that vary from 0 to 0.8 TU and 0.8 to 4 TU are classified as old, i.e., recharged prior to 1952, and mixed water that was recharged before and after 1952, respectively. Based on this classification, the results of 11 samples were interpreted as old water, which was probably recharged before 1952. The remaining 12 samples are composed of tritium values ranging between >0.8 and 1.9 TU, which fall within the 0.8 and 4 TU range, and are classified as a mixture of modern and sub-modern recharged water (Clark and Fritz,1997). In this study, tritium values greater or equal to 1.4 TU indicated the presence of recharge within the past 12.43 years. Low tritium values (< 0.8 TU) suggest that the groundwater slowly circulates and resides in the aquifer for a prolonged period of time due to either limited permeability or a low flow rate that can be driven by a gentle-to-low hydraulic gradient along the flow path.

The average tritium value of 2.8 TU determined by Butler and Verhagen (2013) for Taaiboshgroot in the Limpopo Province is the representative value in the atmosphere with a half-life of approximately 12.43 years.

This tritium value was determined through an analysis of time series rainfall data for the Taaiboshgroet area from the year 2000 to 2005 in comparison with other tritium analyses in the subcontinent. The bomb peak of Harare which followed close to that of the other sites (i.e., Cape Town, Durban, Escourt, Bloemfontein, and Pretoria) in the country was used as a reference and was compared with the Taaiboschgroot to represent the present day pre-bomb value of 2.8 TU (Abiye, 2013).

In comparison with the stable isotopes results, tritium values of <0.8 TU (older water) show low $\delta^{18}O$ and $\delta^{2}H$ compositions ranging between -3.35‰;-18.89‰ to -4.95‰;-30.29‰. These results signify slow circulation of groundwater that allows sufficient time for rock-water interaction to take place over a prolonged period of time resulting in the depletion of stable isotopes of water molecule. Tritium values of > 0.8 (mixed water) have indicated enriched $\delta^{18}O$ and $\delta^{2}H$ compositions in ranges of -0.28;-3.98 to 6.38; 29.95.

Table 5-4: Tritium and stable isotope values for the study area.

Sample ID	Latitudes	Longitudes	Elevation (a.m.s.l)	Tritium (TU)	Classification (Clark and Fritz (1997)	δ18O (‰)	δD (‰)
Groundwater							
DML-001	-23.11860	30.60660	583	0.51	Old water	-4.42	-25.48
FYT-001	-23.30466	30.65190	459	1.30	Mixed water	-3.02	-16.78
H14-0106	-23.22816	30.71604	453	1.33	Mixed water	-2.24	-14.24
H14-0110	-23.15484	30.71428	513	0.91	Mixed water	-2.88	-17.18
H14-0250	-23.25020	30.77499	434	1.86	Mixed water	-1.84	-14.23
H14-0467	-23.32934	30.91855	415	0.60	Old water	-4.95	-30.29
H14-1030	-23.29846	30.63844	476	0.22	Old water	-4.18	-25.59
H14-1617	-23.34867	30.94633	419	0.30	Old water	-3.94	-23.33
H15-0783	-23.10991	30.59513	595	0.20	Old water	-4.69	-27.08
H20-0231	-23.21175	30.47304	519	0.50	Old water	-4.64	-26.50
H20-0836	-23.16711	30.51694	564	0.30	Old water	-4.52	-25.74
H20-1446	-23.17670	30.48963	578	0.90	Mixed water	-4.72	-25.90
KHKP-H1	-23.26695	30.85396	443	1.40	Mixed water	-3.79	-21.84
KL-Shaft	-23.29515	30.56081	479	0.76	Old water	-3.35	-18.89
LM-Shaft 2	-23.22040	30.69584	473	0.46	Old water	-3.93	-22.50
MHW-01	-23.27557	30.88565	447	0.82	Mixed water	-3.34	-20.23
MPV 4	-23.29661	30.57680	470	0.37	Old water	-3.77	-21.49
SIY-BH1	-23.32120	30.67100	460	0.65	Old water	-2.49	-14.78
SHIV-002	-23.15984	30.70547	505	1.40	Mixed water	-3.99	-23.15
Surface Water							
KL-SW	-23.29319	30.56484	474	1.62	Mixed water	6.38	29.95
KLR-1	-23.31220	30.62504	485	0.91	Mixed water	-0.28	-3.98
SHIV-S	-23.15535	30.71338	515	2.07	Mixed water	5.25	24.44

CHAPTER 6 : IMPACTS OF CLIMATE CHANGE

6.1 Introduction

In this chapter, the spatio-temporal trends of rainfall and temperature were analysed to evaluate the influence of climate change on groundwater resources. Rainfall and temperature are two important parameters commonly used to investigate the extent and magnitude of climate change and variability (IPCC, 2007). Groundwater level monitoring data provides important information on the effects of hydrologic stresses on groundwater resources for assessing the quantity of groundwater and understanding the hydrological processes (Seferli et al., 2019).

The Mopani District Municipality, due to its low adaptive capacity, high sensitivity of socio-economic systems, and high reliance on natural resources for livelihood, is considered as one of the most vulnerable areas that are highly affected and still to be affected by the impacts of climate change. The adverse impacts of climate change in the study area are felt mostly by the farmers and rural communities because they are by large dependent on rainfall for growing crops, live stocks drinking, and domestic purposes. To investigate the climate variables (i.e., rainfall and temperature) and assess how their changes affect groundwater resources, statistical and trend analysis methods were used to investigate and characterise their relationship.

6.2 Statistical analysis of rainfall data

The descriptive statistical analysis of monthly, seasonal, and annual data (2007-2016) for stations 06791945 and 30760 is presented in (Table 6-1 and Table 6-2). These results indicate that rainfall distribution varied significantly over the last 10 years with the lowveld areas receiving low rainfall (535 mm per annum), while highveld received high rainfall (945 mm per annum). Summer is the major rain season in the study area which contributes more than 51% of the total rainfall.

Table 6-1: Descriptive statistics and variability analysis of monthly and annual Rainfall (Station 06791945)

Year	Jan	Feb	Mar	Apr	May	Jun	Jul	Aug	Sep	Oct	Nov	Dec	Annual	Summer (Dec-Feb)	Autumn (Mar-May)	Winter (Jun-Aug)	Spring (Sep-Nov)
2007	45,1	40,5	70,5	121	0	9	30,2	15,4	63	104,2	135,8	206,6	841,3	292,2	191,5	54,6	303
2008	173,2	75,4	50,8	38,4	4,6	2,4	9	15,8	7,4	38,6	354,3	207,4	977,34	456	93,8	27,2	400,34
2009	188,98	252,2	79,8	22,8	34,4	52,4	15,4	6,4	1,6	48,8	242,2	130,6	1075,6	571,78	137	74,2	292,6
2010	122,2	131,6	106,8	195,8	12,6	3	26	0	4,4	33,2	202,8	275,4	1113,8	529,2	315,23	29	240,4
2011	452,8	45,8	84,6	268,4	14	2,4	13,8	8,4	5,4	103,4	58,42	77,8	1135,2	576,4	367	24,6	167,2
2012	181,4	114,2	59,6	31,2	8	1,2	3,2	7	126,4	98,6	83,4	161,3	875,5	456,9	98,8	11,4	308,4
2013	564,8	87	49,28	115,2	8	1,02	13	7,2	23,4	60,4	134,6	235	1298,9	886,8	172,48	21,17	218,42
2014	252,98	147,2	143,8	72	4,2	11,2	6,6	14,6	6,4	23,2	64,8	172	918,94	572,14	220	32,4	94,4
2015	76,4	48,8	82,2	68	4,83	1	8,6	0	93,8	21,34	78,2	42,42	525,59	167,62	155,03	9,6	193,34
2016	99,06	77,47	141,4	3,56	52,58	6,35	19,4	0,51	4,57	24,4	105,7	156,2	691,17	332,74	197,54	26,26	134,63
Min (mm)	45,10	40,50	49,28	3,56	0,00	1,00	3,20	0,00	1,60	21,34	58,42	42,42	525,59	167,62	93,80	9,60	94,40
Max (mm)	564,80	252,20	143,80	268,40	52,58	52,40	30,20	15,80	126,40	104,20	354,34	275,40	1298,87	886,80	367,00	74,20	400,34
Mean (mm)	215,69	102,02	86,88	93,64	14,32	9,00	14,52	7,53	33,64	55,61	146,02	166,47	945,33	484,18	194,84	31,04	235,27
%	22,82	10,79	9,19	9,91	1,51	0,95	1,54	0,80	3,56	5,88	15,45	17,61	100,00	51,22	20,61	3,28	24,89
Std. Dev	168,00	64,06	34,02	83,94	16,47	15,66	8,57	6,20	44,90	34,24	94,59	70,35	227,20	197,09	87,97	19,57	92,58
CV (%)	77,89	62,79	39,15	89,64	115,02	174,06	59,07	82,26	133,49	61,57	64,78	42,26	24,03	40,71	45,15	63,03	39,35

Table 6-2: Descriptive statistics and variability analysis of monthly and annual Rainfall (Station 30760)

Year	Jan	Feb	Mar	Apr	May	Jun	Jul	Aug	Sep	Oct	Nov	Dec	Annual	Summer (Dec-Feb)	Autumn (Mar-May)	Winter (Jun-Aug)	Spring (Sep-Nov)
2007	11,1	16,8	69,6	16,1	0	0,9	26,1	10,1	73,2	87,6	59,3	85,4	456,2	113,3	85,7	37,1	220,1
2008	78,3	41,3	27,2	28,2	1,1	0,3	1,1	1,2	0,2	26,3	130,6	46,23	382	165,83	56,5	2,6	157,1
2009	175,4	80,52	51,56	6,1	18,8	28,19	4,83	1,78	10,16	16	223,01	80,01	696,4	335,93	76,46	34,8	249,17
2010	35,56	74,93	13,97	184,8	9,65	1,52	11,68	0,25	3,05	4,06	58,67	183,13	581,3	293,62	208,42	13,45	65,78
2011	161,04	24,13	49,53	33,02	6,6	0,25	11,94	6,1	0,25	86,2	23	71,37	473,4	256,54	89,15	18,29	109,45
2012	155,45	54,36	7,62	4,57	0	0,51	0	0,76	48,77	75,44	44,7	83,06	475,2	292,87	12,19	1,27	168,91
2013	410,97	35,56	30,4	94,23	6,1	0	7,6	2,03	4,06	35,31	69,4	93,73	789,4	540,26	130,73	9,63	108,77
2014	252,98	121,67	123,44	37,34	1,78	0,51	0,25	0,51	1,27	17,78	71,12	120,8	749,5	495,45	162,56	1,27	90,17
2015	9,91	48,8	40,89	48,51	0,4	0,76	0,25	0	22,35	16,8	56,39	24,8	269,9	83,51	89,8	1,01	95,54
2016	69,6	63	81,03	2,8	24,6	1	6,86	0	2,2	13,21	66,4	151,8	482,5	284,4	108,43	7,86	81,81
Min (mm)	9,91	16,80	7,62	2,80	0,00	0,00	0,00	0,00	0,20	4,06	23,00	24,80	269,86	83,51	12,19	1,01	65,78
Max (mm)	410,97	121,67	123,44	184,80	24,60	28,19	26,10	10,10	73,20	87,60	223,01	183,13	789,39	540,26	208,42	37,10	249,17
Mean (mm)	136,03	56,11	49,52	45,57	6,90	3,39	7,06	2,27	16,55	37,87	80,26	94,03	535,57	286,17	101,99	12,73	134,68
%	25,40	10,48	9,25	8,51	1,29	0,63	1,32	0,42	3,09	7,07	14,99	17,56	100,00	53,43	19,04	2,38	25,15
Std. Dev	125,24	30,84	34,68	56,00	8,57	8,72	8,10	3,29	25,02	32,38	57,08	47,11	166,30	148,04	55,00	13,53	61,86
CV (%)	92,07	54,97	70,02	122,90	124,10	257,02	114,77	144,57	151,15	85,51	71,12	50,10	31,05	51,73	53,93	106,33	45,93

The three months of the spring season (September through November) are also significant, contributing approximately 25% of the total rainfall in the study area. The year 2013 experienced the highest rainfall over the study period with more than 780 mm/a in the lowveld and more than 1200 mm/a in the western highveld region. The notable drought events were recorded during the years 2007/2008, 2011/2012, and 2015. The lowest rainfall was recorded in the year 2015 with annual measurements of 525 mm for the highveld and 269 mm for the lowveld. It is evident that rainfall is variable and is characterised by interseasonal drought and flooding periods (Figure 6-1).

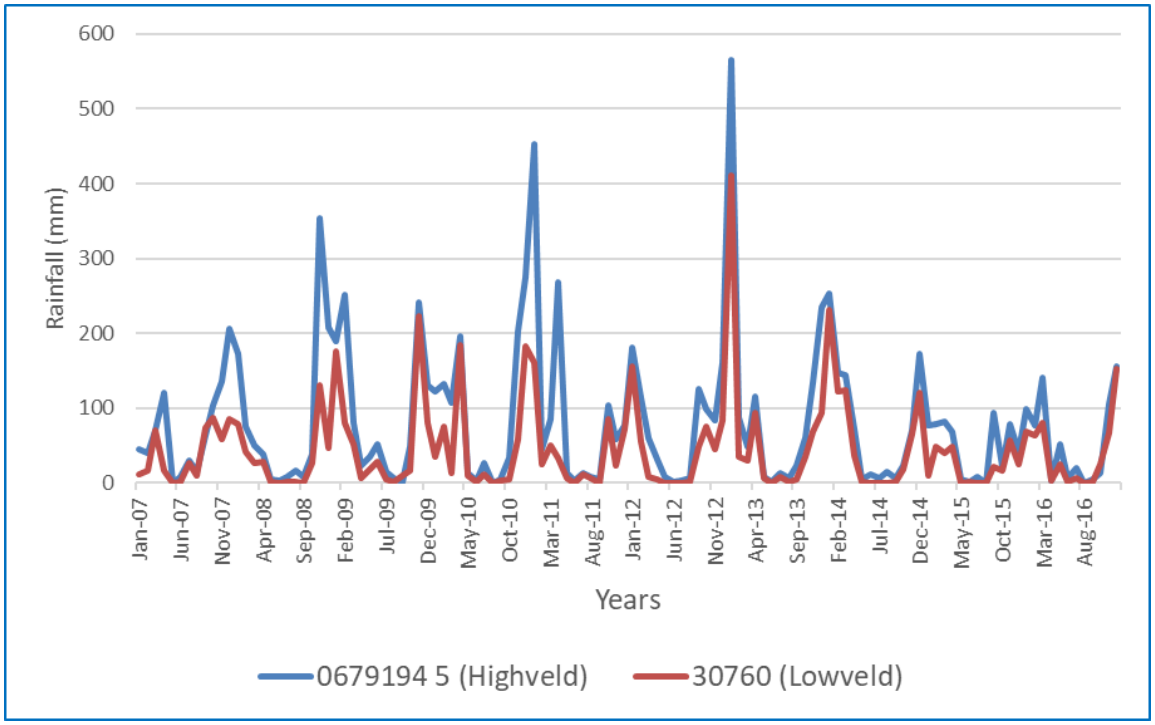

Figure 6-1: Rainfall variability for the highveld and lowveld regions.

The standard deviation and coefficient of variation were determined at 166 and 31 % for station 30760 and 227.20 and 24% for station 06791945, respectively. According to Resende (2002), a general classification range for coefficients of variation (CV) is categorised within the ranges of 0.1 to 15% as low, 15 to 50% as moderate, and greater than 50% as high. Based on the mean annual rainfall (from 2007 to 2016), the CV was determined at 24% and 31% for the highveld and lowveld regions, respectively. These results suggest a moderate rainfall variability for the study area.

Figure 6-2 and Figure 6-3 presents the histogram trends of the annual rainfall variability of the highveld and lowveld regions, respectively. The histograms are both showing a positively skewed distribution with mean values that are greater than the mode in both regions. This signifies that there are large numbers of recorded rainfall that are less than the mean. This indicates that the area received low rainfall throughout the given time, which has a significant impacts on both surface water and groundwater.

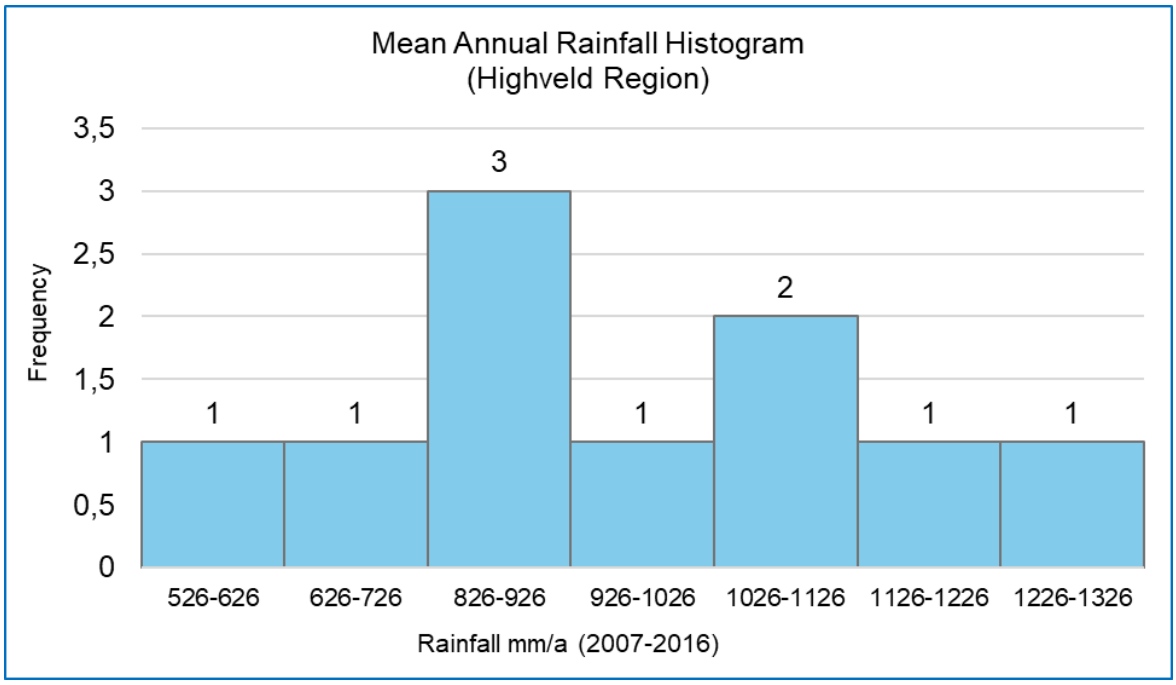

Figure 6-2: Mean Annual Rainfall Histograms for Highveld Region.

These results are consistent with the prevailing groundwater problem in the area. In addition, the histogram shows two populations of rainfall events; one is centered on mode 3 while the other set of data is centered on mode 2. This may be attributed to seasonal fluctuation of rainfall patterns driven by climate change and atmospheric circulation in the region, which impact on availability of water resource in the area.

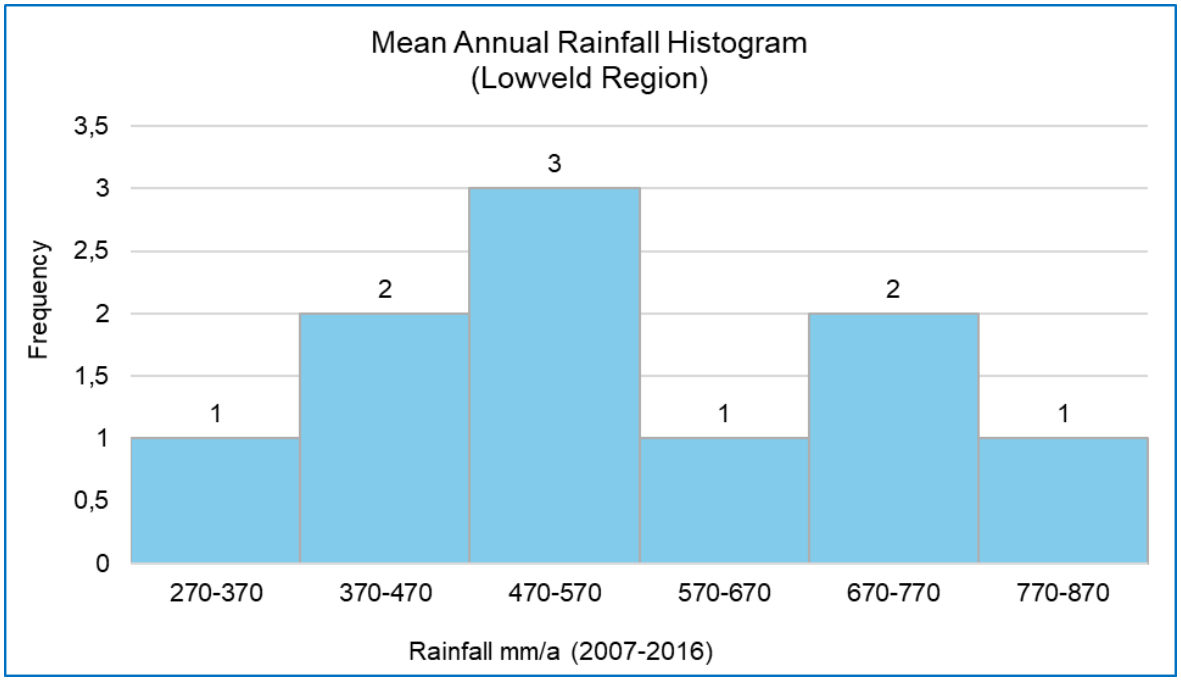

Figure 6-3: Mean Annual Rainfall Histograms for Lowveld Region.

Using a linear regression model, the rate of rainfall change is defined by the slope of the regression line as a function of recorded rainfall versus time. As shown in Figure 6-4, the slope of regression for the highveld region (0679194 5) ranges from -30.3, -4.2, and -23.5 in the annual, summer, and spring rainfall seasons, respectively. The highveld region is showing a declining rainfall trend for annual and spring rainy seasons with summer rainfall characterised by a monotonic decreasing trend. It is evident (Figure 6-4) that the declining rainfall trends could be attributed to the extreme drought as the area is highly prone to severe and frequent drought periods. In a 10-year period (2007-2016), drought accounts for 84.4 %, and wet season accounts for 15.6 %. Drought periods were recorded during 2007/2008 and 2014/2015 classified as moderate, severe, and extreme droughts were recorded in 2015/2016 and 2011/2012, respectively.

In the Lowveld region (30760), the slope of the regression was determined at 2.1, 15.4, and -13.8 for annual, summer, and spring rainfall seasons, respectively (Figure 6-5). The trend test results for the Lowveld region revealed a slightly increasing rainfall trend for the annual and summer seasons while the spring is showing a declining trend.

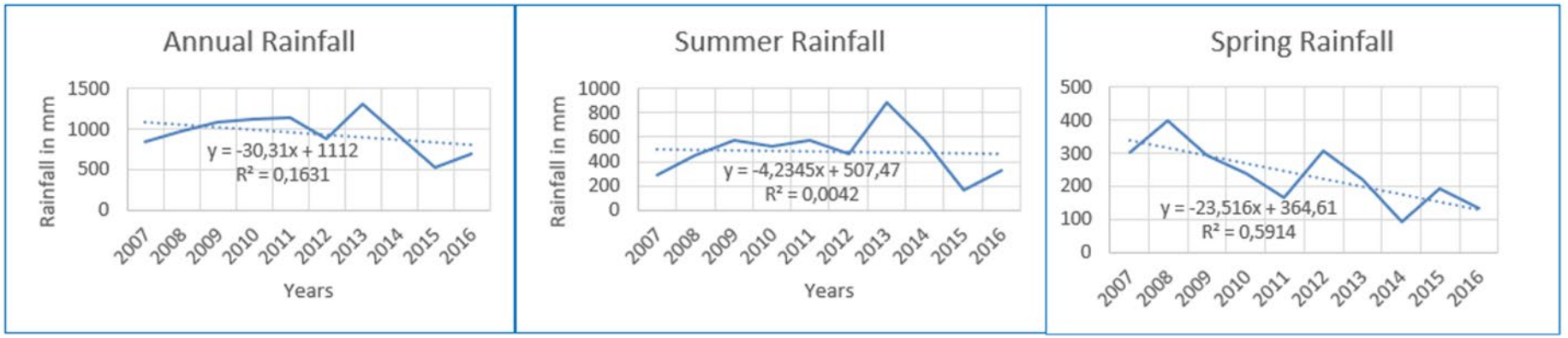

Figure 6-4: Rainfall pattern (Mean, Summer, and Spring) linear least square regression lines for Highveld region (0679194 5).

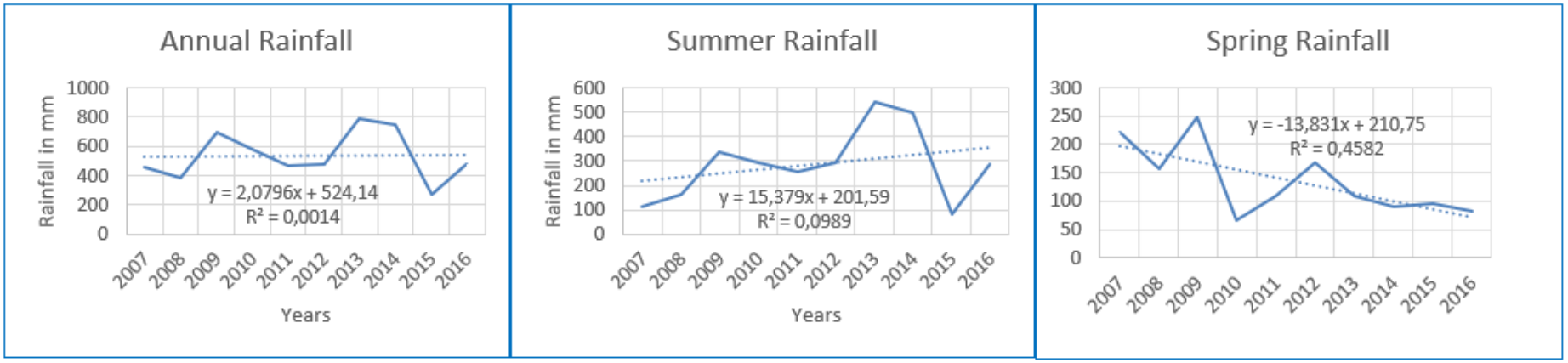

Figure 6-5: Rainfall pattern (Mean, Summer, and Spring) linear least square regression lines for the Lowveld region (30760).

The minimal increasing rainfall trend for the annual and summer seasons could relate to the 52.3 % of the wet seasons and 47.4 % of drought season over 10 years indicating significant fluctuation between the wet and dry seasons, but with the wet events being slightly dominant (Nembilwi et al, 2021).

According to Shikwambana (2021), the highveld region is more prone to severe and extreme drought than the lowveld region which is mainly characterised by moderate and extreme droughts. Rainfall totals in the Mopani district have decreased by 38% from 1960 to 2018 (Shikwambana, 2021). However, for the same interval period, the regression analysis has suggested a non-significant decrease in rainfall over time.

6.3 Statistical and trend analysis of temperature data

The increase in temperature is one of many factors that are considered to be indicators of global climate change. The annual and monthly maximum temperature data analyses were conducted to determine the variability and trend of temperature change in the study area for a period of 10 years (2007 to 2016). Table 6-3 and Table 6-4 displays the monthly and annual temperatures (minimum, maximum, and coefficient variation) for the 2 selected stations (06791945 and 30760) representing the highveld and lowveld regions. The mean annual maximum temperature in the study area ranges between 26.9ºC for the Highveld and 27.4ºC in the Lowveld, with the eastern Lowveld showing much warmer temperatures, while the highveld displaying cooler temperatures (Figure 6-6). The years with the highest temperature are 2012, 2015, and 2016.

According to the classification of Resende (2002), the temperature variability in the study area falls within <15 % implying that the degrees of variability of temperature are very low ranging between 3 to 7 % in the highveld and lowveld regions. This could be due to the minor variability of warm temperatures that the Mopani district generally experiences throughout the year. This suggests that temperature nearly remains the same throughout the warm season, which has a significant impacts on water resources.

Table 6-3: Descriptive statistics and variability analysis of monthly and annual temperature (Station 06791945)

Year	Jan	Feb	Mar	Apr	May	Jun	Jul	Aug	Sep	Oct	Nov	Dec	Annual	Summer (Dec-Feb)	Autumn (Mar-May)	Winter (Jun-Aug)	Spring (Sep-Nov)
2007	29,60	31,20	29,90	26,90	24,80	23,00	22,60	25,30	27,80	25,00	27,70	26,30	26,68	29,03	27,20	23,63	26,83
2008	26,80	29,10	27,00	25,70	24,60	23,10	23,10	25,40	28,20	28,40	27,40	28,10	26,41	28,00	25,77	23,87	28,00
2009	28,80	27,70	26,40	25,80	24,90	23,00	20,70	24,40	28,50	27,70	27,20	29,50	26,22	28,67	25,70	22,70	27,80
2010	28,40	28,80	28,60	24,80	24,40	22,10	21,20	24,20	28,20	28,50	27,60	28,90	26,31	28,70	25,93	22,50	28,10
2011	27,60	27,70	29,70	24,80	25,80	23,40	20,50	22,70	27,80	27,10	23,90	27,20	25,68	27,50	26,77	22,20	26,27
2012	28,60	30,10	29,60	25,50	25,60	23,10	23,10	26,50	24,70	25,80	27,60	28,00	26,52	28,90	26,90	24,23	26,03
2013	27,90	28,80	27,20	25,10	24,50	24,30	22,30	24,40	27,90	26,20	29,20	25,40	26,10	27,37	25,60	23,67	27,77
2014	27,80	27,40	27,20	25,30	25,10	24,10	22,70	25,20	27,40	26,60	26,60	27,80	26,10	27,67	25,87	24,00	26,87
2015	29,20	29,90	29,40	26,30	27,90	23,60	24,70	27,00	26,00	30,10	30,70	32,50	28,11	30,53	27,87	25,10	28,93
2016	30,60	30,80	30,00	28,00	23,50	23,60	22,50	26,60	28,40	29,90	28,60	29,00	27,63	30,13	27,17	24,23	28,97
Min	26,80	27,40	26,40	24,80	23,50	22,10	20,50	22,70	24,70	25,00	23,90	25,40	25,68	27,37	25,60	22,20	26,03
Max	30,60	31,20	30,00	28,00	27,90	24,30	24,70	27,00	28,50	30,10	30,70	32,50	28,11	30,53	27,87	25,10	28,97
Mean	28,53	29,15	28,50	25,82	25,11	23,33	22,34	25,17	27,49	27,53	27,65	28,27	26,57	28,65	26,48	23,61	27,56
Std. Dev	1,09	1,33	1,40	1,01	1,17	0,63	1,26	1,31	1,21	1,70	1,77	1,94	0,74	1,07	0,80	0,90	1,03
CV (%)	3,83	4,56	4,92	3,90	4,67	2,68	5,65	5,21	4,41	6,19	6,38	6,87	2,79	3,74	3,02	3,81	3,72

Table 6-4: Descriptive statistics and variability analysis of monthly and annual temperature (Station 30760)

Year	Jan	Feb	Mar	Apr	May	Jun	Jul	Aug	Sep	Oct	Nov	Dec	Annual	Summer (Dec-Feb)	Autumn (Mar-May)	Winter (Jun-Aug)	Spring (Sep-Nov)
2007	28,84	32,36	30,66	26,93	25,22	23,7	22,29	25,19	28,35	25,29	28,27	26,21	26,94	29,14	27,60	23,73	27,30
2008	27,13	29,91	27,54	26,76	25,5	23,28	22,92	25,86	28,68	29,16	28,03	29,08	26,99	28,71	26,60	24,02	28,62
2009	29,27	27,76	26,16	26,36	25,52	23,3	20,77	24,52	27,46	28,26	28,28	28,94	26,38	28,66	26,01	22,86	28,00
2010	28,56	29,43	29,47	24,59	24,09	22,03	21,34	24,29	28,85	29,28	28,34	28,32	26,55	28,77	26,05	22,55	28,82
2011	26,82	27,31	29,75	25,46	26,03	23,81	21,07	23,28	28,18	28,03	28,72	28,53	26,42	27,55	27,08	22,72	28,31
2012	29,68	30,22	30,18	26,18	26,24	23,36	23,33	26,53	25,81	26,69	28,7	29,74	27,22	29,88	27,53	24,41	27,07
2013	27,86	28,76	26,85	24,97	24,36	24,05	21,9	24,74	28,83	26,64	29,43	26,06	26,20	27,56	25,39	23,56	28,30
2014	27,15	26,52	27,02	25,04	25,17	24,09	22,56	25,34	27,84	27,66	27,85	27,54	26,15	27,07	25,74	24,00	27,78
2015	28,9	30,55	29,44	26,52	28,1	23,03	24,48	26,85	25,74	30,08	30,82	33,12	28,14	30,86	28,02	24,79	28,88
2016	31,19	32,16	31,12	30,34	25,12	24,1	23,18	27,1	29,16	31,32	30,29	29,74	28,74	31,03	28,86	24,79	30,26
Min	26,82	26,52	26,16	24,59	24,09	22,03	20,77	23,28	25,74	25,29	27,85	26,06	26,15	27,07	25,39	22,55	27,07
Max	31,19	32,36	31,12	30,34	28,10	24,10	24,48	27,10	29,16	31,32	30,82	33,12	28,74	31,03	28,86	24,79	30,26
Mean	28,54	29,50	28,82	26,32	25,54	23,48	22,38	25,37	27,89	28,24	28,87	28,73	26,97	28,92	26,89	23,74	28,33
Std. Dev	1,35	1,95	1,76	1,63	1,12	0,64	1,15	1,22	1,22	1,79	1,00	2,02	0,86	1,35	1,12	0,82	0,91
CV%	4,73	6,62	6,12	6,20	4,37	2,71	5,14	4,82	4,39	6,34	3,45	7,02	3,18	4,67	4,15	3,45	3,20

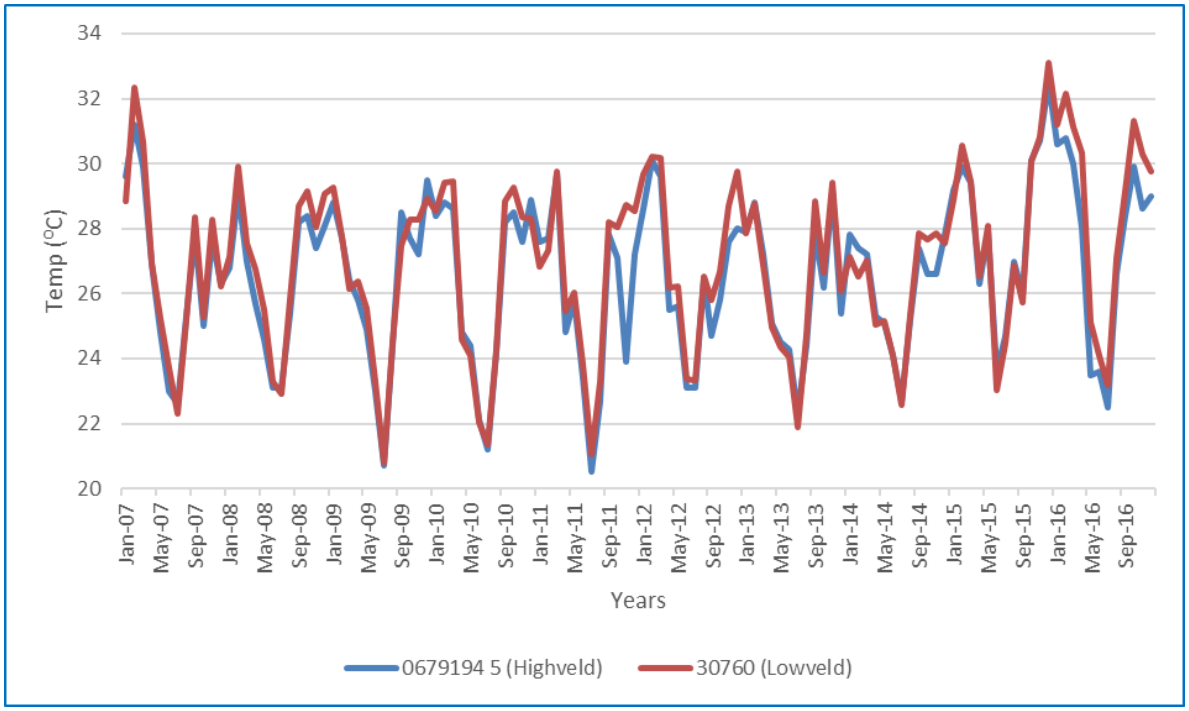

Figure 6-6: Interannual temperature variability for the highveld and lowveld regions.

The slope of the regression lines (Figure 6-7 and Figure 6-8) for the highveld and lowveld regions were determined at 0.2, 0.1, and 0.6ºC and 0.2, 0.1, and -0.02 ºC, respectively for the minimum, mean, and maximum temperature. These findings are consistent with the mean annual temperature anomalies calculated from 26 spatially well-distributed and representative climate stations in South Africa (SAWS, 2023). This data indicates that South Africa experienced a warm year, about 0.36 ºC above the average of the reference period (1991- 2020), making it approximately the 8th hottest year on record since 1951. A warming trend of 0.17 ºC per decade is indicated for the country, over the period 1951-2023, which is statistically significant at the 5% level. The long-range anomalies (Figure 6-9) of mean annual temperature showed inter-annual variability, while the trend after 2014 has been higher than the long-term average which is evidence for the present warming trend.

Due to the high temperature and frequent occurrences of heatwaves in the study area, evapotranspiration is significantly high resulting in decreased availability of the limited surface water resources. This consequently causes an increase in demand for groundwater resources.

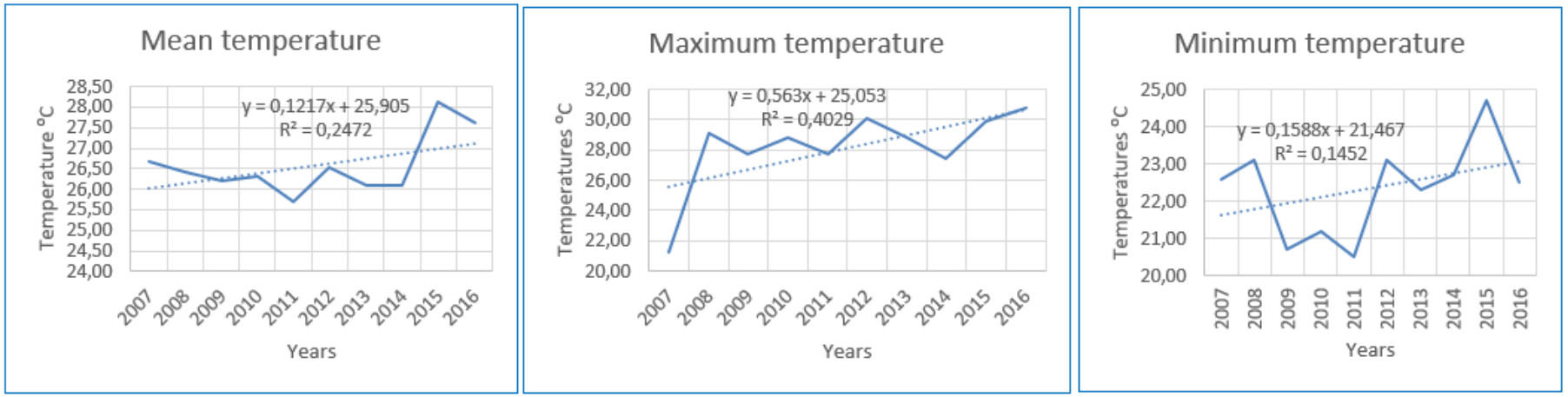

Figure 6-7: Temperature pattern (Mean, Maximum and Minimum) with linear least squarre regression lines for highveld region (0679194 5).

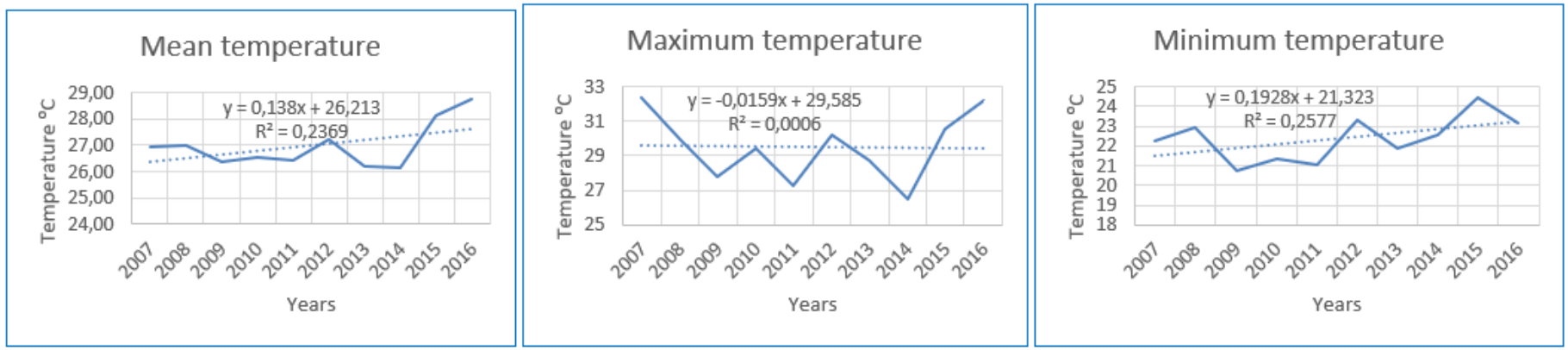

Figure 6-8: Temperature pattern (Mean, Maximum, and Minimum) with linear least square regression lines for the lowveld region (30760).

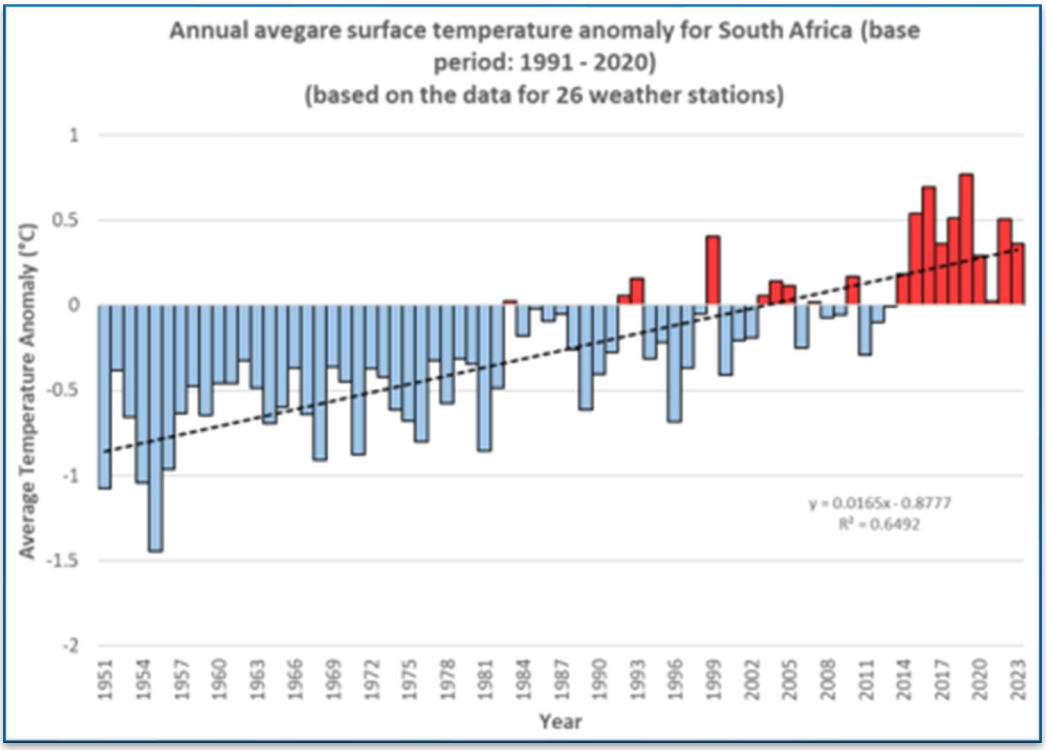

Figure 6-9: Temperature anomalies for South Africa relative to 1951 to 2023.

Reference evapotranspiration values (ET_0) were plotted against rainfall and temperature. The results indicate that the mean monthly ET_0 is generally greater than the mean monthly rainfall for most months of the year except for January where ET_0 is observed to be slightly lower or equal to the monthly rainfall (Figure 6-10 and Figure 6-11). ET_0 is generally high during the Summer due to elevated temperatures.

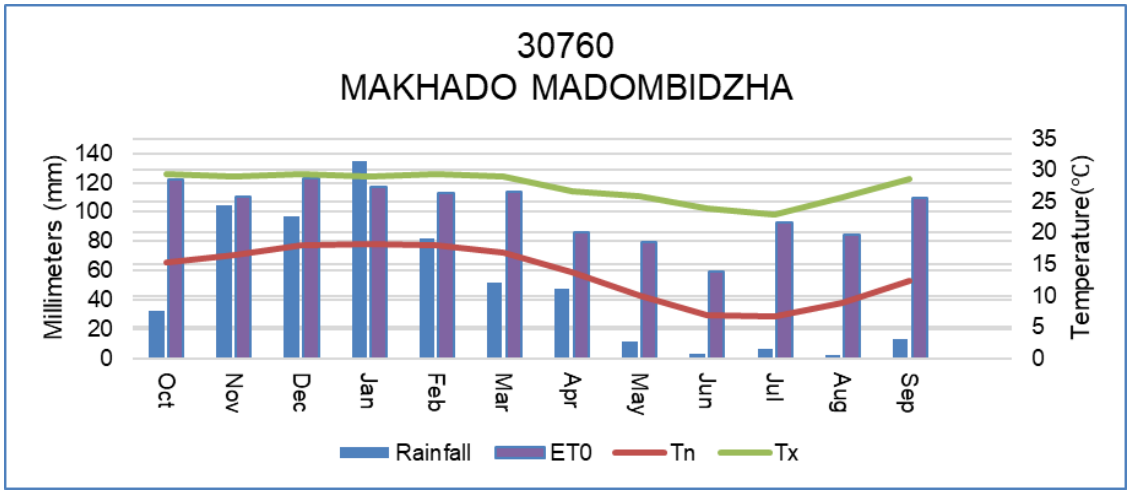

Figure 6-10: Relationship between rainfall, evapotranspiration and temperature.

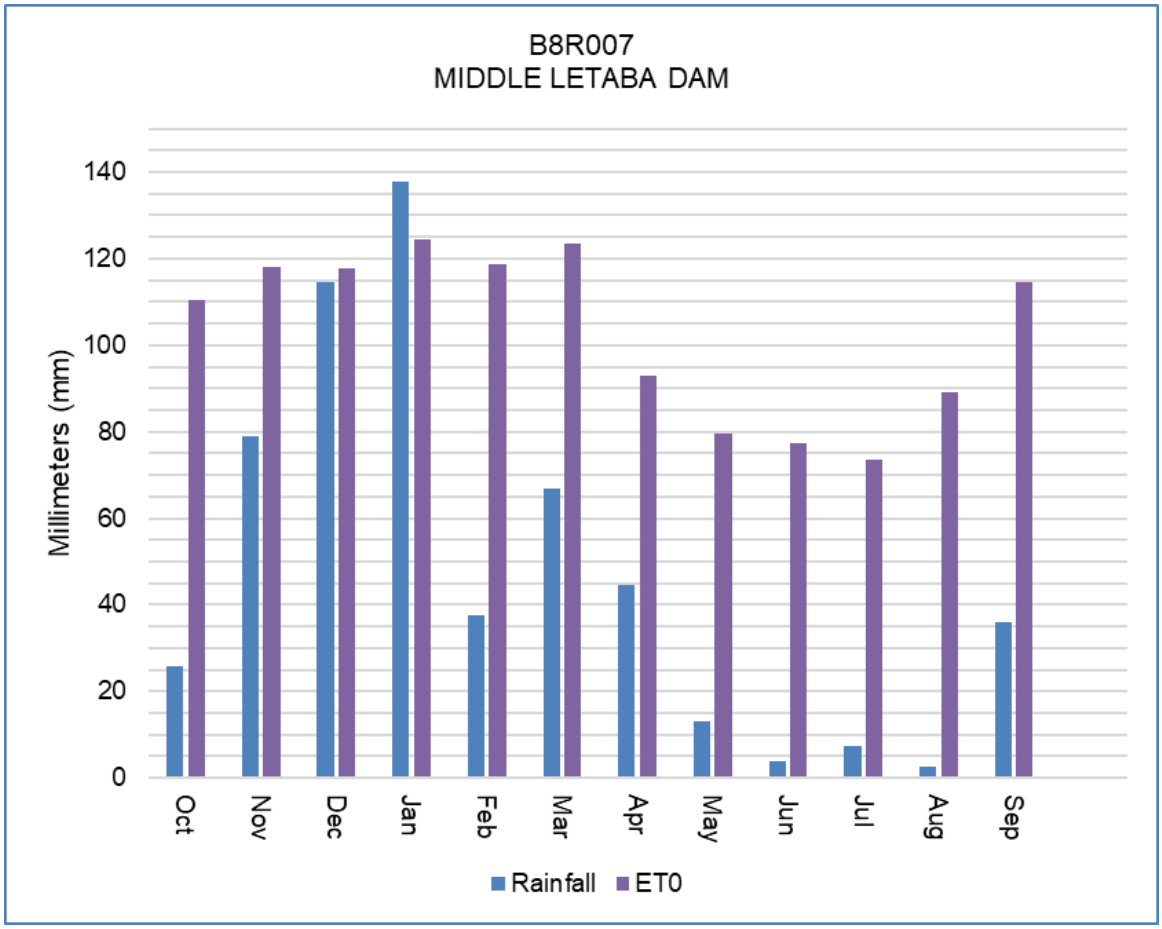

Figure 6-11: Relationship between reference evapotranspiration and rainfall.

6.4 Impacts of climate change on water resources

Meadows (2006), predicted that the future increase in temperature over South Africa will bring a decrease in rainfall and more severe and frequent droughts. This makes understanding climate change impacts significant for effective decision-making in mitigating and reducing the risks that may occur (Hayes et al., 2011). The impacts of climate change were assessed using rainfall data, temperature data, dam water level, and groundwater level data. As shown in Table 6-5 and Figure 6-12, the years with the highest temperatures have the lowest rainfall and these correspond with the drought seasons recorded in the study area.

Figure 6-12 is a graphical presentation of the relationship between rainfall and temperature on an annual basis. The data indicate that there is a non-linear relationship between temperature and rainfall during the years (2007, 2012, 2015, and 2016) with the highest temperature corresponds to the lowest rainfall.

Table 6-5: Comparison between annual rainfall and temperatures

	06791945 (Highveld)		30760 (Lowveld)	
Years	**Rain (mm)**	**Temp (°C)**	**Rain (mm)**	**Temp (°C)**
2007	841,3	26,68	456,2	26,94
2008	977,34	26,41	382,03	26,99
2009	1075,58	26,22	696,36	26,38
2010	1113,83	26,31	581,27	26,55
2011	1135,2	25,68	473,43	26,42
2012	875,5	26,52	475,24	27,22
2013	1298,87	26,10	789,39	26,20
2014	918,94	26,10	749,45	26,15
2015	525,59	28,11	269,86	28,14
2016	691,17	27,63	482,5	28,74

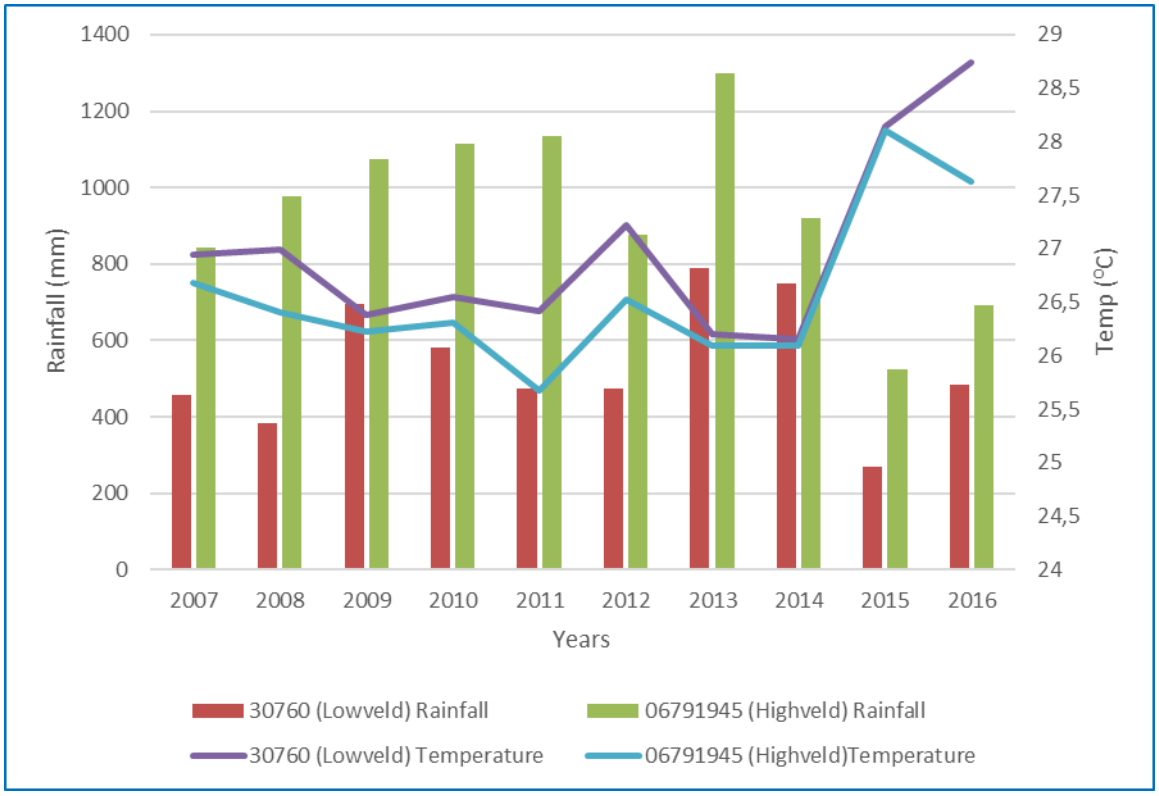

Figure 6-12: Comparison of annual rainfall and maximum temperatures

6.4.1 Impacts of climate change on surface water resources

Nsami and Middle Letaba dams are the two major dams in the study area with a storage capacity of 21.9 Mm^3 and 173 Mm^3, respectively. The 21-year (1999 to 2020) period of water level data is showing consistent declining dam water level trends with sharp and sporadic fluctuations.

This is due to the minimal periods of wet seasons coupled with numerous periods of drought (Figure 6-13 and Figure 6-14). On numerous occasions, the Mopani Municipality had to effectively enforce abstraction restrictions in these dams due to the significantly low levels. During these periods, water levels in boreholes also dropped significantly due to the stress applied to groundwater resources as a result of the declining availability of water from the Middle Letaba dam.

To understand the impacts of climate change on surface water resources, this study focuses on the Middle Letaba dam due to its persistent low water level that has resulted in the continued water supply crisis for the targeted communities in Giyani Local Municipality. For more than 20 years, this local municipality has been the most water-stressed area in the Limpopo Province. For this study, impact analysis is only focused on 10-year period data (from 2007 to 2016).

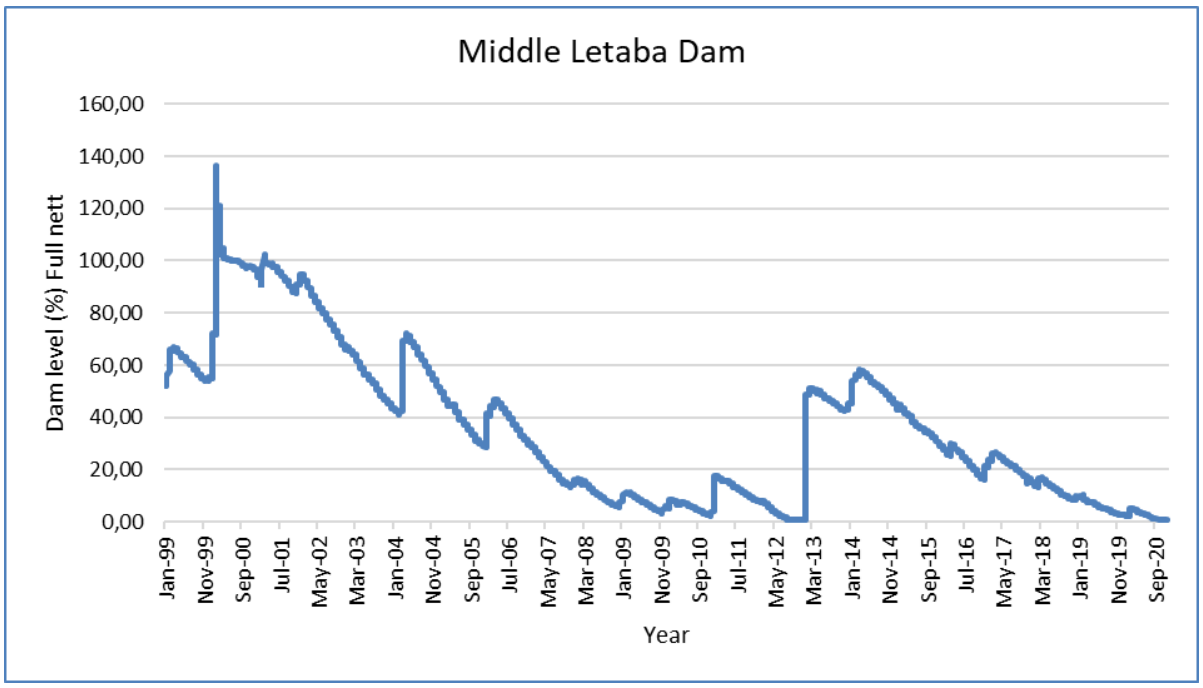

Figure 6-13: Middle Letaba Dam water levels from 1999 to 2020.

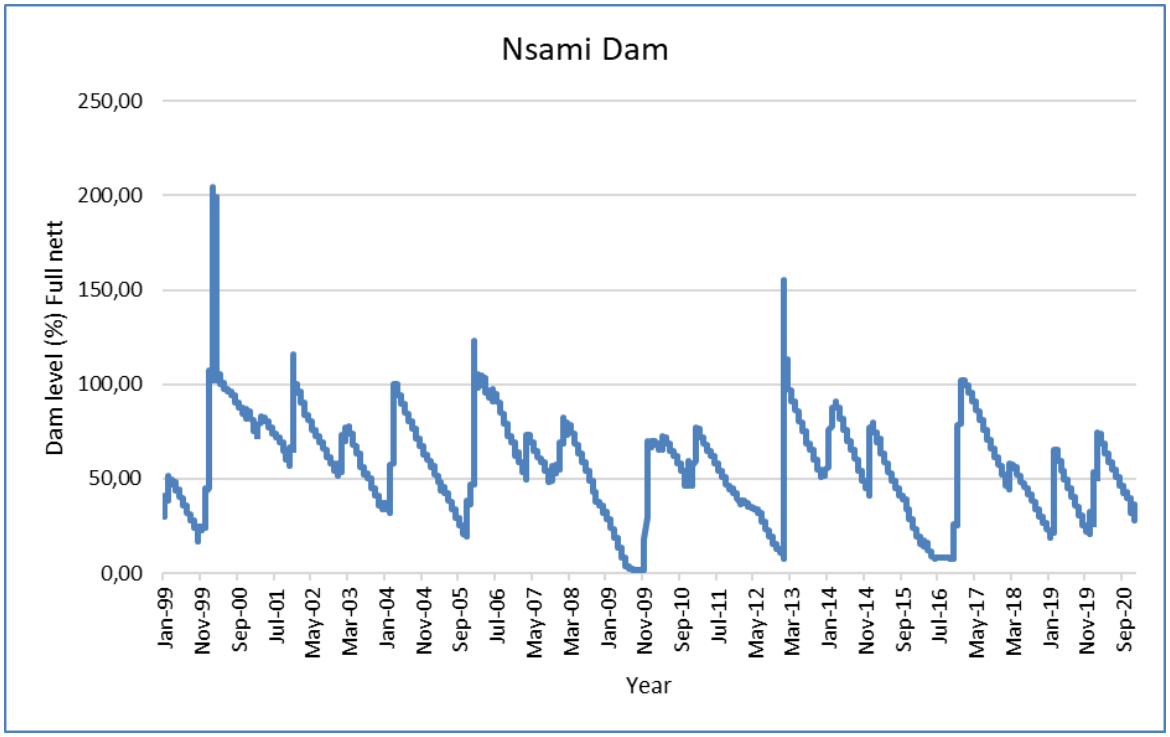

Figure 6-14: Nsami Dam water levels from 1999 to 2021.

As shown in Figure 6-15, the mean monthly rainfall received on the surface area of the Middle Letaba dam varied significantly across different months over the 10 years (2007 to 2016). The dam receives more water from direct rainfall during the summer months, with January having the highest rainfall. Furthermore, Figure 6-15 reveals that reference evaporation around the Middle Letaba dam is often higher than rainfall except in a few events where monthly rainfall is above average (i.e. <100 mm/m). This could be one of the reasons for the persistent low water levels and failure to fulfill water supply obligations to the community who live in the area. Higher reference evaporation is associated with higher temperature because when water is heated more energy is created to evaporate the water. As a result, dam storage volume in the Middle Letaba dam has been consistently below 20% for more than 6 years (from July 2007 to January 2013), with the lowest recorded in Dec 2012 at 0.62 %. The increased rain event of the year 2013/ 2014 was the wettest season recorded for the study area in the last 10 years, resulting in an increased dam storage volume of about 50 to 60% (Figure 6-15). However, this was short-lived because in May 2014 the storage volume was already on a declining trend which continued until the year 2020 (Figure 6-13).

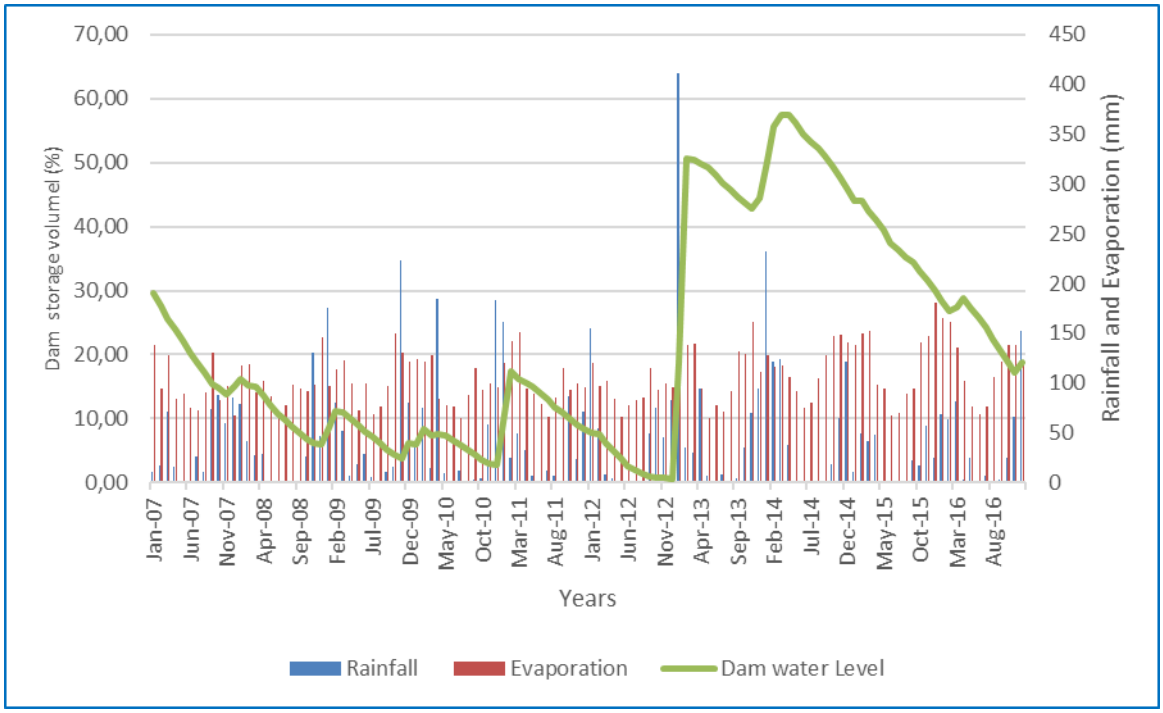

Figure 6-15: Relationship between rainfall and Middle Letaba dam volume

Based on the analysis of the rainfall, temperature, and dam storage volume trends, it is evident that climate change is negatively influencing the rainfall and temperature which in turn affect the availability of water resources in the study area. Since the year 2000, this dam has been on a declining trajectory and at its lowest with storage volume only improving during floods. This indicates that the Middle Letaba dam cannot meet its obligation of sustainable water supply from only rainfall as the main source of water supply in the region.

6.4.2 Impacts of climate change on groundwater resources

The groundwater level in the study area ranges between 8.29 mbgl (B8N0521) and 38.69 mbgl (B8N0509), indicating a shallow unconfined aquifer which is generally characterised by a constant decline with some sharp seasonal fluctuation pattern. The effect of climate change on fluctuations in groundwater resources was evaluated and the linear regression line (Figure 6-16) indicates an increasing trend with time. This shows that groundwater level is increasing in depth from time to time, which suggests that groundwater in the study area is diminishing. This situation can be alarming and raise concern for the sustainable use of groundwater by various communities in the area.

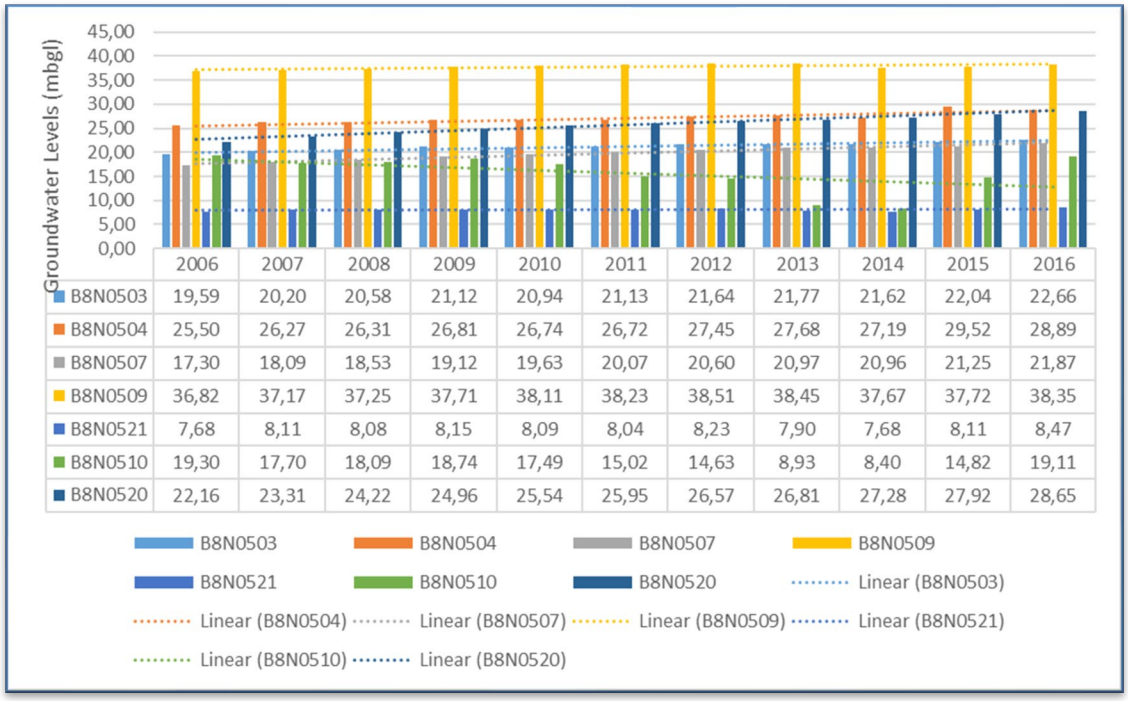

	2006	2007	2008	2009	2010	2011	2012	2013	2014	2015	2016
B8N0503	19,59	20,20	20,58	21,12	20,94	21,13	21,64	21,77	21,62	22,04	22,66
B8N0504	25,50	26,27	26,31	26,81	26,74	26,72	27,45	27,68	27,19	29,52	28,89
B8N0507	17,30	18,09	18,53	19,12	19,63	20,07	20,60	20,97	20,96	21,25	21,87
B8N0509	36,82	37,17	37,25	37,71	38,11	38,23	38,51	38,45	37,67	37,72	38,35
B8N0521	7,68	8,11	8,08	8,15	8,09	8,04	8,23	7,90	7,68	8,11	8,47
B8N0510	19,30	17,70	18,09	18,74	17,49	15,02	14,63	8,93	8,40	14,82	19,11
B8N0520	22,16	23,31	24,22	24,96	25,54	25,95	26,57	26,81	27,28	27,92	28,65

Figure 6-16: Groundwater level in response to rainfall

As shown in Figure 6-17, groundwater level fluctuations are in response to seasonal rainfall variability and drought events that occur in the study area. This shows that even though groundwater is protected from the direct effects of climate change, piezometric surface is indirectly influenced by reduced recharge, discharge or even influencing water quality (Moseki, 2017). The area experienced significant wet seasons during 2010-2011 and 2012-2013 and this resulted in a direct positive response of the aquifer which led to the recovery of the groundwater level. The impact of drought event that occurred between 2014 to 2015 had a negative impact resulting in declining groundwater levels. The variations in weather patterns have a serious negative impact on water resources, agricultural yield, livelihood, and the national economy.

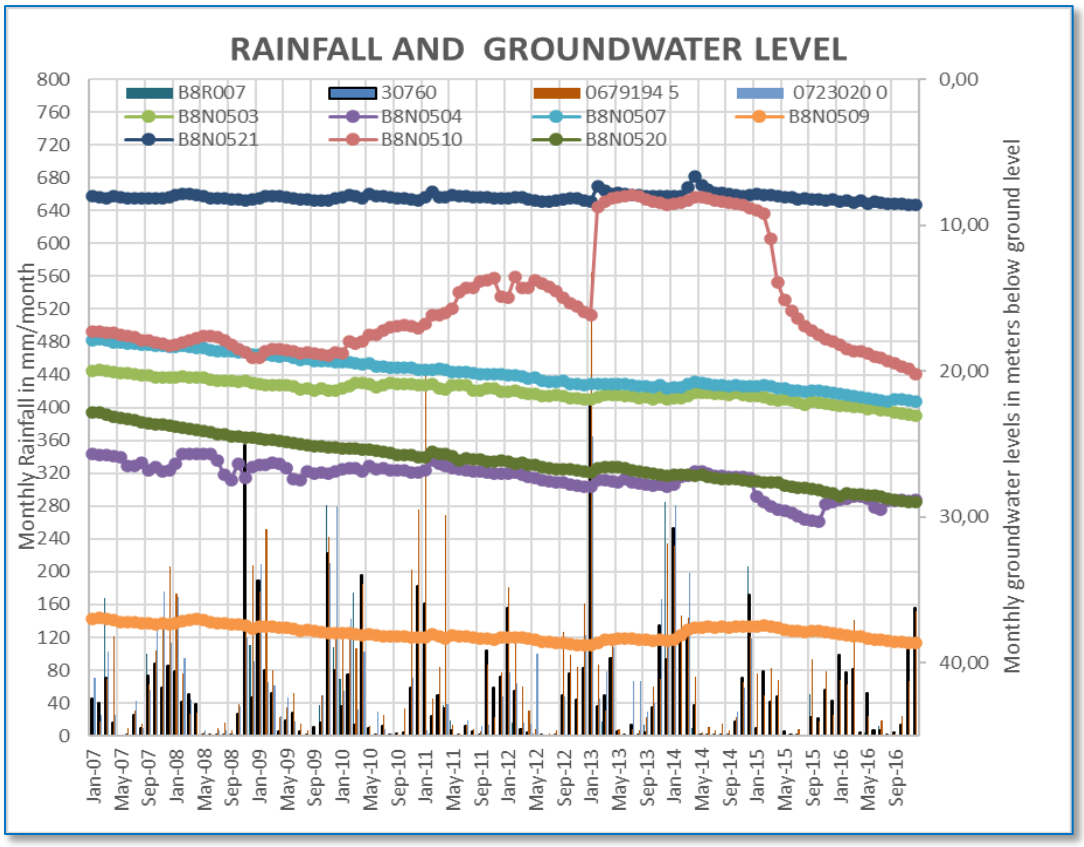

Figure 6-17: Trends of groundwater level change and monthly rainfall during the historical observation.

CHAPTER 7 : MODEL RESULTS AND DISCUSSION

7.1 Introduction

Water is a limited and scarce resource for the rural and farming communities in the Klein Letaba River catchment. The area has been experiencing severe water shortages over the past years. The decline in groundwater level is partly due to an increase in abstraction. This problem is further exacerbated by low rainfall and prolonged periods of droughts. To determine the sustainable use of water, the impacts of climate and man-made-induced hydrological stresses have to be thoroughly assessed. This can be achieved through the implementation of a steady-state numerical model of groundwater flow. Below are the model results and discussion.

7.2 Evaluation of model calibration

Five observation wells were considered for comparison with the simulated hydraulic heads, and the results are presented in Figure 7-1 and Table 7-1. The model was calibrated manually by adjusting the hydraulic conductivity of different rock types, recharge, evapotranspiration, dam, and river bed conductance to obtain the best fit between the observed and simulated heads. The mean error (ME), mean absolute error (MAE) and root mean squared error (RMS) were calculated to evaluate the level of fitness between the observed and simulated heads. The best-fitting line is represented by a coefficient of determination R^2=0.99, i.e. this parameter defines how the simulated hydraulic heads closely fit the observed heads as illustrated in Figure 7-1.

The simulated water level contour maps for the two layers (weathered and fractured aquifers) are presented in Figure 7-2. These maps suggest that the groundwater flow direction is SW-NE, with the maximum level on the SW (1070 m.a.s.l), and minimum in the northeastern part of the area (485 m.a.s.l). The rivers and dams are superimposed on the simulated water level contour map. Along the river channels and the dam, the simulated water level is consistently lower than elsewhere, suggesting that the aquifer supplies water to the river and dam.

The amount of water gained by the river and dam appears to be driven by a hydraulic gradient, i.e., the leakage is increasingly high towards the lower reach of the river, while towards the upper reach, the volume of water that leaks from the aquifer to the river is low. The patterns of the simulated water level contour lines along the rivers are also accordant with the results of the water budget shown in Table 7-2.

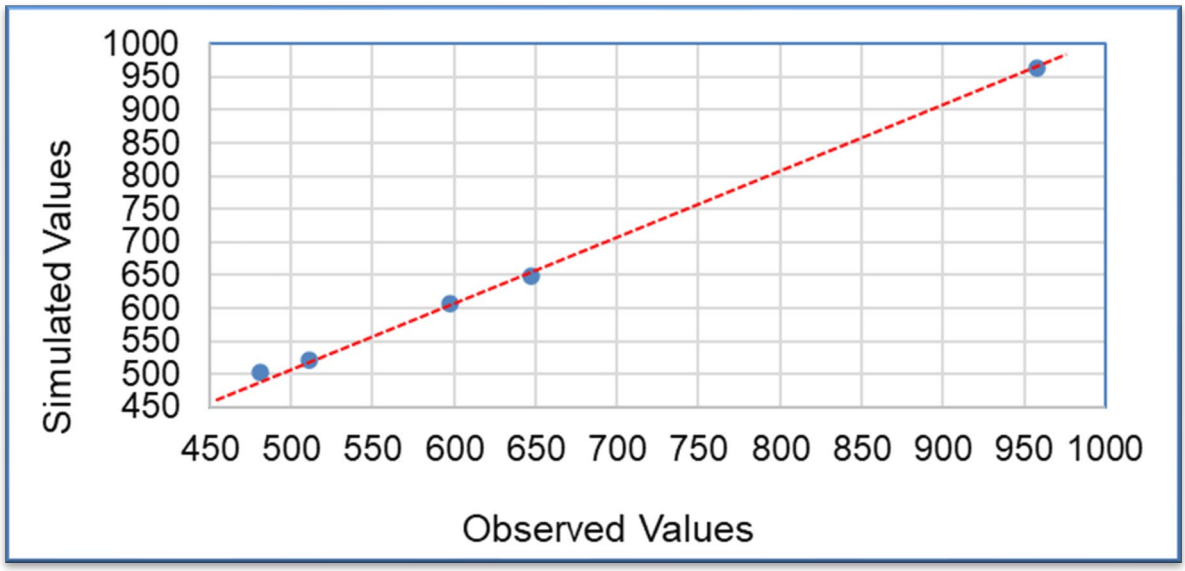

Figure 7-1: Scatter plot of the comparison between observed and simulated heads.

Table 7-1: Comparison between observed and simulated heads.

BH ID	Latitudes	Longitudes	Observed Values	Simulated Values	Differences	Root Mean Square (Obsi-Simi)^2	Mean Error (Obsi-Simi)	Mean Absolute Error (Obsi-Simi)
BH 1	-23.20531	30.14028	598	606	-7.70	60.84	-7.80	7.80
BH 2	-23.26800	30.38180	511	520	-9.11	82.99	-9.11	9.11
BH 3	-23.46550	30.15652	647	648	-0.87	0.79	-0.89	0.89
BH 4	-23.34400	29.99800	958	964	-6.04	36.48	-6.04	6.04
BH 5	-23.24500	30.47400	481	502	-20.91	437.23	-20.91	20.91
					Sum	**618.33**	**-44.75**	**44.75**
					Minimum	**0.79**	**-0.89**	**0.89**
					Maximum	**437.23**	**-20.91**	**20.91**
					Mean	**123.67**	**-8.95**	**8.95**
					Standard Deviation	**177.92**	**7.38**	**7.38**
					Mean Errors	**11.12**	**-8.95**	**8.95**

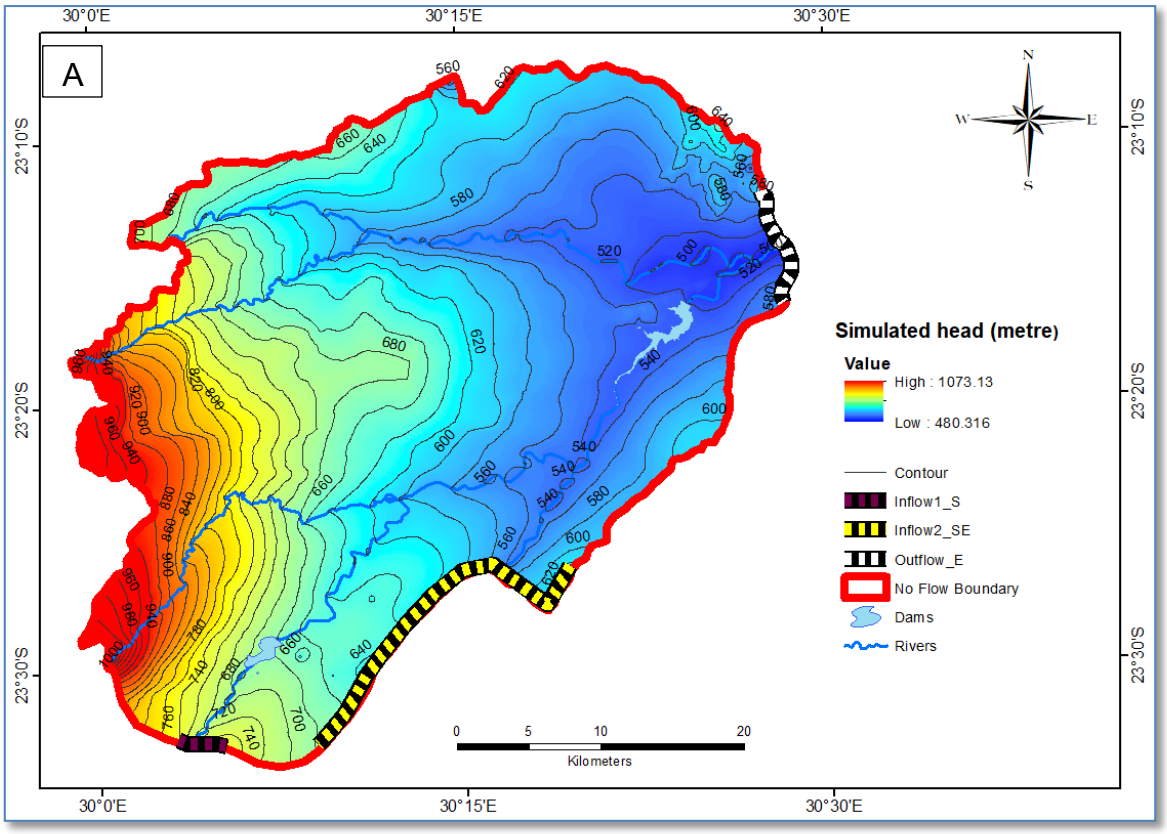

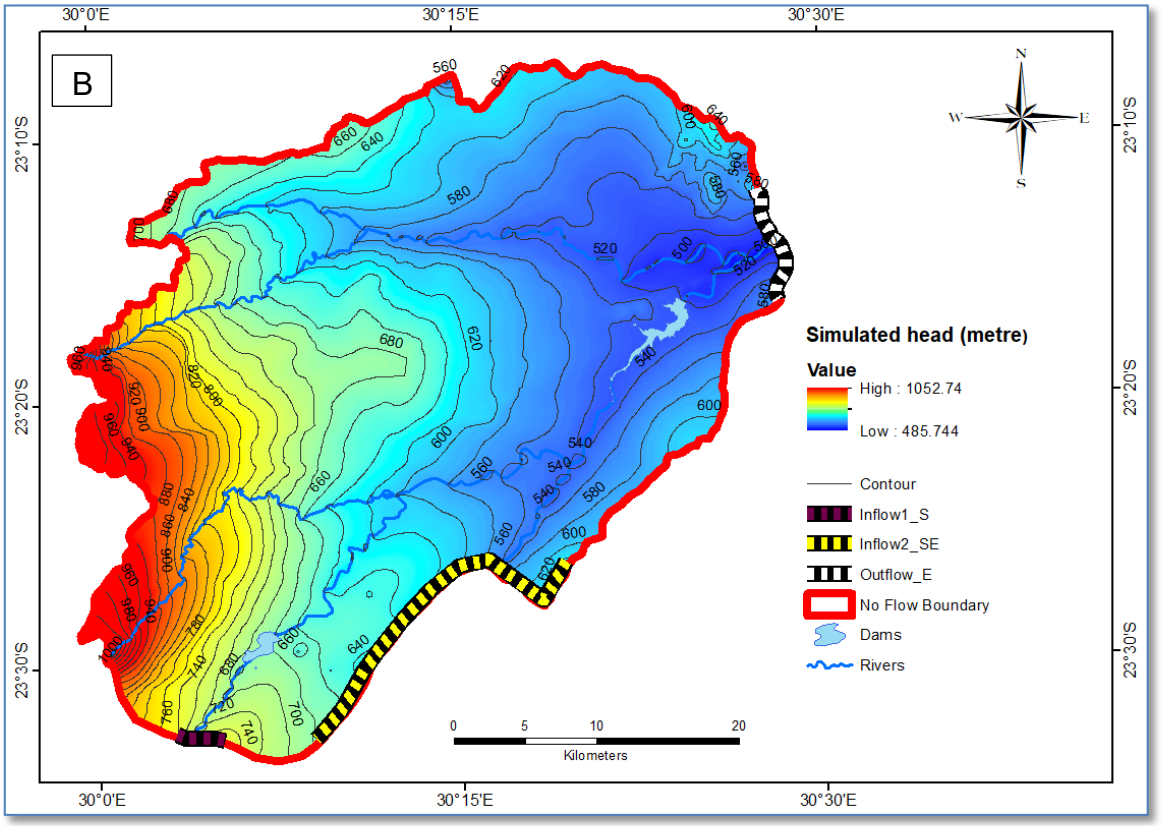

Figure 7-2: Simulated groundwater level, (A) Weathered Aquifer and (B) Fractured Aquifer.

7.3 Analysis of Water Budget

The water budget was used to quantify the main components that control the inflows and outflows of the groundwater as shown on Table 7-2. The inflow components consist of recharge through interaction between the rivers and the aquifer, head-dependent boundaries of the model domain, and rainfall. The outflow components include abstraction wells, evapotranspiration, gaining river and head-dependent boundaries (subsurface outflow). The total volume of water that flows into the aquifer is 3.085E+08 m^3/day, while the total discharge (outflow) is estimated at 3.083E+08 m^3/day. The water budget shows that rainfall recharge is the major source of inflow contributing 1.35E+08 m^3/day (i.e., equivalent to 44%), followed by the leakages from the river with a flux rate of 1.25E+08 m^3/day (i.e., equivalent to 40%).

Abstraction wells were considered to be the lowest outflow component, only taking approximately 2% of the total outflow, i.e., it accounts for an abstraction volume of 5.70E+06 m^3/day. This is followed by the general head-dependent boundaries (GHB) and evapotranspiration with 3.50E+07 m^3/day (i.e., equivalent to 11%) and 7.61E+07 m^3/day (i.e., equivalent to 25%) of the total outflow volumes, respectively. A significant amount of water, approximately 1.92E+08 m^3/a (i.e., equivalent to 62% of the total groundwater outflows) is lost from the aquifer through river leakage. The water budget results are presented in Table 7-2 and further displayed in Figure 7-3.

Table 7-2: Results of the steady-state water budget.

Sources/Sinks	Inflows (m^3/day)	Inflows (%)	Outflows (m^3/day)	Outflows (%)
WEL	0	0	5.70E+06	2
EVT	0	0	7.61E+07	25
RIV LEAKAGE	1.25E+08	40	1.92E+08	62
GHB	4.88E+07	16	3.50E+07	11
RCH	1.35E+08	44	0	0
Total	**3.08493E+08**		**3.08258E+08**	

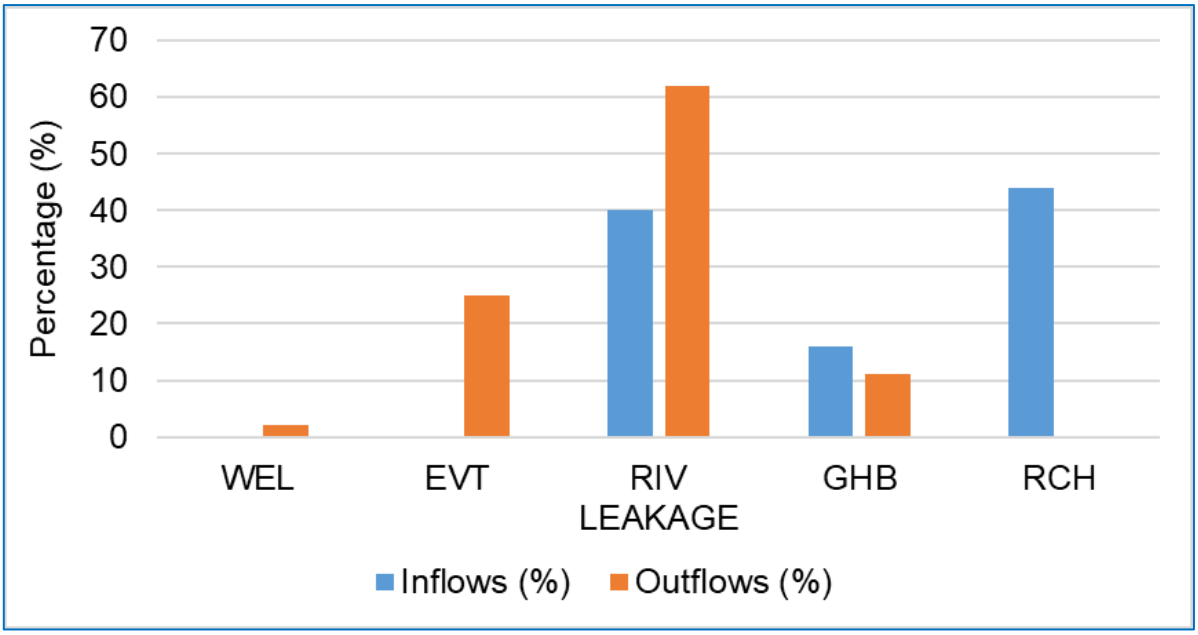

Figure 7-3: Graphical display of the results of the water budget showing the flux corresponding to each component of inflows and outflows.

7.4 Analysis of Zone Budget

To investigate the interaction between the various components of the surface water and groundwater, the Zone Budget package was implemented. Four zones that are 1, 2, 3, and 4 were assigned to the weathered aquifer, fractured aquifer, dam, and rivers, respectively.

The results are shown in Table 7-3 and Figure 7-4 indicate that surface and groundwater aquifers are hydraulically connected, which is accordant with the results of stable isotope composition suggesting mixing of groundwater and surface water. The zone budgets indicate that there is a significant interaction between the weathered aquifer (zone 1) with the fractured aquifer (zone 2) and the rivers (zone 4). The weathered aquifer supplies approximately 1.04E+08 m^3/day (i.e. equivalent to 36% of the total inflow) to a fractured aquifer, while the latter supplies approximately 9.86E+07 m^3/day to the weathered aquifer. This result suggests that the total volume of recharge 1.35E+08 m^3/day is redistributed to the fractured aquifer across the weathered aquifer. Thus, the weathered aquifer acts as a layer through which the fractured aquifer is being replenished.

In addition, the result indicates that the storage capacity of the weathered aquifer is lower than the fractured aquifer, which is consistent with the borehole log results. Furthermore, the results signify the importance of the underlying fractured aquifer as the main source of water owing to its good hydraulic conductivity compared to the weathered aquifer.

Table 7-3: Results of the zone budget.

Zones Budget Components	Interactions	Inflow (m^3/day)	Inflows (%)	Outflows (m^3/day)	Inflows (%)
Zone 1 (Weathered Aquifer) and River	Zone 1 to 0	0	0	1.21E+08	42
	Zone 1 to 2	0	0	1.04E+08	36
	Zone 1 to 3	0	0	2.16E+05	0.07
	Zone 1 to 4	0	0	6.64E+07	23
	Zone 0 to 1	1.71E+08	1	0	0
	Zone 2 to 1	9.86E+07	34	0	0
	Zone 3 to 1	2.30E+05	0.08	0	0
	Zone 4 to 1	2.27E+07	8	0	0
Totals		**2.92326E+08**	**42**	**2.91940E+08**	**100**
Zone 2 (Fractured Aquifer)	Zone 0 to 2	0	0	5.70E+06	5
	Zone 1 to 2	1.04E+08	100	0	
	Zone 2 to 1	0	0	9.86E+07	95
Totals		**1.04000E+08**	**100**	**1.04302E+08**	**95**
	Zone 0 to 3	1.39E+07	98	0	0
	Zone 1 to 3	2.16E+05	2	0	0
	Zone 3 to 0	0	0	1.38E+07	98
	Zone 3 to 1	0	0	2.30E+05	2
	Zone 3 to 4	0	0	4.85E+04	0
Totals		**1.40767E+07**	**100**	**1.40765E+07**	**100**
Zone 4 (Rivers)	Zone 4 to 0		0	2.33E+08	91
	Zone 4 to 1		0	2.27E+07	9
	Zone 0 to 4	1.89E+08	74	0	0
	Zone 1 to 4	6.64E+07	26	0	0
	Zone 3 to 4	4.85E+04	0.02	0	0.00
Totals		**2.55882E+08**	**100**	**2.55879E+08**	**100**

Note: Zone 0: GHB, RCH, WEL and EVT; Zone 1: Weathered aquifer; Zone 2: Fractured aquifer; Zone 3: Dam and Zone 4: River.

The river (zone 4) supplies about 9% (2.27E+07 m^3/day) of the total inflows to the weathered aquifer. As the river stage drops, the hydraulic head is reversed causing the discharge of water from the aquifer storage to return to the river through baseflow.

In this case, an amount of 6.63E+07 m^3/day (i.e., equivalent to approximately 23% of the total outflows) is lost to the river system through base flow from the weathered aquifer. The interaction between the dam and the aquifer was considered insignificant, with the dam (zone 3) only contributing 2% (2.30E+05 m^3/day) of the total inflows to the weathered aquifer. The weathered aquifer, in turn, supplies 0.07 % of the total outflows (equivalent to 2.16E+05 m^3/day) to the dam.

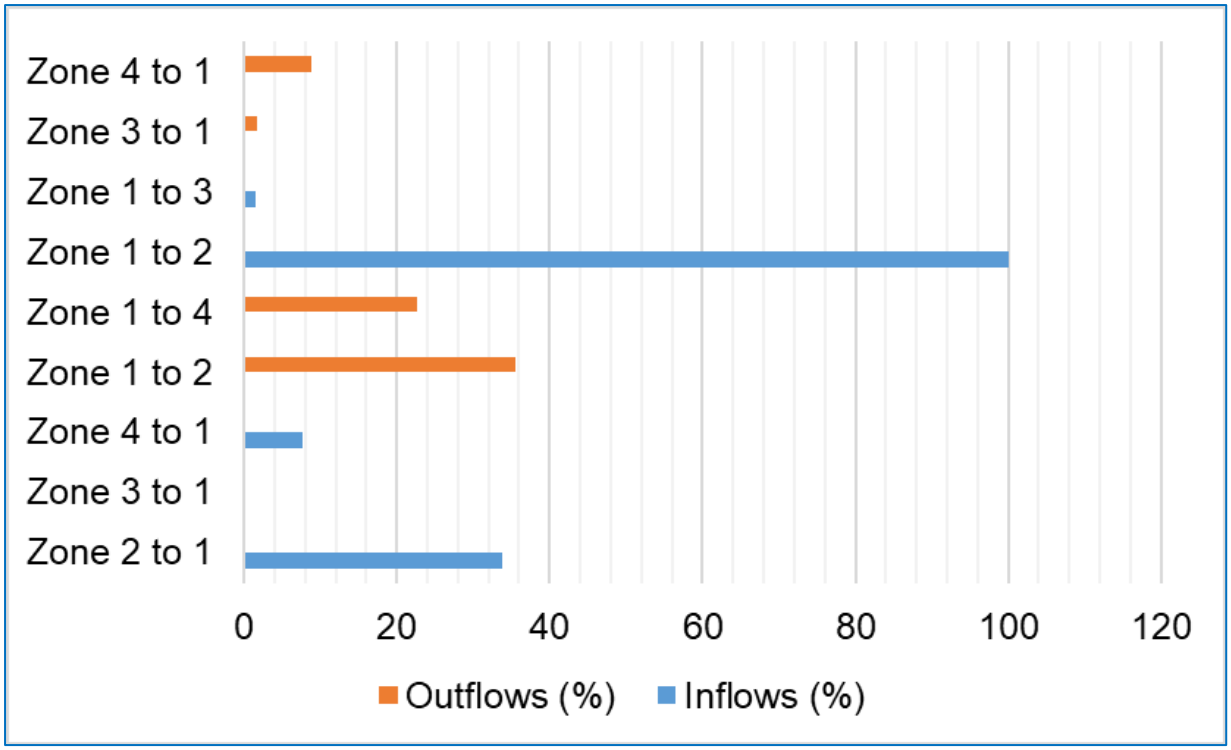

Figure 7-4: Graphical display of results of water zone budget.

7.5 Prediction of Aquifer Response

A calibrated groundwater flow model was used to predict the potential impacts of climate change and anthropogenic factors on groundwater resources. The interactions between aquifers, river, and dam were simulated to understand the response of the groundwater level to the impacts of reduced recharge i.e., climate change, and increased abstraction i.e., man-made induced stress. These were implemented by decreasing the recharge and increasing the groundwater withdrawal, by 25%, 50%, 75%, and 100%, respectively. Groundwater levels in unconfined aquifers are the first to respond to the effects of climate change and human-induced stresses.

The effects of the stress were evaluated based on the observed aquifer heads at the end of each simulation time. The different scenarios are discussed in the following sections.

7.5.1 Scenario 1: Reduced Recharge

To assess the impacts of reduced recharge on groundwater level, the recharge rate was decreased by 25%, 50%, 75% and 100%. The model was found to be sensitive to the decreased recharge and the effects are apparent in the aquifer water levels, where the simulated heads decline as the recharge rate progressively decreases. Table 7-4 and Figure 7-5 show the results of the water budget as recharge decreases from 25% to 100% step by step.

The total inflows corresponding to 25%, 50%, 75% and 100% recharge reduction were determined at 2.79452E+08 m^3/day, 2.51130E+08 m^3/day, 2.23862E+08 m^3/day and 1.99230E+08 m^3/day, respectively. The results of the simulated groundwater head distribution (Figure 7-6) show a spatially variable reduction in groundwater levels. However, these changes were less pronounced at 25% recharge reduction with the impacts becoming more significant when recharge was decreased to 50%, 75%, and 100%. These changes or declines in the groundwater level are well observable in the highly elevated areas towards the south western part of the model domain.

As shown in Figure 7-6 C and D, lower groundwater levels resulted in a reduction of hydraulic gradients from the recharge area (south west boundary) to the discharge area (north eastern boundary). Thus, causing a baseflow reduction toward the north eastern boundary. These results indicate that a decline in rainfall intensity will have detrimental environmental effects due to the changes in baseflow dynamics in rivers.

Table 7-4: Scenario 1 water balance.

Scenario	Sources/Sinks	Inflows (m^3/day)	Inflows (%)	Outflows (m^3/day)	Outflows (%)
Scenario 1: 25% decreased recharge rate	WEL	0	0	5.70E+06	2
	EVT	0	0	5.94E+07	21
	RIV LEAKAGE	1.29E+08	46	1.81E+08	65
	GHB	4.96E+07	18	3.37E+07	12
	RCH	1.01E+08	36	0	0
	Total	**2.79452E+08**	**100**	**2.79444E+08**	**100**
Scenario 1: 50% decreased recharge rate	WEL	0	0	5.70E+06	2
	EVT	0	0	4.33E+07	17
	RIV LEAKAGE	1.33E+08	53	1.70E+08	68
	GHB	5.07E+07	20	3.24E+07	13
	RCH	6.75E+07	27	0	0
	Total	**2.51130E+08**	**100**	**2.51130E+08**	**100**
Scenario 1: 75% decreased recharge rate	WEL	0	0	5.70E+06	3
	EVT	0	0	2.86E+07	13
	RIV LEAKAGE	1.38E+08	62	1.58E+08	71
	GHB	5.19E+07	23	3.12E+07	14
	RCH	3.37E+07	15	0	0
	Total	**2.23862E+08**	**100**	**2.23854E+08**	**100**
Scenario 1: 100% decreased recharge rate	WEL	0	0	5.70E+06	3
	EVT	0	0	1.82E+07	9
	RIV LEAKAGE	1.46E+08	73	1.45E+08	73
	GHB	5.36E+07	27	3.01E+07	15
	RCH	0	0	0	0
	Total	**1.99230E+08**	**100**	**1.99238E+08**	**100**

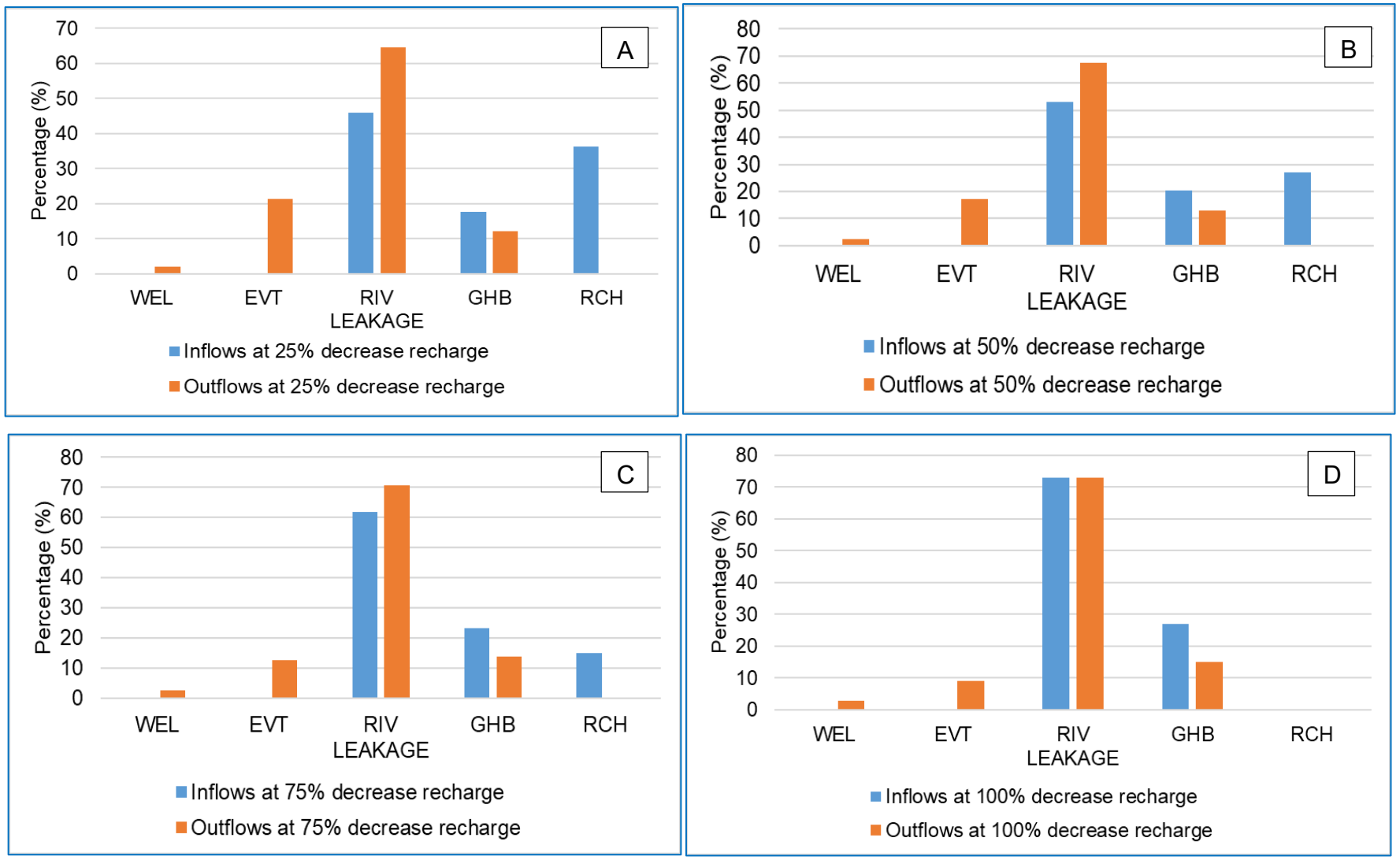

Figure 7-5: Water balance results with varying recharge rate reduction, (A) 25%, (B) 50%, (C) 75% and (D) 100%.

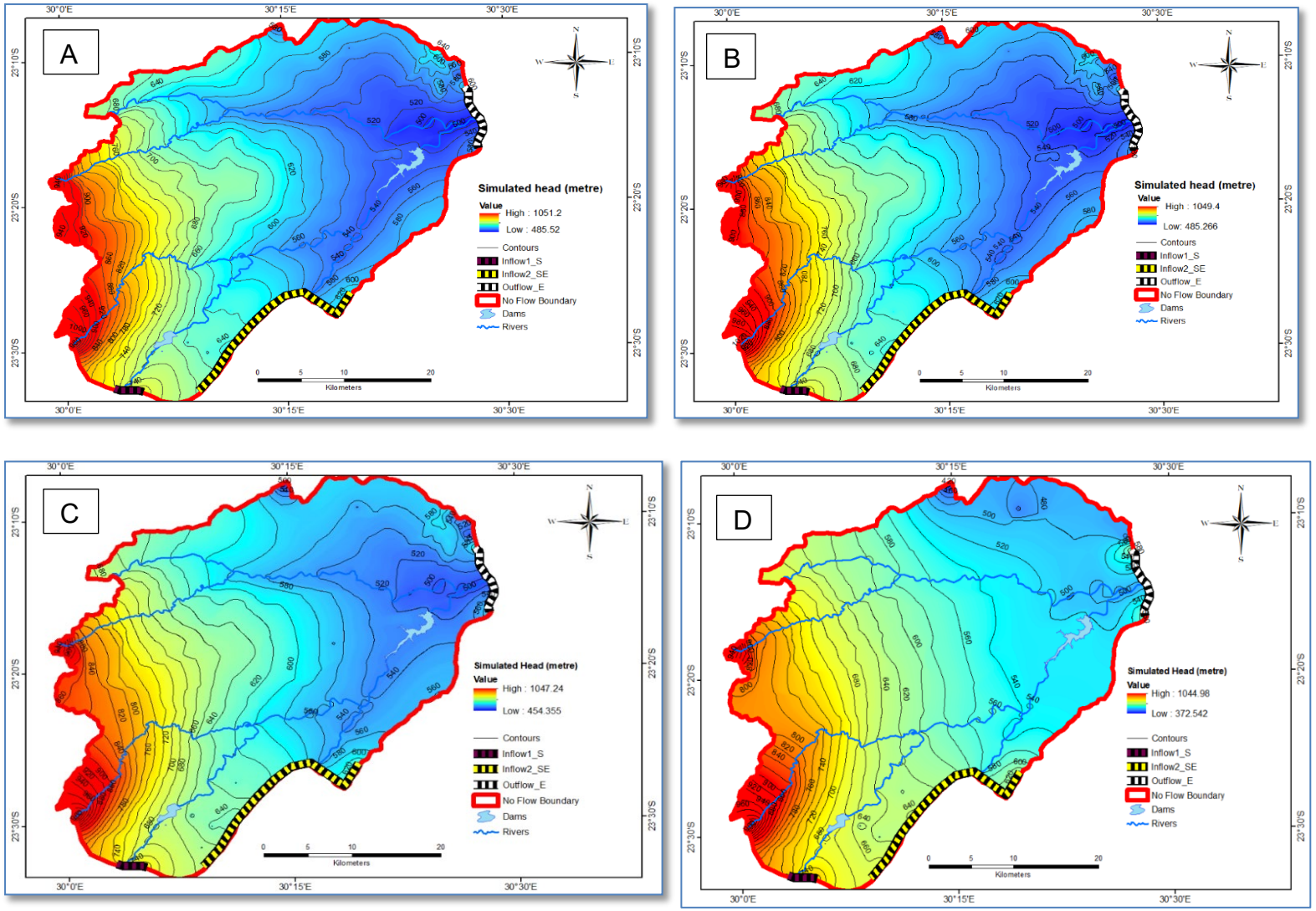

Figure 7-6: Simulated groundwater head distribution with varying recharge rate reduction, (A) 25%, (B) 50%, (C) 75% and (D) 100%.

To enhance our understanding of the response of the aquifer to the reduction in recharge rate, water table cross-sections were plotted to correspond to the four scenarios of decline in the rate of recharge (25%, 50%, 75%, and 100%). The lengths of the cross-sections are approximately 45 km west to east and 54 km south west to north east (Figure 7-7). The water table cross-sections are illustrated in Figure 7-8. The results show a steeper slope of decline in groundwater level resulting from a decrease in recharge rate.

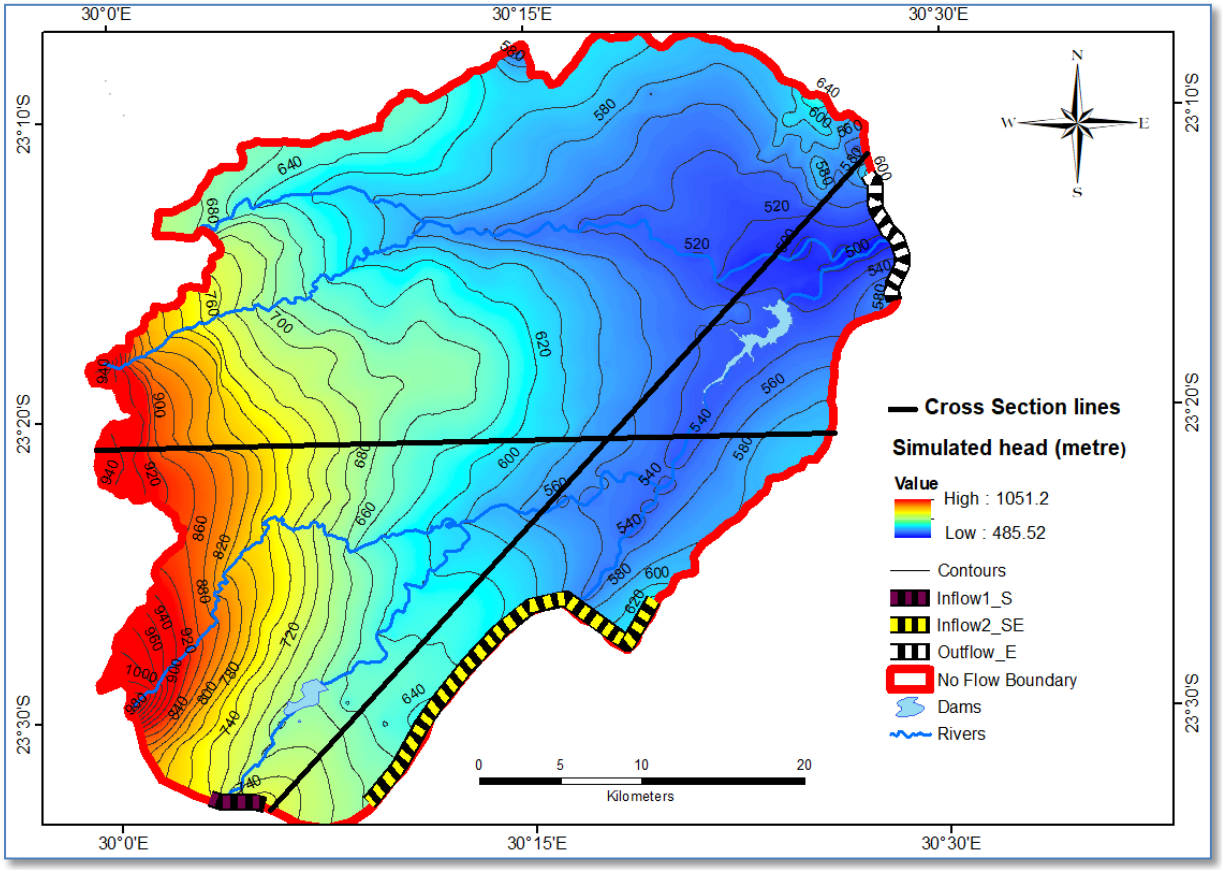

Figure 7-7: Map showing the spatial position of the water level cross-section for the boundary of the model domain.

As depicted in Figure 7-8 A and B, the high elevated areas are more vulnerable to reduced recharge than low elevated areas. This is shown on the graph (stations 1 to 25) whereby a decrease in recharge rate from 25% to 100% resulted in a decline in water level from approximately 880 m to 780 m, i.e., a 100 m drop in water level. The decline in water level elevation is obvious as the recharge rate decreases from 25% to 100% of the current recharge rate throughout the study area.

However, the impact of the decrease in recharge rate on the aquifer system is overprinted by the interaction between the river and aquifer (see the cross-section where the points on the cross-section coincide with the river channel). This result is consistent with the discussions presented in sections 7.4 and 7.5 attesting groundwater and surface water interactions.

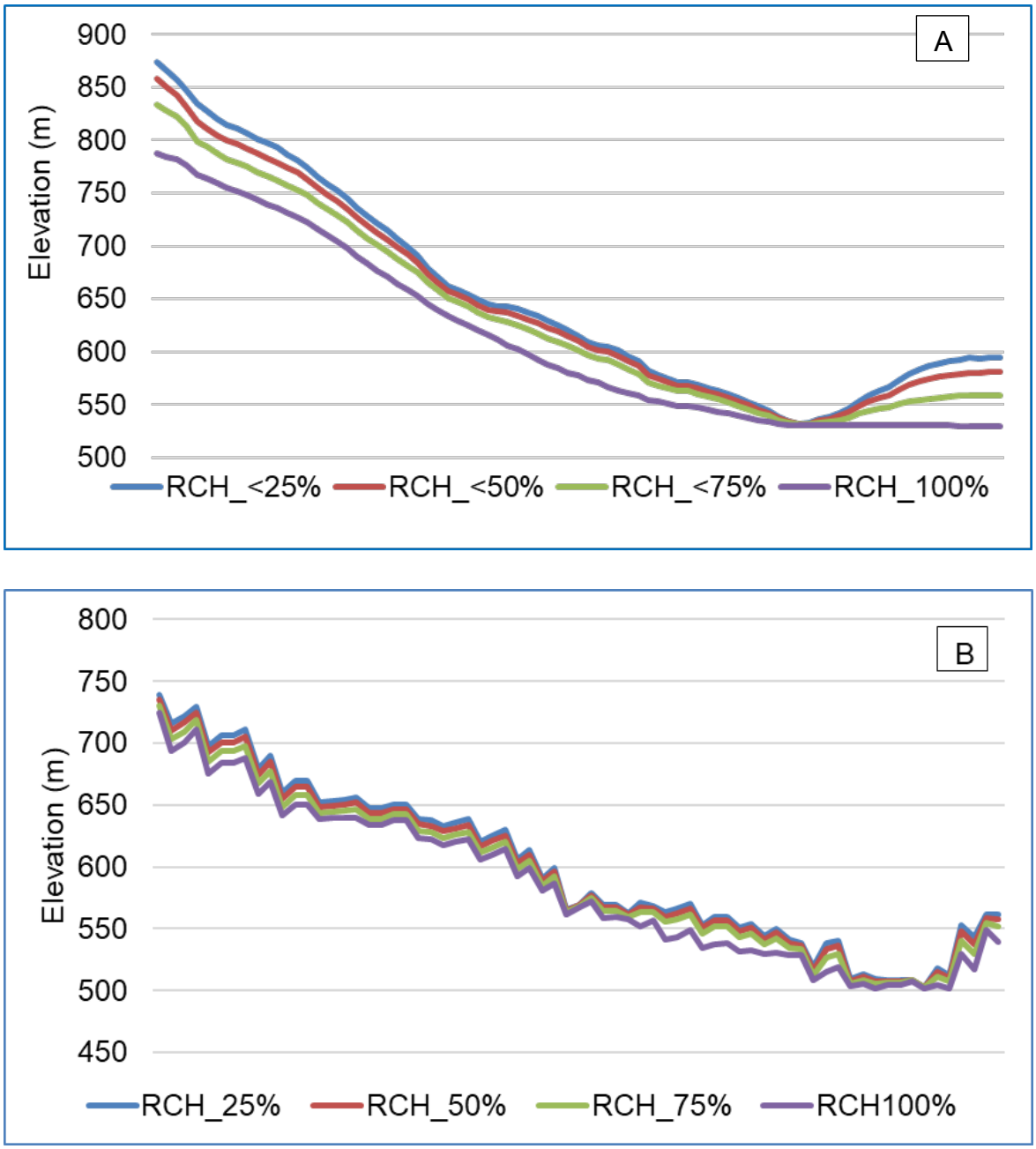

Figure 7-8: Cross-section of water table corresponding to recharge reduction rates of 25%, 50%, 75%, and 100% recharge reduction, (A) west to east and (B) south west to north east.

7.5.2 Scenario 2: Increased Abstraction

Groundwater is significantly impacted by extensive use of water for irrigation, particularly in the south western part of the study area. The second scenario is implemented by considering 12 abstraction wells which are assumed to be applying significant stress to the groundwater resource in the area. The abstraction scenario was simulated using a 25%, 50%, 75%, and 100 % increase in abstraction rate. The response of the aquifers to the different abstraction scenarios is presented in Table 7-5 and Figure 7-9. The total outflows at 25%, 50%, 75% and 100% increased abstractions were determined at 3.36087E+08 m^3/day, 3.45211E+08 m^3/day, 3.55018E+08 m^3/day and 3.64703E+08 m^3/day, respectively. The EVT decreases continuously as the abstraction rate increases from 25% to 100% with a step of 25%. This suggests that due to a continuous increase in the abstraction rate, the EVT extinction depth becomes shallower and shallower than the depth of the water level in the aquifer. In addition, the inflows and outflows corresponding to the GHB increase and decrease, respectively as the abstraction rate increases. This implies that the volume of water that flows from the GHB to the aquifer increases as the water level in the aquifer drops making the aquifer gain water from the dams and other features that were defined as GHB. Similarly, the amount of water that is discharged out of the aquifer through interaction with the features that were defined as GHB decreases continuously due to a drop in water level resulting in from high abstraction rate.

The simulated contour maps of aquifer water levels due to the impact of the increased groundwater abstraction are presented in Figure 7-10. Interestingly, the water level around the wells is significantly lower than elsewhere due to an immediate response of the aquifer to an increased abstraction rate. This implies that a future increase in the demand for groundwater use will have an adverse effect on the sustainable supply of water for various types of use. This is a distinct indication of the impact of abstraction causing groundwater level depressions in the immediate vicinity of the abstraction boreholes. These depressions have a strong influence on groundwater flow, as can be seen by the convergence of groundwater toward the abstraction boreholes.

In the absence of proper monitoring, management of groundwater level, and abstraction, the cone of depression around the individual boreholes has the potential to extend beyond the nearby boreholes. Thus, lowering the groundwater levels and consequently increasing the volume of water that flows from the surface such as rivers and dams to the aquifer. This may result in possible contamination of groundwater due to strong interaction between surface water and groundwater. Thus, some of the negative effects associated with the declining groundwater level include escalated pumping costs, deterioration of water quality, reduction of water in streams and lakes, or land subsidence (Kwon, 2017). It is therefore important to implement regular sampling and analysis of the chemistry of water as well as water level monitoring to mitigate the adverse impacts of increased abstraction rate.

Table 7-5: Scenario 2 water balance.

Scenario	Sources/Sinks	Inflows (m^3/day)	Inflows (%)	Outflows (m^3/day)	Outflows (%)
Scenario 2: 25% increase in abstraction	WEL	0	0	8.55E+07	25
	EVT	0	0	5.21E+07	15
	RIV LEAKAGE	1.39E+08	41	1.71E+08	51
	GHB	6.23E+07	19	2.75E+07	8
	RCH	1.35E+08	40	0	0
	Total	**3.36087E+08**	**100**	**3.36087E+08**	**100**
Scenario 2: 50% increase in abstraction	WEL	0	0	1.03E+08	30
	EVT	0	0	4.91E+07	14
	RIV LEAKAGE	1.44E+08	42	1.67E+08	48
	GHB	6.67E+07	19	2.67E+07	8
	RCH	1.35E+08	39	0	0
	Total	**3.45220E+08**	**100**	**3.45211E+08**	**100**
Scenario 2: 75% increase in abstraction	WEL	0	0	1.20E+08	34
	EVT	0	0	4.64E+07	13
	RIV LEAKAGE	1.49E+08	42	1.62E+08	46
	GHB	7.15E+07	20	2.60E+07	7
	RCH	1.35E+08	38	0	0
	Total	**3.55018E+08**	**100**	**3.55018E+08**	**100**
Scenario 2: 100% increase in abstraction	WEL	0	0	1.37E+08	38
	EVT	0	0	4.42E+07	12
	RIV LEAKAGE	1.54E+08	42	1.58E+08	43
	GHB	7.62E+07	21	2.54E+07	7
	RCH	1.35E+08	37	0	0
	Total	**3.64703E+08**	**100**	**3.64703E+08**	**100**

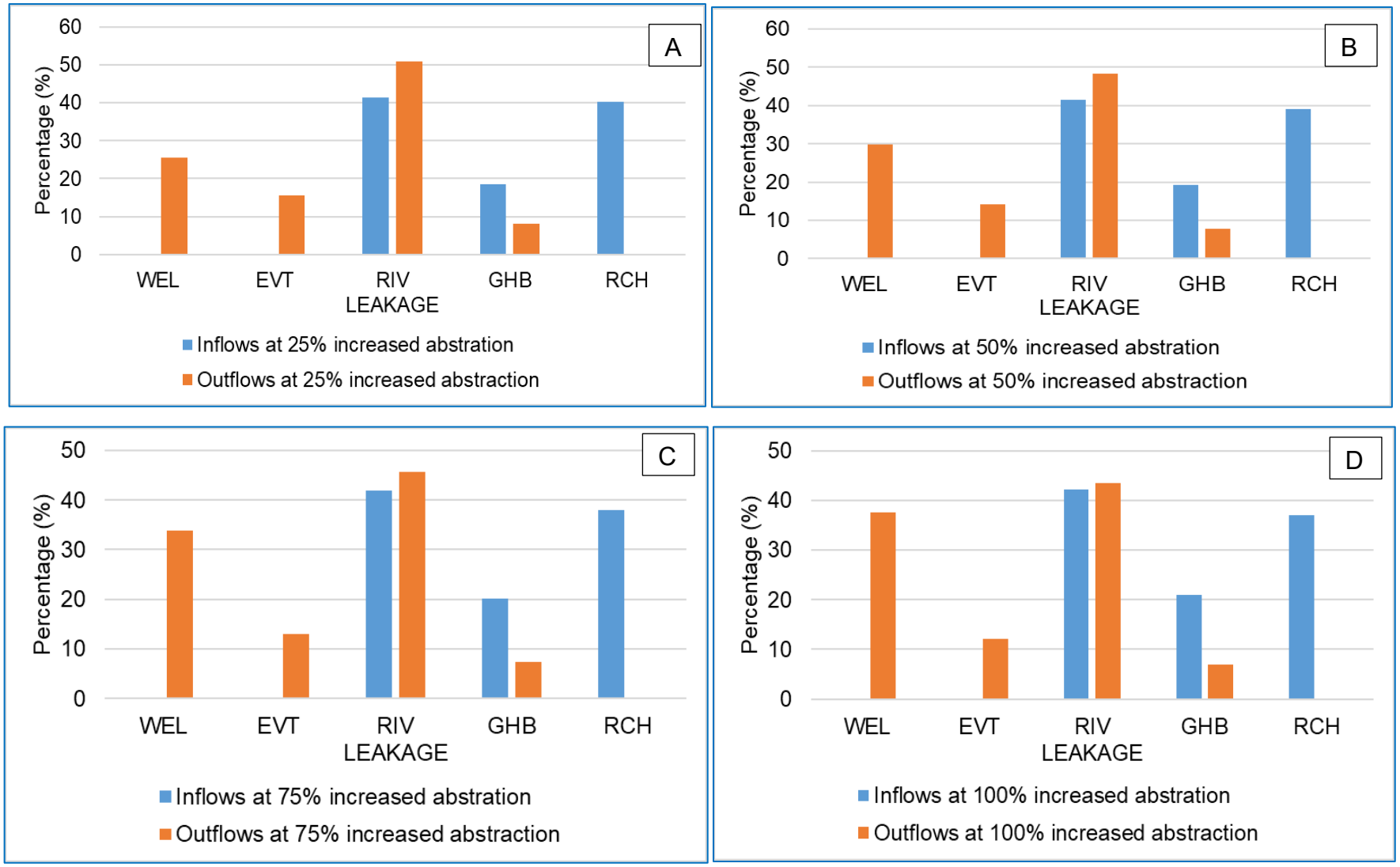

Figure 7-9: Water balance results in varying abstraction rate increment, (A) 25%, (B) 50%, (C) 75% and (D) 100%.

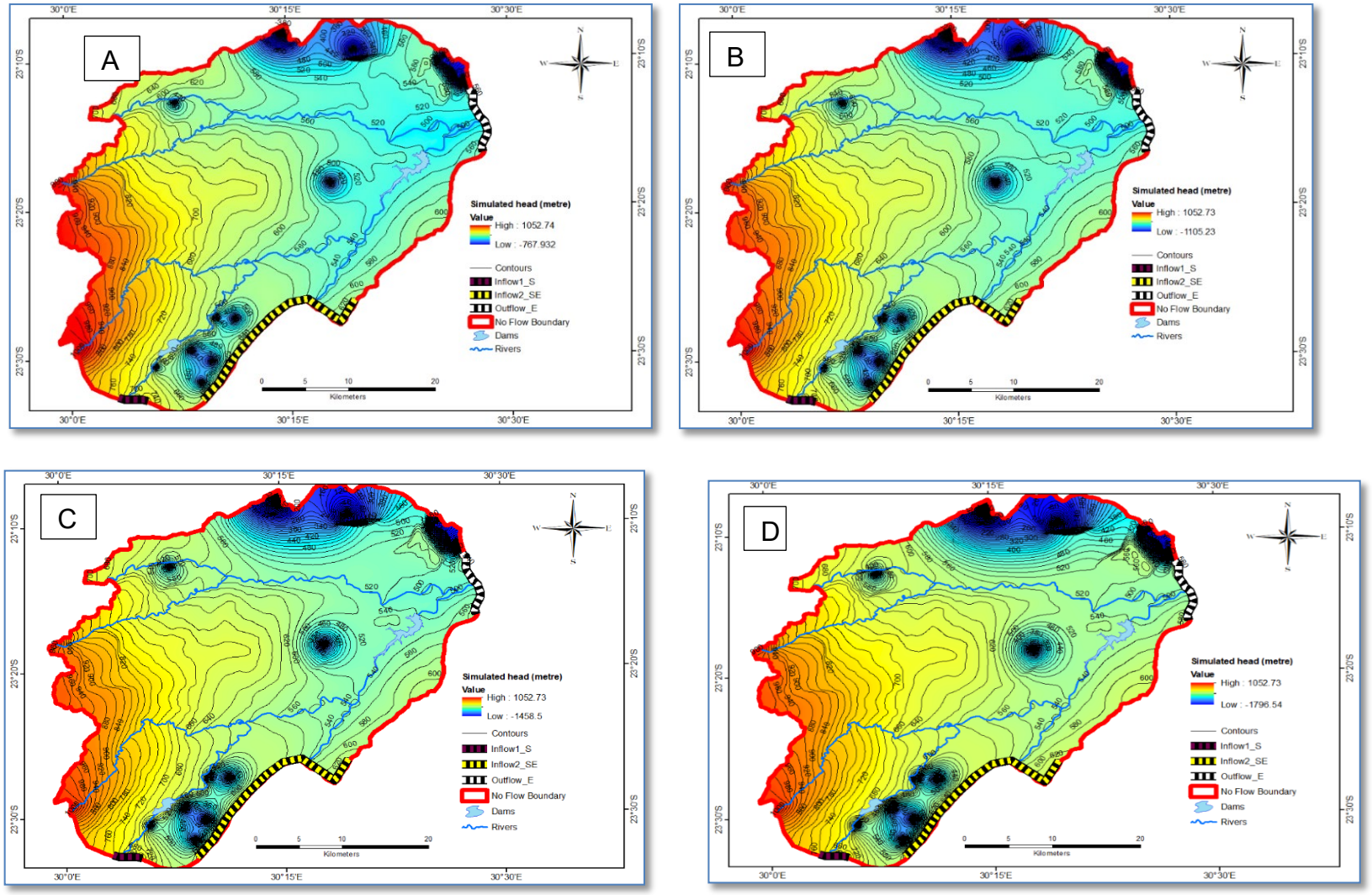

Figure 7-10: Simulated groundwater head distribution with varying abstraction rate increment, (A) 25%, (B) 50%, (C) 75% and (D) 100%.

The groundwater level cross-section corresponding to the different scenarios of increased abstraction rates shows no abstraction impact on the western part of the model domain (highly elevated areas) due to the lack of the availability of abstraction boreholes (Figure 7-11A). However, the impact is obvious at stations 45 to 66 on the east towards the river, with simulated groundwater elevation ranging between 600 to 550m. The trends are showing a gentle slope suggesting less stress due to abstraction possibly resulting from the interaction of the river and aquifer system, similar to the response of the aquifer to a decrease in recharge rate at the vicinity of the river channel (Figure 7-8A).

The south west to north east water level cross-section exhibits a significant impact of abstractions on the aquifer at stations 6 to 36 with simulated groundwater elevation ranging between 200 to 640 m (Figure 7-11B). At stations 66-91, the simulated groundwater level ranges between 550m and 400m due to the impact of the increased groundwater abstraction.

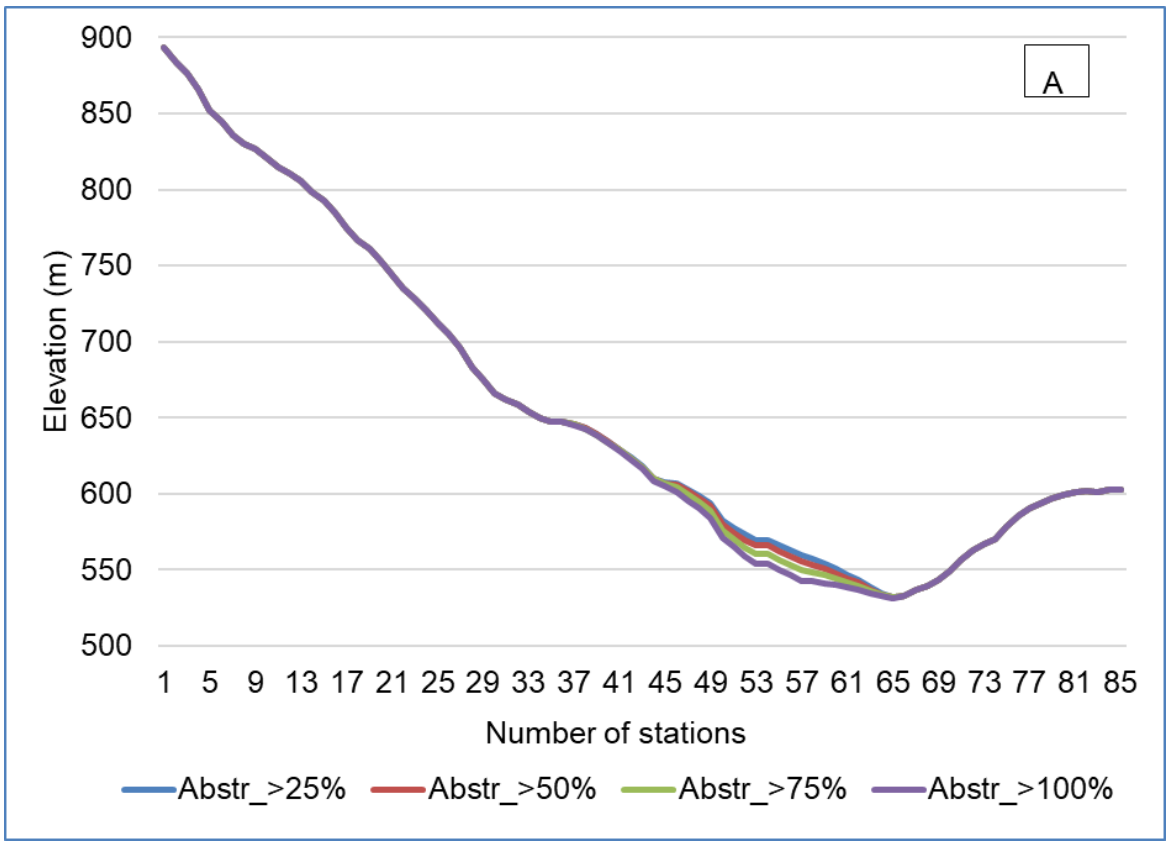

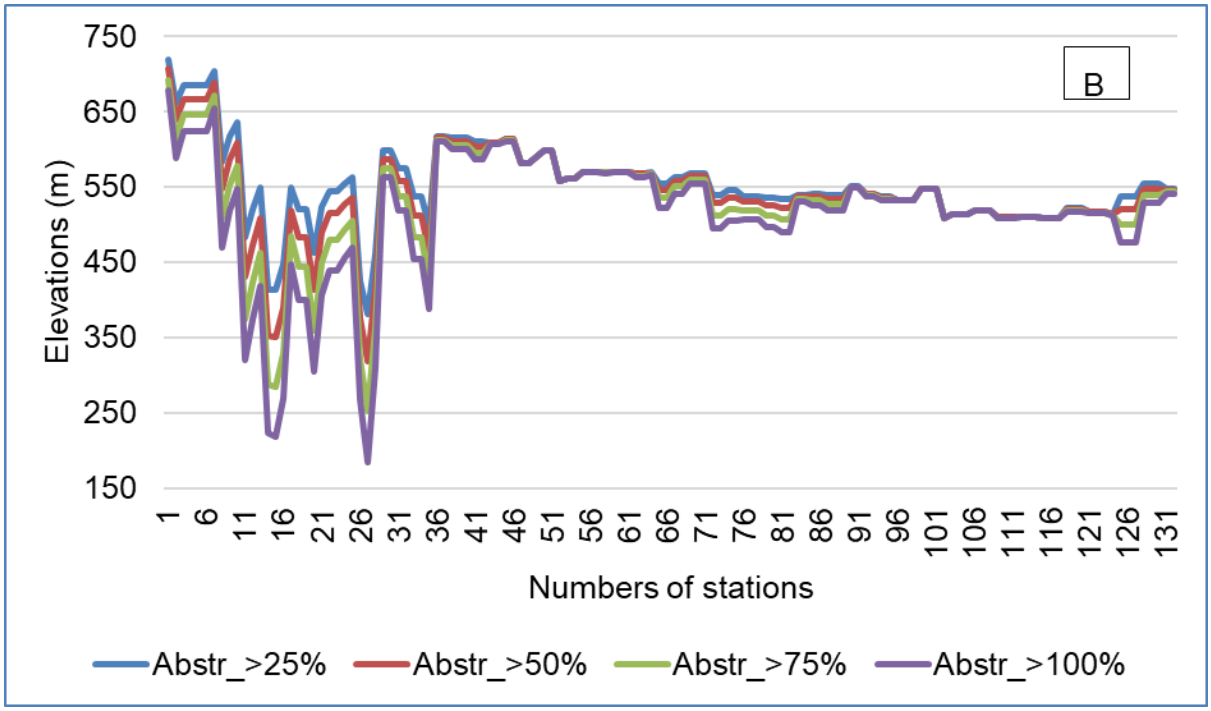

Figure 7-11: Simulated groundwater level cross-section corresponding to an increase in abstraction rate of 25%, 50%, 75%, and 100%, (A) west to east and (B) south west to north east.

7.6 Model Limitations

Numerical models are generally known to be the best approaches and most suitable for modelling complex groundwater systems which most of the analytical solutions cannot achieve. They represent a simplified version of the real system, and therefore always contain limitations due to several assumptions that may represent real-world conditions. The parameters that represent boundary conditions and layer parameters are based on assumptions. In addition, there is uncertainty in model results due to assumptions of the boundary conditions such as inflows, outflows, hydraulic conductivity, depth of screen elevation, etc. The limitations of the steady-state groundwater flow model are presented as follows:

- A limited number of piezometric boreholes in the model domain area affects the model calibration,

- Due to the limited availability of subsurface geologic information, hydraulic conductivity is simulated as uniform per lithological unit. Despite the evidence that borehole yields are highly variable within a short distance, even within the

same rock type. This does not reflect the true complexity of the geology in the study area,

- Lack of abstraction boreholes limits the ability of the model to simulate the impact of groundwater abstraction in the western part of the model domain area,

- Parameters such as river leakages and dam conductance, are simplified because of the lack of detailed information, and

- Several assumptions were used to simplify the construction of the model. One of the most important assumptions was that layer 3 (fractured aquifer) is confined. However, layer 2 and layer 3 have proven to be hydraulically connected and layer 3 depended solely on recharge from layer 2.

These limitations can affect the accuracy of the model results such that it does not capture all the complexities of the system being modeled. For example, this model does not consider the influence of the complex geological structural settings, hydraulic conductive zones, and climatic variabilities which have significant implications on the availability and sustainable management of groundwater and surface water resources. In addition, the groundwater recharge is based on the chloride mass balance method which can substantially under-estimate the long-term average annual recharge by not accounting for the effects of localised surface water inputs (Somaratne and Smettem, 2014). Despite all the challenges related to the limitations, the model results are credible and can be considered for planning and management of the groundwater in the study area.

CHAPTER 8: CONCLUSION AND RECOMMENDATION

8.1 Conclusion

Hydrogeological characterisation of the groundwater resource was conducted to establish a baseline understanding of the aquifer parameters, recharge, groundwater flow mechanisms, water budget, and boundary conditions for the development of the conceptual model in the Klein Letaba River catchment. The hydrochemical and environmental isotope data were used to trace the groundwater flow path and ascertain the inflow and outflow boundaries of the conceptual model of groundwater flow. In addition, a tritium radiogenic isotope was utilised to estimate the mean groundwater resource time based on the methods that were outlined in the previous studies. The results suggest that low tritium concentrations ranging from 0.2 to 1.9 TU correspond to the presence of old water that was probably recharged before 1952 (<0.8 TU), while tritium values > 0.8 TU, suggests a mixture of old (e.g., older than 1952), and recently recharged water.

Statistical and trend analysis of climate data depicted a rainfall variability that appears to have a negative impact on the availability of water resources. Based on the classification of Resende (2002), the rainfall and temperature variability in the study area are classified as moderate (<50%) and low (<15%), respectively. The lowveld has the highest rainfall variability of 31%. The degrees of temperature variability is very low ranging between 2.7 to 6.9% in the highveld and 2.7 to 7.0% in the lowveld. This could be due to the warm temperatures that the Mopani district generally experiences throughout the year. Reference evaporation around the Middle Letaba dam is often higher than rainfall except in a few events where monthly rainfall is above average (<100 mm/m). This could be one of the reasons for the persistent low water levels and failure to fulfill water supply obligations in the area.

Based on the monitoring boreholes, groundwater level trends are also showing increasing depth with time indicating that groundwater level in the study area is diminishing. This situation is considered alarming and raises a concern for the sustainable use of groundwater.

The steady-state groundwater flow simulation results indicate that recharge through rainfall and river leakage accounts for 44% and 40%, respectively. The major outflow components include river leakage and evapotranspiration, with 62% and 25%, respectively to the total water loss from the aquifer system. These findings reveal that interactions between groundwater and surface water are critical in controlling the hydrological water balance. In that, the depletion of groundwater determines the future fate of surface water and vice versa through a hydraulic link between the two reservoirs of water.

The results of the zone budgets show that weathered aquifer acts as a medium through which the fractured aquifer and the rivers are being replenished. It supplies approximately 36% and 23% of the total outflow of its zone to the fractured aquifer and the rivers, respectively. The fractured aquifer has a total inflow volume of 1.04E+08 m^3/day, and approximately 95% and 5% of the total volume is lost to the overlying weathered aquifer and abstraction. These results suggest that the fractured aquifer is the most important source of water supply in the area.

A calibrated groundwater flow model was used to predict the potential impacts of climate change and anthropogenic factors on groundwater resources. This was implemented by decreasing the recharge and increasing the groundwater withdrawal, by 25%, 50%, 75%, and 100%, respectively. The results suggest that groundwater level will significantly decline with the progressive decrease and increase of recharge and abstraction rates, respectively.

The present study shows that there is strong evidence about the vulnerability of groundwater due to the impacts of climate (i.e., a decline in rainfall intensity and increased evapotranspiration), and human-induced stress (e.g., increased abstraction rate). Therefore, the development and management of water resources require a well-planned management that ensures the protection and sustainable use of water in the area.

8.2 Recommendations

Based on the model results, it is anticipated that climate change will have a considerable impact on both surface water and groundwater.

Detailed investigations are therefore required to collect site-specific information that improves the present results, and enables the implementation of transient simulation of groundwater flow. Both modelling approaches will certainly enhance the accuracy of prediction of the impacts of climate change and an increase in groundwater demand. The following recommendations for further study are made:

- Streamflow measurements and groundwater level monitoring can be recommended at upstream of the Middle Letaba River. These datasets will help to accurately predict the behavior of the aquifer in response to both climate change and high abstraction rate,

- Measurements of the permeability of the different types of soil types are important to improve the reliability of the hydraulic conductivity zones corresponding to the model top,

- Additional observed heads and reliable screen depth of each abstraction borehole help improve the discrepancy between the simulated and observed heads,

- The increase in the number of head observation wells is very helpful to improve the reliability of the simulated heads. Future work therefore recommends the availability of at least 20 head observation wells, and

- The boundary between layer groups is interpolated from borehole log data, which may have compromised the actual representation of layer boundaries. Thus, future work may recommend adequate borehole distribution within the model domain.

REFERENCES

Abiye, T., 2016. Synthesis on groundwater recharge in Southern Africa: A supporting tool for groundwater users. Groundwater for Sustainable Development. 2. 182-189.

Abiye, T., 2013. The use of isotope hydrology to characterize and assess water resources in Southern Africa. Report to the Water Research Commission by School of Geosciences, University of the Witwatersrand Contributors. WRC Report No TT 570/13.

Achite, T., Caloiero, T., Wałega, A,. Krakauer, N., and Hartani, T., 2021. Analysis of the spatiotemporal annual rainfall variability in the Wadi Cheli- basin (Algeria) over the period 1970 to 2018. Water, vol. 13, no. 11, p. 1477.

Adams, S., Titus, R. and Xu, Y., 2004. Groundwater recharge assessment of the basement aquifers of central Namaqualand. WRC Report No. 1093/1/04. Water Research Commission, Pretoria.

Aggarwal, P.K., Dillon, M.A., and Tanweer, A., 2004. Isotope fractionation at the soil atmosphere interface and the 18O budget of atmospheric oxygen. Geophys. Res. Lett., 31, L14202.

Ahzegbobor, P. A., Kehinde, D.O. and Adebola, A., 2017. An overview of the potential impacts of climate change on groundwater resources. Journal of Informatics and Mathematical Sciences, Vol 9 (2). 437-453.

Allen, R.G., Pereira, L.S., Raes, D and Smith, D., 1998. Crop evapotranspiration: Guidelines for computing crop water requirements. Irrigation and Drainage Paper, No. 56. Rome: Food and Agriculture Organisation of the United Nations, 300.

Anhaeusser, C.R., 1992. Structures in granitoid gneisses and associated migmatites close to the granulite boundary of the Limpopo Belt, South Africa. Precambrian Res., 55. 81-92.

Anderson, M.P., Woessner, W.W. and Hunt, R.J., 2015. Applied groundwater modelling: Simulation of flow and advective transport. Academic Press, Inc. 564.

Anderson, M. P., and Woessner, W. W., 1992. Applied Groundwater Modelling: Simulation of Flow and Advective Transport. Academic Press. London. 381.

Anderson, M.P., Hunt, R.J., Krohelski, J., and Chung, K., 2002. Using High Hydraulic Concudctivity Nodes to Simulate Lakes. Ground Water 40, 117-122.

Ayuba, R., Tijani, M.N., and Snow, D., 2019. Hydrochemistry and stable isotopes (18O and 2H) characteristics of groundwater in Lokoja and its environs, central Nigeria. Environmental Earth Sciences (2019) 78:582.

Barrat, J.C., 2018. Episodic recharge of groundwater due to cyclonic events within the Limpopo Province, South Africa. Dissertation submitted in fulfillment of the requirements for the degree Master of Science in Environmental Sciences at the North-West University.

Belyanin, G.A., Rajesh, H.M., Sajeev, K., Van Reenen, D.D., 2012. Ultrahigh-temperature metamorphism from an unusual corundum+orthopyroxene intergrowth bearing Al-Mg granulite from the Southern Marginal Zone, Limpopo Complex, South Africa. Mineral Petrol 164. 457-575.

Bird, P., Be-Avraham, Z., Schubert, G., Andreoli., M., and Viola, G,. 2006. Patterns of stress and strain in southern Africa. Journal of Geophysical Research 111, B08402.

Botai, M.C., Botai, J.O. and Adeola, A.M., 2018. Spatial distribution of temporal precipitation contrast in South Africa. S Afr J Sci, 114(7/8).

Brandl, G., 1987. The geology of the Tzaneen area. Explanation Sheet 2330 (1:250 000), Geological Survey of South Africa. 55.

Brandl, G. and Kröner, A., 1993. Preliminary results of single zircon studies from various Archaean rocks of the north-eastern Transvaal. Abstracts, 16th Colloquium of African Geology, Mbabane, Swaziland, Volume 1, 54—56.

Brandl, G., Cloete, M., and Anhaeusser, C. R., 2006. Archaean Greenstone Belts in The Geology of South Africa (M R Johnson, C R Anhaeusser and R J Thomas editors), Geological Society of South Africa/ Council for Geoscience, 9—56.

Brodrick, C., Rahiz, M., and New, M., 2014. Analysis of downscaled climate model results for the areas of Mopani and Namakwa, South Africa, at the district municipality scale. African Climate and Development Initiative (ACDI), University of Cape Town.

Buchanan, P., Koeberl, C. & Reimold, W., 1999. Petrogenesis of the Dullstroom Formation, Bushveld Magmatic Province, South Africa. Contributions to Mineralogy and Petrology, 137(1). 133-146.

Butler, M.J., and Verhagen, B.Th., 2013. Towards a management model for the exploitation of groundwater from the Taaibosch Karoo Graben, Limpopo Province.

Cai, X., Magidi, J., Nhamo, L., van Koppen, B., 2017. Mapping Irrigated Areas in the Limpopo Province, South Africa. Colombo, Sri Lanka: International Water Management Institute (IMWI). 37. IWMI working paper 172.

Cavé, L., Beekman, H.E., and Weaver, J., 2003. Impact of climate change on groundwater recharge estimation. UNESCO IHP Series No. 64. 189-197.

Chandrasekar, N., Selvakumar, S., Srinavas, Y., Wilson, J.J., Peter, T.S. and Magesh, N., 2014. Hydrogeochemical assessment of groundwater quality along the coastal aquifers of southern Tamil Nadu, India, Environmental earth sciences, vol. 71, no, 11. 4739-4750.

Chinoda, G., Moyce, W., Matura, N., and Owen, R., 2009. Baseline report on the geology of the Limpopo Basin Area, a contribution to the Challenge Program on Water and Food Project 17. Integrated Water Resource Management for Improved Rural Livelihoods: Managing risk, mitigating drought and improving water productivity in the water scarce Limpopo Basin". Water Net Working Paper 7, Harare, 44.

Clark, I. D., Fritz, P., 1997. Environment Isotopes in Hydrogeology. Lewis Publishers, New York. 328.

Clifton, C., Evans R., Hayes S., Hirji, R., Puz, G. and Pizarro C., 2010. Water and climate change: impacts on groundwater resources and adaptation options.

Cook, P.G., 2003. A guide to regional groundwater flow in fractured rock aquifers. Seaview Press. Adelaide. Australia.

Cooper, H.H., and Jacob, C.E., 1946. A generalized graphical method for evaluating formation constant and summarizing well field history. American Geophysical Union Transactions, 27:526-534.

Craig, H., 1961. Isotopic variation in meteoric waters. Science 133, 1702-1703.

Dansgaard, W., 1964. Stable isotopes in precipitation. Tellus, 16, 436–468.

Davis, C., 2010. Climate change handbook for north-eastern South Africa. Council for Scientific and Industrial Research (CSIR). Pretoria, South Africa.

Davis, S.N., 1969. Porosity and permeability of natural materials in flow through porous media, R.J.M De Wiest, ed., Academic Press, New York, 54-89.

Deák, J., 1999. Comparison of groundwater flow modeling and environmental isotope results on the Great Hungarian Plain. Use of isotopes for analyses of flow and transport dynamics in groundwater systems. Results of a co-ordinated research project. International Atomic Energy Agency, Vienna (Austria); 394; 2002; (23).

Deák, J., 1978. Environmental isotopes and water chemical studies in Hungary for groundwater research. International symposium on isotope hydrology; Neuherberg/Muenchen, Germany, F.R; 19 - 23 Jun 1978; IAEA-SM-228/13.

Demiroglu, M., 2017. Identifying the groundwater basin boundaries, using environmental isotopes: a case study. Appl Water Sci 7:1161–1167.

Dennis, I and Dennis R., 2011: Climate change index for South Africa aquifers. International Conference of Groundwater: Our source of security in an uncertain future, Pretoria, 19-21 September.

Department of Water and Sanitation (DWS)., 2015. Development of a Reconciliation Strategy for the Levuvhu and Letaba Water Supply System. Groundwater Utilization Scenarios.

Department of Water Affairs (DWA)., 2013. National Water Resource Strategy Second Edition: Water for an Equitable and Sustainable Future. Department of Water Affairs, Pretoria.

Department of Water Affairs and Forestry (DWAF)., 1996. South African water quality guidelines (2nd Ed.). Vol. 1: Domestic Use. Pretoria: Department of Water Affairs and Forestry.

De Silva, R.P., 1999. A comparison of different methods of estimating actual evapotranspiration from potential evapotranspiration in the dry zones of Sri Lanka. Sabaragamuwa University Journal, 2(1): 87-100.

De Vries. J.J. and Simmers. I., 2002. Groundwater Recharge: an Overview of Process and Challenges. Hydrogeology Journal, 10. 5-17.

Dewandel, B., Lachassagne, P., Wyns, R., Marechal, J.C and Krishnamurthy, N.S., 2006. A generalized 3-D geological and hydrogeological conceptual model of granite aquifers controlled by single or multiple weathering. J.Hydrol., 330, 260-284.

Dewandel, B., Lachassagne, P., Chadra, S. and Zaidi, F.K., 2011. Conceptual Hydrodynamic model of a geological discontinuity in hard rock aquifers: Example of quartz reef in granitic terrain in South India. J. Hydrol. (in press).

Dewandel, B., Marechal, J.C., Ladouche, B., Ahmed, S., Chandra, S., Pauwels, H., 2012. Upscaling and regionalizing hydraulic conductivity and effective porosity at watershed scale in deeply weathered crystalline aquifers. J. Hydrol., 416-417, 83-97.

De Wit, M., Van Reenen, D., and Roering, C., 1992. Geologic observations across a tectono-metamorphic boundary in the Babangu area, Giyani (Sutherland) Greenstone Belt, South Africa. Precambrian Research, 55, 111-122.

Dippenaar, M.A., Van Rooy, J.L., Moyo, A., Freeze, R and Makonto, O.T., 2010. Preliminary Vadose Zone Classification Methodology (Molototsi and Middle Letaba Quaternary Catchments). Water Research Commission (South Africa). Project Number K8/876. 14.

Döll, P., and Florke, M., 2005. Global-scale estimation of diffuse groundwater recharge: model tuning to local data for semi-arid and arid regions and assessment of climate change impact. Frankurt Hydrology Paper. August 2005.

Dubinina, E.O., Aranovicha, L.Y., van Reenenb, D.D. Avdeenkoa, A.S., Varlamovc, D.A., Shaposhnikova, V.V. and Kurdyukova, E.B., 2015. Involvement of fluids in the metamorphic processes within different zones of the Southern Marginal Zone of the Limpopo complex, South Africa: An oxygen isotope perspective. Precambrian Research, Volume 256, January 2015, 48-61.

Du Toit, W. H., 2001. An investigation into the occurrence of groundwater in the contact aureole of large granite intrusions (batholiths) located west and northwest of Pietersburg. Pretoria: Department of Water Affairs.

Du Toit, W. H. and Van Lelyveld, M., 2006. An explanation for the 1:500 000 general hydrogeological map: Phalaborwa 2330. Pretoria: Department of Water Affairs and Forestry.

Ebrahim, G. Y., Villholth, K. G. and Boulos, M., 2019. Integrated hydrogeological modelling of hard-rock semi-arid terrain: Supporting sustainable agricultural groundwater use in Hout catchment, Limpopo Province, South Africa.

Environmental Defence Fund (EDF)., 2015. South Africa, The World's Carbon Markets: A Case Study Guide to Emissions Trading, South Africa.

Environomics., 2009. Environmental Management Framework for the Olifants and Letaba Rivers Catchment Areas (OLEMF) Environmental Management Framework Report December 2009.

Esri Environmental Simulations (EES) Inc., 2000. Guide to using Groundwater Vistas, version 8.

European Commission., 1995. Soil terrain database. Land Management and Natural Hazards Unit. IES and JRC, European Commission, Brussels.

Fetter, C.W., 2001. Applied Hydrogeology, 4th Edt., Prentice Hall, New Jersey, P. 598.

Fitts, C. R. (2002). Groundwater Science. Academic Press: London. ISBN 0-12-257855-4.

Freeze, R.A. and Cherry, J.A., 1979. Groundwater. Prentice-Hall, Englewood Cliffs, NJ, 604.

Greater Giyani Local Municipality (GGLM)., 2024. Integrated Development Plan Draft 2024/25.

Geyh, M., Amore, F.D., Darling, G., Paces, T., Pang, Z. and SILAR, J.,2000. Environmental Isotopes in the Hydrological Cycle: Principles and Applications – Volume 4: Saturated and Unsaturated Zone. IAEA, Vienna. 196.

Gummandi, S., Rao, K. P. C., and Seid et al., 2018. Spatio-temporal variability and trends of precipitation and extreme rainfall events in Ethiopia in 1980‐2010," Theoretical and Applied Climatology, vol. 134, no. 3‐4, pp. 1315‐1328.

Günay, G., 2006. Hydrology and hydrogeology of Sakaryabas, ı karstic springs, Cifteler, Turkey. Environ Geol. 51:229–240.

Harris, G., 2009. Salinity, in Encyclopedia of inland waters.

Harbaugh, A.W., and McDonald, M.G., 1996. User's documentation for MODFLOW-96. An update to the U.S. Geological survey modular finite-difference ground-water flow model: U.S. Geological Survey Open-File Report 96-485. 56.

Harbaugh, A.W., 2005. MODFLOW-2005, The U.S. Geological Survey Modular Ground-Water Model – the Ground-Water-Flow Process: U.S. Geological Survey Techniques and Methods, 253.

Habaugh, A. W., Banta, E.R., Hill, M.C., McDonald, M.G., 2000. MODFLOW-2000, The U.S. Geological Survey Modular Ground-Water Model- User guide to modularization concepts and the ground-water flow process. U.S. Geological Survey Open-File Report, No. 92, 121.

Hayes, M., Svoboda, M., and Wall, N., and Widhalm, M., 2011. The Lincoln declaration on drought indices: Universal Meteorological drought index recommended. Bulletin of the American Meteorological Society, 92., 485-488.

Holland, M., 2011. Hydrogeological characterisation of crystalline basement aquifers within the Limpopo Province of South Africa, PhD Thesis at the University of Pretoria.

Houston, J.F.T. and Lewis, R.T., 1988. The Victoria Province drought relief project, II. Borehole yield relationships. Ground Water 26 (4), 418–426.

Hunt, R.J. and Feinstein, D.T., 2012. MODFLOW-NWT: Robust Handling of Dry Cells Using a Newton Formulation of MODFLOW-2005. Groundwater, Vol. 50, No. 5.

International Atomic Energy Agency (IAEA)., 2012. Global Network of Isotopes in Precipitation. The GNIP Database.

International Association of Hydrogeologists (IAH),. 2016. Strategic Overview series on the global change and groundwater.

Intergovernmental Panel on Climate Change (IPCC)., 2007, a and b. Impacts, adaptation and vulnerability, Contribution of working group II to the Fourth Assessment Report of the Intergovernmental Panel on Climate Change. Cambridge University Press, Cambridge, 176.

Jones, M.J., 1985. The weathered zone aquifers of the basement complex areas of Africa. Quarterly Journal of Engineering London 18, 35–46.

Krasny, J., 1992. Classification of Transmissivity Magnitude and Variation. Ground Water, 31, 7.

Khwashaba, M.E., 2018. Vulnerability and resilience in the Mopani district municipality in a changing climate. Dissertation submitted in fulfillment of the requirements for the degree Master of Science in Geography and Environmental Management at the North-West University.

Kumar, C.P., 2013. Hydrological Studies Using Isotopes. International Journal of Innovative Research and Development, Vol 2 Issue 13.

Kusangaya,S., Warburton. M.L., Van Garderen.E.A. and Jewitt, G,P., 2014. Impacts of climate change on water resources in southern Africa: A review. Physics and Chemistry of the Earth, Parts A/B/C. 67.47-54.

Kwon, A.J., 2017. Declining groundwater level effects on supply well operations. Dissertation submitted in partial satisfaction for the requirements for the degree of Master of Science in Hydrologic Science, University of California Davis.

Langevin, C.D., Hughes, J.D., Banta, E.R., Niswonger, R.G., Panday, Sorab, and Provost, A.M., 2017. Documentation for the MODFLOW 6 Groundwater Flow Model. United States of Geological Survey Techniques and Methods, book 6, chap. A55.197.

Lachassagne, P., Wyns, R., and Dewandel, B., 2011. The fracture permeability of Hard Rock Aquifers is due neither to tectonics, nor unloading, but to weathering processes. Terra Nova, 145-161.

Lachassagne, P., Dewandel, B., and Wyns, R., 2021. Review: Hydrogeology of weathered crystalline/hard-rock aquifers—guidelines for the operational survey and management of their groundwater resources. Springer, Hydrogeology Journal.

Lachassagne, P., Dewandel, B., and Wyns, R., 2014b. The conceptual model of weathered hard rock aquifers and its practical applications. In: Fractured rock hydrogeology. IAH Selected Papers, no. 20. CRC, Boca Raton, FL, 13–46.

Leaney F, Crosbie R, O'Grady A, Jolly I, Gow L, Davies P, Wilford J, Kilgour P (2011) Recharge and discharge estimation in data-poor areas: scientific reference guide. CSIRO: Water for a Healthy Country National Research Flagship, Canberra, Australia

Levin, M and Verhagen, B., 2013. Application of isotope techniques to trace location of leakage from dams and reservoirs.

Lerner, D.N., Issar, A.S., and Simmers, I., 1990, Groundwater recharge—A guide to understanding and estimating natural recharge: International Association of Hydrogeologists, International Contributions to Hydrogeology, v. 8, 147.

Libby, W.F., 1946. Atmospheric Helium Three and Radiocarbon from Cosmic Radiation. Physical Review 69(11–12):671–672. doi:10.1103/Phys Rev.69.671.2.

Low, A.B. and Rebelo, A.T., 1998. Vegetation of South Africa, Lesotho and Swaziland, edition 2. Dept of Environmental Affairs and Tourism, Pretoria.

Magaia, L.A., 2009. Processing Techniques of Aeromagnetic Data. Case Studies from the Precambrian of Mozambique. Examensarbete vid Institutionen för geovetenskaper ISSN 1650-6553 Nr 185.

Madisha, M.E., 1996. Carbonate alteration of Serpentinite in the Murchison Greenstone Belt, Kaapvaal Craton: Implications for gold mineralization. Dissertation for Masters of Science in geology, Rand Afrikaanse University.

Makonto, O.T., 2013. Vadose zone classification and aquifer vulnerability of the Molototsi and Middle Letaba Quaternary Catchments, Limpopo Province. A dissertation submitted at the University of Pretoria in partial fulfillment for the Degree of Master of Science in Engineering and Environmental Geology.

Maponya, P.I., 2013. Climate change and agricultural production in Limpopo: Impacts and Adaptation Options, PhD Thesis, University of South Africa, Pretoria, South Africa.

Marechal, J.C., Dewandel, B. and Subrahmanyam, K., 2004. Use of hydraulic tests at different scales to characterize fracture network properties in the weathered-fractured layer of a hard rock aquifer. Water Resour. Res., 40, 17.

Mato, R.A.M.M., 2002. Groundwater Pollution in Urban Dar es Salaam, Tanzania: Assessing Vulnerability and Protection Priorities, PhD Thesis, Eindhoven University, The Netherlands.

Mazor, 1991. Applied and chemical isotopic groundwater hydrology. USA, Canada and Latin America: Halsted Press.

Mazor, 2004. Chemical and Isotopic groundwater Hydrolysis, 3rd Edition, Marcel Dekker Inc. New York.

McDonald. M.G., and Harbaugh. A. W., 1988, A modular three-dimensional finite-difference ground-water flow model: U.S. Geological Survey Techniques of Water Resources Investigations. Book 6. Chap.A1. 586.

McCourt, S., Van Reenen, D., 1992. Structural geology and tectonic setting of the Sutherland Greenstone Belt, Kaapvaal Craton, South Africa. Precambrian Research, 55: 93-110.

McFarlane, M.J., 1992. Groundwater movement and water chemistry associated with weathering profiles of the African surface in Malawi. In: Wright, E.P., Burgess, W.G. (Eds.), Hydrogeology of Crystalline Basement Aquifers in Africa, vol. 66. Geological Society Special Publication, London. 101–129.

Meadows, M.E., 2006. Global change and southern Africa. Geographical Research, 44,135-145.

Mkali, A.T., 2020. Developing a hydrogeological conceptual model for subterranean groundwater control areas using remote sensing techniques, Hout catchment, Limpopo, South Africa. MSc Thesis submitted at the Department of Earth Sciences, Faculty of Natural Sciences, University of the Western Cape.

Monroe, J., Wicander, R. & Hazlett, R., 2007. Physical Geology. 6th ed. Belmont, CA: Thomson Books/Cole.

Moon, B.P. and Heritage, G.L., 2001. The Contemporary geomorphology of the Letaba River in the Kruger National Park, Koedoe 44 (1). 45-55.

Mopani District Municipality (MDM)., 2020. Draft Reviewed Integrated Development Plan: 2016-2021.

Morrice, J., Valett, H., Dahm, C., and Campana, M., 1997. Alluvial characteristics, groundwater-surface water exchange and hydrological retention in headwater streams. Hydrological Processes, 11(3). 253–267.

Moseki, M.C., 2017. Climate change impacts on groundwater: literature review. Environ Risk Assess Remediate, Vol 2 (1).16-17.

Mukheibir, P., 2007. The impact of climate change on small municipal water resource management. The case of Bredasdorp, South Africa. Energy Research Centre, University of Cape Town.

Mukheli, A., 2018. Investigation of factors influencing borehole yields in the Nzhelele-Makhado Areas in Limpopo Province, South Africa. Dissertation submitted to the Departmental Sciences, in fulfillment of the requirements for the degree of Master of Earth Science in Mining and Environmental Geology, University of Venda.

Nel, J., Nel, M., Dustay, S., Siwawa, S., and Mbali, S., 2014. Towards a guideline for the delineation of groundwater protection zones in complex aquifer settings. WRC Report No. 2288/1/14, Water Research Commission, October 2014.

Nembilwi, N., Chikoore,H., Kori, E., Munyai, R.B., and Manyanya, T.C., 2021. The Occurrence of Drought in Mopani District Municipality, South Africa: Impacts, Vulnerability and Adaptation. Climate 2021, 9, 61.

Nistor, M.M., Dezsi, S., Cheval, S., Baciu, M., 2016. Climate change effects on groundwater resources: a new assessment method through climate indices and effective precipitation in Belis District, Western Carpathians. Meteorological Applications, Vol 23. 554-561.

Niswonger, R.G., Panday, Sorab, and Ibaraki, Motomu, 2011, MODFLOW-NWT, A Newton formulation for MODFLOW-2005: U.S. Geological Survey Techniques and Methods 6–A37, 44.

Orpen, W.R.G., 1994, A recommended map legend and mapping methodology for the compilation of regional hydrogeological maps of the Republic of South Africa as a scale of 1: 500 000. Department of Water Affairs and Forestry.

Pathak, R., Awashi M.K., Sharma S.K., Hardaha, M.K., and Nema, R.K., 2018. Groundwater Water Flow Modelling Using MODFLOW-A Review. International Journal of Current Microbiology and Applied Sciences 7(2): 83-88. ISSN: 2319-7706 Volume 7 Number 02.

Penman, H.L., 1956. Evaporation: An introductory survey. Netherlands J. Agric. Sci. 1:9-29, 87-97,151-153.

Piper, A.M., 1994. A graphic procedure in the geochemical interpretation of water analyses, EOS, Transactions American Geophysical Union, Vol. 25.6. 914-928.

Poujol, M., Robb, L.J., Anhaeusser, C.R., and Gericke, B., 2003. A review of the geochronological constraints on the evolution of the Kaapvaal Craton, South Africa: Precambrian Research, volume 127, 181-213.

Reason, C.J.C. and Keibel, A., 2004. Tropical cyclone Eline and its unusual penetration and impacts over the Southern African mainland. Weather and forecasting, 19, 789-805.

Resende, M.D.V., 2002. Genética biométrica e estatística no melhoramento de plantas perenes. Embrapa Informação Tecnológica, Brasília, 975p.

Robb, L. J., Brandl, G., Anhaeusser, C. R. and Poujol, M., 2006. Archaean Granitoid Intrusions in The Geology of South Africa (Johnson, M. R., Anhaeusser, C. R ., and Thomas, R. J., editors), Geological Society of South Africa/ Council for Geoscience, 57—94.

Somaratne, N., and Smettem, R.J., 2014. Theory of the generalised chloride mass balance method for recharge estimation in groundwater basins characterised by point and diffuse recharge. Hydrol.Earth Syst.Sci.Discuss., 11, 307-332.

Sander, P., 2007. Lineaments in groundwater exploration: a review of applications and limitations. Hydrogeol J., 15: 71‑74.

Scanlon, B.R., Healy, R. W. and Cook, P.G., 2002. Choosing Appropriate Techniques for Quantifying Groundwater Recharge. Hydrogeology Journal, 10, 18-39.

Scholes, R., and Walker, B., 1993. An African Savannah: Synthesis of the Nylsvley study. Cambridge, UK: Cambridge University Press.

Schulze, R.E., 1995. Hydrology and Agrohydrology. A text to accompany the ACRU – 3.00 Agrohydrological Modelling System. School of Bioresources Engineering and Environmental Hydrology. University of KwaZulu-Natal. Pietermaritzburg. South Africa.

Seaber, P.R., 1988, Hydrostratigraphic units; in, Back, W., Rosenschein, J.R., and Seaber, P.R., Hydrogeology: The Geology of North America, Geological Society of America, Volume O-2. 9-14.

Shikwambana, S., Malaza, N., and Shale, K., 2021. Impacts of Rainfall and Temperature Changes on Smallholder Agriculture in the Limpopo Province, South Africa. Water 2021, 13, 2872. https://doi.org/10.3390/w13202872.

Simmers, I., 1996. Challenges in estimating groundwater recharge. WRC: Groundwater-Surface Water Issues in Arid and Semi-arid Areas, Pretoria.

South African Weather Services (SAWS)., 2023. Annual State of the Climate of South Africa.

Smith, J.M.B., 1996. Encyclopedia Article. Associate Professor of Geography and Planning, University of New England, Armidale, New South Wales. Station Leader, 1996 Australian National Antarctic Research Expedition to Macquarie Island, Australian Cooperative Research Centre, Hobart, Tasmania. Editor of A History of Australasian Vegetation.

Smit, C., Roering, C., and Van Reenen, D., 1992. The structural framework of the Southern Margin of the Limpopo belt, South Africa, Precambrian Research, 55, 51-67.

South African National Standards (SANS 241)., 2015. South African National Standards for water for domestic supplies. The Council for the South African Bureau of Standards, Pretoria.

South African Committee for Stratigraphy (SACS)., 1980. Stratigraphy of South Africa. Part 1 (Comp. L. E. Kent). Lithostratigraphy of the Republic of South Africa, South West/ Namibia, and the Republics of Bophuthatswana, Transkei and Venda: Handb. Geol. Survey. S. Afr., 8, 53.

Statistics South Africa (Stats)., 2011. General Household Survey (dataset).

Seferli,S., Modis, K. and Adam, K., 2019. Interpretation of groundwater hydrographs in the West Thessaly basin, Greece, using principal component analysis. Environmental Earth Sci., 78 (8), p. 257.

Stettler, E.H, de Beer, J.K and Blom, M.P, 1989. Crustal domains in the northern Kaapvaal as defined by magnetic lineaments. Precambrian Res. 45:263-276.

Sophocleous, M. A., 2004. Climate change—Why should water professionals care? Ground Water, in press.

Sophocleous, M. A., 2004. Global and Regional Water Availability and Demand: Prospects for the Future. Natural Resources Research, Vol. 13, No. 2.

Tshiala, M. F. and Olwoch, J. M., 2010. Impact of climate variability on tomato production in Limpopo Province. South Africa.African Journal of Agricultural Research, Vol. 5 (21).2945-2951.

Taylor, R., 2014. Hydrology: When wells run dry. Nature, Vol 516 (7530): pp179-180.

Taylor, R.G., Koussis, A.D., Tindimugaya, C., 2009. Groundwater and climate in Africa, A Review of Hydrological Sciences Journal, 54(4):655-664.

Taylor, R. and Howard, K., 2000. A tectono-geomorphic model of the hydrogeology of deeply weathered crystalline rock: Evidence from Uganda. Hydrogeol J 8(3):279–294.

Taylor, R. & Howard, K., 1999. The influence of tectonic setting on the hydrological characteristics of deeply weathered terrains: evidence from Uganda. Journal of Hydrology, 218(1-2). 44-71.

Toth, J. 1999. “Groundwater as a geologic agent: an overview of the causes, processes, and manifestations.” Hydrogeology Journal 7:1-4.

Tredoux, G. and Talma, A.S., 2006. Nitrate pollution of groundwater in southern Africa. In: Xu, Y & Usher, B (Eds), Groundwater pollution in Africa, Taylor & Francis/Balkema, Leiden, The Netherlands. 15-36.

Tredoux, G., Engelbrecch, J.F.P., and Talma, A.S., 2001. Nitrate in groundwater in southern Africa. In: new approaches characterizing groundwater flow, Seiler & Wohnlich (eds), Swets & Zeitlinger, Lisse. 663-666.

Todd, D., and Mays, L., 2005. Groundwater Hydrology. 3rd Edition, John Wiley and Sons, Inc., Hoboken, 652.

Tripathi, R.P., and Singh, H.P., 1998. Soil erosion and conservation. New Age International, LTD Publishers.

Turpie, J., Visser, M., 2012. The impact of climate change on South Africa’s rural areas. Technical Report: Submission for the 2013/14 Division of Revenue.

Uken, R., Watkeys, M.K., 1997. An interpretation of mafic dyke swarms and their relationship with major mafic magnetic events on the Kaapvaal Craton and Limpopo Belt. S.Afr.J. Geol. 100(no.4): 341-348.

UNESCO., 1983. International Association of Hydrogeologists (IAH), International Association of Hydrogeological Sciences (IAHS) United Nations Education, Scientific Cultural Organisation (UNESCO. International Legend for Hydrogeological Maps, Revised version.

United Nations (UN)., 2007. Coping with Water Scarcity: Challenges of the Twenty-First Century. United Nations (UN)-Water and Food and Agriculture Organisation of the United Nations (FAO), New York.

United Nations., 2023. What is climate change? https://www.un.org/en/climate change.

Van Tonder, G. and Xu, Y., June 2000. A guide for the estimation of groundwater recharge in South Africa.

Van Tonder, G.J., Botha, J.F., Chiang, W.H., Kunstmann, H. and Y.Xu, Y., 2001. Estimation of the sustainable yields of boreholes in fractured rock formations.

Van Wyk, E., 2010. Estimation of episodic groundwater recharge in semi-arid fractures hard rock aquifers. An unpublished Dissertation submitted in fulfillment of the requirements for the degree of Doctor of Philosophy in the Faculty of Natural and Agricultural Science, University of Free State.

Van der Gun, J., 2012. Groundwater and global change: Trends opportunities and challenges. United Nations World Water Assessment Programme.

Van Reenen, D., Roering, C., Brandl, G., Smit, C., and Barton, J., 1990. The granulite-facies rocks of the Limpopo belt in Southern Africa. In: D. Vielzeuf and Ph. Vidal (Editors), Granulites and Crustal Evolution. Kluwer, Dordrecht, 257-289.

Van Reenen D.D., Roering, C., Ashwal, L. D., and De Wit, M.J., 1992. Regional Geological setting of the Limpopo Belt. Precambrian Research, 55 (1-4), 1-5.

Vassolo, S., Tiberghien, C., Heckmann, M., Hahne, C. and Baranyikwa, D., 2019. Hydrogeology of a weathered fractured aquifer system near Gitega, Burundi, Hydrogeology Journal, 27(2). 625–637.

Vegter, J.R., 2003. Hydrogeology of Groundwater: Region 19 Lowveld. WRC Report No. TT 208/03. Pretoria, Water Research Commission.

Weaver, J.M.C., Cave, L., Talma, S., 2007. Groundwater Sampling. A Comprehensive Guide for Sampling Methods. Water Research Commission. Report No, TT 303/07, 183.

Weaver, J. M. C., Cave, L., Talma, S., 2007. Groundwater Sampling a Comprehensive Guide for sampling methods: Water Research Commission. Report No TT 303/07, 183.

Weitz, J.C., 2016. Hydrogeological and three-dimensional numerical groundwater flow modelling of the Lake Sibayi catchment, Northern KwaZulu-Natal, South Africa. Submitted in fulfillment of the academic requirements of Doctor of Philosophy, University of KwaZulu-Natal.

Witthüser, K.T., Holland, M., Rossouw, T.G., Rambau, E., Bumby,A.J., Petzer,K.J., Dennis, I., Beekman, H., van Rooy, J.L., Dippenaar, M. and de Wit, M., 2011. Determining Sustainable Yields of Potential Productive Well Fields in the Basement Aquifers of the Limpopo Province With Special Emphasis on the Limpopo (WMA a) and Luvuvhu/Letaba (WMA 2) Water Management Areas. Water Research Commission (South Africa) Project Number K5/1693/1, 5.

Woldeamak, S.T., Batelaan, O., Smedt, F., 2007. Effects of climate change on the groundwater system in the Grote-Nete catchment, Belgium. Hydrogeology Journal, 15:891-901.

World Health Organisation (WHO)., 2011. Guidelines for drinking-water quality (4th Ed). WHO Library Cataloguing-in-Publication Data.

Wright, E.P. and Burgess, W.G., 1992. Hydrogeology of Crystalline Basement Aquifers in Africa, vol. 66, 1-27. Geological Society Special Publication, London. 101–129.

Wu, Y., 2005. Groundwater recharge estimation in Table Mountain Group aquifer systems with a case study of the Kammanassie area. Dissertation submitted in the fulfillment of the requirements for the degree of Doctor of Philosophy in the Faculty of Natural Science, University of the Western Cape.

Xu, Y., and Beekman. H.E., 2003. Groundwater recharge estimation in Southern Africa. UNESCO IHP Series No. 64, UNESCO Paris.

Yidana, S. M., Fynn, O. F., Cheggeleh, L. P., Nude, P. M., Asiedu, D.K., 2013. Hydrogeological conditions of a crystalline aquifer: Simulation of optimal abstraction rates under scenarios of reduced recharge, The Scientific World Journal.

Zhang, L., Dawes, W.R., and Walker, G.R., 1999. Predicting the Effect of Vegetation Changes on Catchment Average Water Balance. Cooperative Research Centre for Catchment Hydrology, CSIRO Land and Water, Technical Report 12, 42.

Zhou, P., Li, M and Lu, Y., 2017. Hydrochemistry and Isotope Hydrology for Groundwater Sustainability of the Coastal Multilayered Aquifer System (Zhanjiang, China). Hindawi Geofluids Volume 2017, Article ID 7080346.